This is to certify that the

dissertation entitled

A Miniturized Chemiluminescence Detector and an Automatic Sample Introduction System in Capillary Zone Electrophoresis

presented by

CHUNHONG PENG

has been accepted towards fulfillment
of the requirements for

Ph.D degree in Chemistry

Major professor

Date May 5, 2000

O-12771

A MINIATURIZED CHEMILUMINESCENCE DETECTOR AND AN AUTOMATIC SAMPLE INJECTION SYSTEM IN CAPILLARY ELECTROPHORESIS

By

Chunhong Peng

A DISSERTATION

Submitted to
Michigan State University
in partial fulfillment of the requirements
for the degree of

DOCTOR OF PHILOSOPHY

Department of Chemistry

1999

ABSTRACT

A Miniaturized Chemiluminescence Detector and an Automatic Sample Introduction System in Capillary Zone Electrophoresis

by

Chunhong Peng

A miniaturized, high collection-efficiency, post-column, sheath-flow chemiluminescence (CL) detector for use with capillary zone electrophoresis (CZE) is described. The stainless steel detector body significantly cuts down the electrical noise associated with AC power supply. The inner wall of this CL detector was carefully machined to a high smoothness to increase retro-reflection. The other advantage of this novel CL detector arises because the PMT is placed extremely close to the separation capillary to increase the solid angle for light collection. This simple detector requires no lens or concave reflection mirror for enhancement of collection efficiency. Calculations predict that the collection efficiency of this chemiluminescence detector is $\approx 58\%$.

The miniaturized CE-CL detector is characterized using transition metal cations as the sample species. The major problem for the separation of transition metal cations is their strong adsorption to the surface of the fused silica capillary. We are able to achieve a detection limit of 1.5×10^{-12} M for Co^{2+}, 5.0×10^{-8} M for Cr^{3+}, 3.0×10^{-8} M for Cu^{2+}, and a theoretical plate number of 340,000 for 1.0×10^{-11} M Co^{2+}. This is by far the best separation efficiency that has been achieved with post-column reaction detector in capillary zone electrophoresis.

An automatic sample injection device is also described. This novel sample injector requires neither the relocation of separation capillary nor the disconnection of the high voltage during sample injection. Sample throughput is greatly enhanced compared to that of traditional sample injection. This automatic sample injection system includes a mechanical system, an electronic control circuit and a computer. The whole system is mounted on a 10" x 18" x ½" home-made aluminum optical breadboard.

In this sample introduction system, the separation capillary is fixed on a capillary holder, which is mounted on a optical translation stage. The sample capillary is held on the sample platform mounted on a rotary alignment system. A computer controls the electromagnet to pull the platform to a precise position. The rotary alignment system assures the precise alignment of sample capillary and separation capillary during sample injection. A damping device is used to minimized the shock when the sample capillary joins the separation capillary. The new injection system is characterized in chapter 5. The automatic injection system shows a better reproducibility of injection (10.9% RSD) than the manual injection system (27.0% RSD).

Acknowledgements

I would like to thank all the people who were helpful in the preparation of this thesis. No one can do everything by himself although I am the sole author of this dissertation.

I would like to express the greatest gratitude to my adviser, Dr. Stanley R. Crouch. Stan is not only an adviser, but also a friend who understands his students. I learned many things from the course he taught and from regular conversations with him. He is not someone who tells you what to do, but someone who makes you to think what you should do. Special thanks go to Dr. Gary Blanchard for serving as my second reader and for providing suggestions during the writing of this dissertation. I would also like to thank the rest of the committee members, Dr. Dantus and Dr. Hollingsworth for their support.

My special thanks go to Russell Geyer and Richard Menke in the chemistry machine shop for teaching me various machining skills. Also thanks to Ron Haas, Scott, Glen in the Electronic shops for their excellent service whenever help is needed.

Finally I would also want to thank some former group members, David Short, Dana Spence, Yi Shi, Tom Cullen and Dan Severs (the Karate man) for the help during my Ph.D journey at Michigan State University.

TABLE OF CONTENTS

LIST OF TABLES

TABLE PAGE

LIST OF FIGURES

Chapter 1

Introduction to Chemiluminescence and Capillary Zone Electrophoresis

This chapter describes some basic principles of chemiluminescence, such as the mechanism of chemiluminescence and the factors affecting the emission intensity. Several popular chemiluminescence reagents are listed. Chemiluminescence detection in static and flow systems is also described. The historical background of capillary electrophoresis is also presented. The advantages of capillary zone electrophoresis over conventional electrophoresis are described. Some basic principles of capillary zone electrophoresis, including electroosmosis, sample injection, and various detection techniques including chemiluminescence are given. The interface between chemiluminescence and capillary electrophoresis is summarized in detail. Sample injection techniques such as electrokinetic injection and hydrodynamic injection in CE are also discussed.

1.1 Introduction to Chemiluminescence

1.1.1 Theoretical Aspects of Chemiluminescence Reactions

Chemiluminescence (CL) is the emission of light from a chemical reaction (1). Chemiluminescence reactions generally yield a product in an electronically excited state. Visible light is produced when the excited state relaxes to the ground state. The typical CL reaction can be represented as:

$$A + B \text{ ----> } C^* \text{ ----> } C + h\nu \qquad (1.1)$$

where A and B are the reactants, C* is the excited intermediate, and C is the final product. For CL to occur, three general conditions must be met. First, there must be sufficient energy to produce an excited state. Thus, the reaction must be sufficiently exothermic that

$$-\Delta G = \frac{h\,c}{\lambda_{ex}} \tag{1.2}$$

Here ΔG is the free-energy change (kcal/mol) of the reaction, h is Planck 's constant, c is the speed of light, and λ_{ex} is the long-wavelength limit in nm for excitation of the luminescent species. For CL emission in the visible region, -ΔG must be 40 to 70 kcal / mol (1). Second, there must be a favorable reaction pathway to produce the excited state. Third, photon emission must be a favorable deactivation process.

The emission intensity I_{CL}, defined as photons emitted per second, depends on the chemiluminescence quantum yield, ϕ_{CL}, defined as the number of photons emitted per molecule reacting and the rate of reaction, dC/dt (2):

$$I_{CL} = \phi_{CL} \frac{dC}{dt} \tag{1.3}$$

ϕ_{CL} depends on how efficiently the excited states are generated from the molecules reacting (ϕ_{EX}, excitation efficiency) and on how efficiently the excited states luminesce (ϕ_L, luminescence efficiency) (4):

$$\phi_{CL} = \phi_{EX}\ \phi_L \tag{1.4}$$

Combine Equations 1.3 and Equation 1.4, we have:

$$I_{CL} = \phi_{EX}\ \phi_L \frac{dC}{dt} \tag{1.5}$$

Equation 1.5 indicates that the intensity of chemiluminescence depends on the rate of chemical reaction, the efficiency of production of the excited state, and the efficiency of light emission from the excited state. For most CL reactions, the emission intensity quickly increases to a maximum after mixing and then slowly decays to the background level as the CL reagents are consumed, giving rise to a peak-shaped transient signal.

The advantages of chemiluminescence detection include high sensitivity, wide linear dynamic range, and simple instrumentation (1). Chemiluminescence is considered a dark field technique because it generates a signal against a dark background. No external light source is needed as in UV absorption, and thus the background signal is very low. Unlike fluorescence, the CL background signal is usually determined by reagent purity rather than by Raman scattering. Small changes in a small background are more easily detected than small changes in a large background. The problem with chemiluminescence detection is the lack of selectivity. CL emission depends on a variety of environmental factors, such as pH, temperature, ionic strength, solvent and species other than that of interest. CL emission is transient; the emission vs. time profile can be different from one compound to another, making the detection more complicated. Furthermore, CL reactions with complex kinetics can give rise to nonlinear calibration curves (3).

1.1.2. Chemiluminescence Reagents

Several CL reactions have been used for analytical purposes, including the peroxyoxalate, acridinium, firefly luciferase, lucigenin, and luminol (5-amino-2,3-dihydro-1,4-phthalazine-dione) reactions. Luminol is one of the most widely used CL reagents. In aqueous alkaline solution, luminol is oxidized by H_2O_2 or other oxidant such

as MnO_4^-, ClO^- and I_2 (5) to 3-aminophthalate in the presence of catalysts (peroxidase, hemin and transition metal ions). The CL intensity is proportional to the concentrations of luminol, H_2O_2 and catalysts (2). Thus, measurements of CL intensity can be used to quantitate luminol or derivatives of luminol, H_2O_2 or species that can be converted into H_2O_2, and catalysts. The mechanism of the luminol-H_2O_2 reaction can be described below. Luminol is first ionized to an anion carrying two electrons in alkaline media, which then reacts with active O_2* to generate an excited state intermediate. When the excited state of 3-aminophthalate returns to the ground state, blue light is emitted at 425 nm.

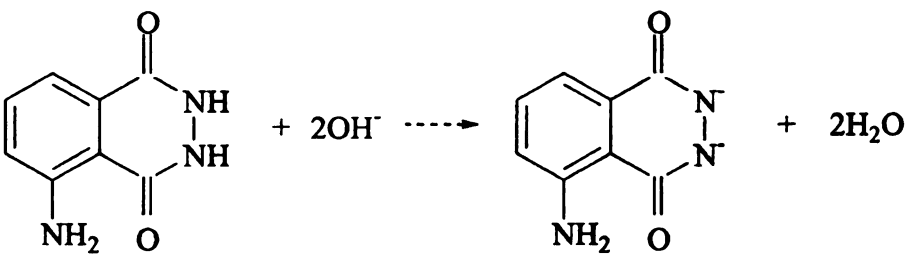

Luminol 3-aminophthalate

$$H_2O_2 \xrightarrow{\text{catalyst}} H_2O + O_2^*$$

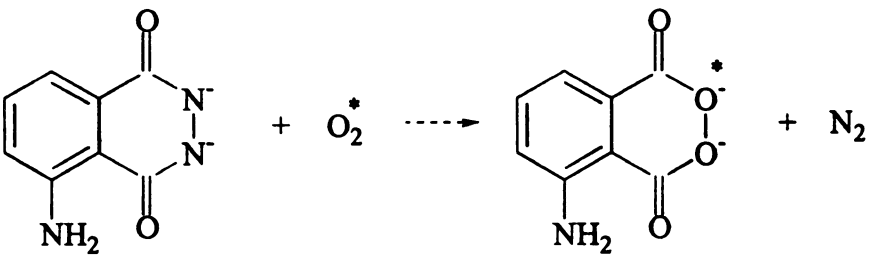

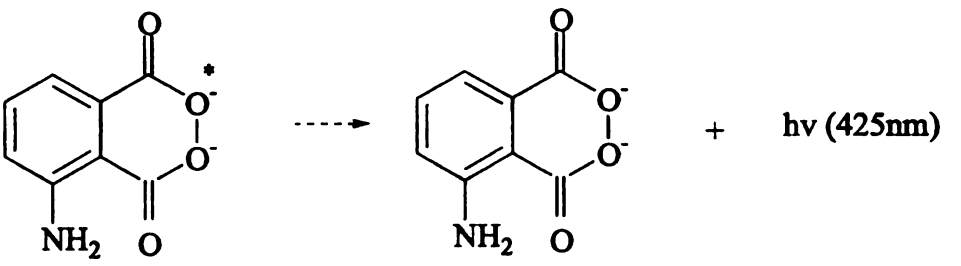

1.1.3 Historical Background of Chemiluminescence Detection

Many transition metal ions are known to activate or inhibit the chemiluminescence of luminol in basic solution. Seitz and Neary (6), and Isacsson and Wetermark (7) have reviewed analytical applications. When the reagents are in excess, the CL emission can be related to the concentration of metal ions (8). In 1962, Babko and coworkers (9-12) did the earliest determination of cobalt, copper and iron based on their catalysis of the luminol reaction in static mode. By simply mixing the reactants while exposing the container to a photographic film and measuring the exposure as a function of concentration, they found detection limits of 1 ppb, 3 ppb and 10 ppb for cobalt, copper and iron, respectively. In 1972, Seitz and Hercules developed specific methods for the determination of Cr^{3+} (13) and Fe^{2+} (14). The CL responds more sensitively to Co^{2+} than to other metal ions, and the detection limit for Co^{2+} has been estimated to be 10^{-11} M (8). The early work laid the foundation for on-line CL detection of transition metal ions separated by ion chromatography (15, 16). CL has been used as a sensitive means of detection in capillary zone electrophoresis; a detailed description is given in section 1.2.6 of this chapter.

1.2 Introduction to Capillary Zone Electrophoresis

1.2.1 Historical Background of Capillary Electrophoresis

Electrophoresis is the separation of charged species based on differential migration under an applied electric field. It was first described by Arne Tiselius in 1937 (17). In 1967, Hjerten presented the pioneering demonstration of capillary electrophoresis (18). In 1974, Virtanen described electrophoretic separations in 0.2 - 0.5 mm id. glass tubes with potentiometric detection (19). In 1979, Mikkers and Everaerts performed the separation of organic and inorganic anions in Teflon tubes (20, 21). However, high separation efficiency was not achieved due to sample overloading. In 1981, Jorgensen and Lukacs demonstrated the first high efficiency separation of more than 400,000 theoretical plates using a narrow bore glass capillary (22). This work has become the landmark in modern capillary zone electrophoresis. The literature of capillary electrophoresis has been reviewed in detail by several workers (23-26). In this section, the important theory and various detection techniques, including chemiluminescence detection, are reviewed.

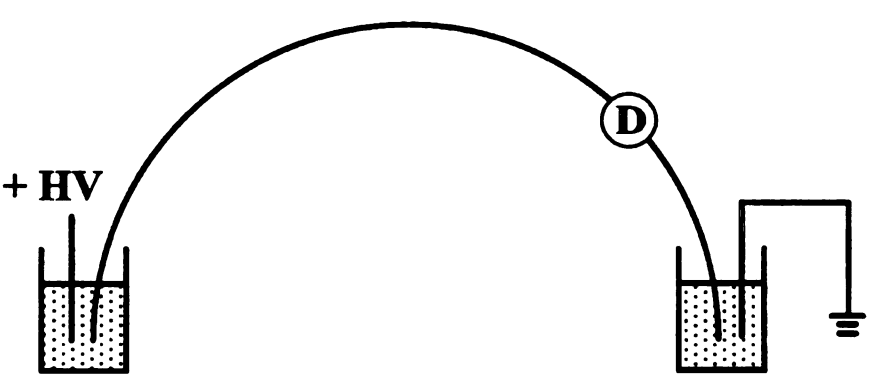

Figure 1.1 Schematic Representation of Capillary Electrophoresis

In capillary zone electrophoresis, a narrow plug of sample is introduced into the buffer-filled capillary from the high voltage end, as illustrated in figure 1.1. When a high electric field is applied across the capillary, different species in the sample migrate differentially, according to ionic mobility.

1.2.2 Advantages of Capillary over Conventional Electrophoresis

The major limitation in conventional electrophoresis is the temperature rise induced by Joule heating which results in temperature gradients across the capillary. The subsequent convection increases zone broadening. Severe Joule heating can lead to boiling of the electrophoretic buffer. The unique advantage of capillary electrophoresis is the enhanced heat dissipation. A narrow bore capillary provides better heat dissipation due to the large surface area / volume ratio, and permits the use of very high electric fields which are required for fast and efficient separations. Other advantages of using a capillary include minimal convection due to the small radius, sampling from a microenvironment like a single cell and simple automation.

1.2.3 Electroosmosis

Electroosmosis is the flow of bulk solvent caused by the electrical double layer adjacent to the inner surface of a capillary under the influence of an electric field. This phenomenon can be explained by the interaction of silanol groups with aqueous solution at the inner wall of the fused-silica capillary. The surface Si-OH group is ionized to $Si\text{-}O^-$ in alkaline and slightly acidic media; thus, the inner wall of the capillary is negatively charged and positive counter ions are present in the stagnant double layer and diffuse

layer as shown in figure 1.2. In strongly acidic media (pH < 2), electroosmotic flow is very small. The potential across the double layer is termed the zeta potential, ζ, and is given by:

$$\zeta = \frac{4 \pi \eta \mu_{eo}}{\varepsilon} \tag{1.6}$$

Here η is the viscosity of the operating buffer, μ_{eo} is the electroosmotic flow coefficient, and ε is the zero frequency dielectric constant of the carrier buffer.

$$\mu_{eo} = \frac{\varepsilon \zeta}{4 \pi \eta} \tag{1.7}$$

The thickness of the double layer is usually a few nanometers to a few hundred nanometers. When an electric field is applied across a narrow bore capillary, the solvated counterions in the diffuse layer migrate with a flat flow profile toward the cathode. The direction and rate of electroosmotic flow depend on the polarity and magnitude of the zeta potential, respectively. The direction of electroosmotic flow is normally toward the cathode in aqueous solutions, but can be reversed by introducing a cationic surfactant such as cetyltrimethylammonium bromide (CTAB) into the separation buffer due to its adsorption to the negatively charged capillary wall (27).

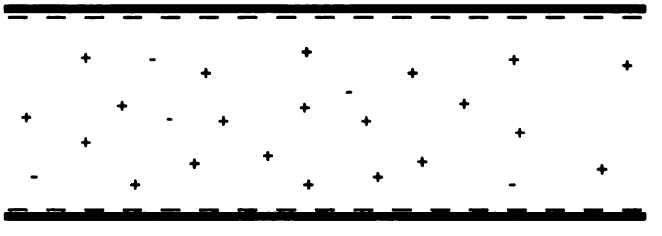

Figure 1.2 Schematic Representation of Silica-Solution Interface

1.2.4. Theoretical Aspects of Capillary Zone Electrophoresis

1.2.4.1 Migration Time

In capillary zone electrophoresis, the migration time t_r is the time for a charged species to travel the distance L′ from the beginning of capillary to the detector (22).

$$t_r = \frac{L' L}{V_{ep} (\mu_{ep} + \mu_{eo})} \tag{1.8}$$

where L is the entire length of capillary, μ_{ep} is the electrophoretic mobility of the sample, and V_{ep} is the electrophoretic voltage. The length of capillary has a profound influence on migration times as can be seen from Equation 1.8.

1.2.4.2 Separation Efficiency

Separation efficiency in terms of the total number of theoretical plates, N, is given by (22):

$$N = \frac{(\mu_{ep} + \mu_{eo}) V_{ep}}{2D} \tag{1.9}$$

Here D is the solute 's diffusion coefficient. Equation 1.4 indicates that the separation efficiency has nothing to do with the length of capillary. This is somewhat different from chromatography where the theoretical plate number increases with the length of column. Ideally, high efficiency separation is best performed with high voltage across a short capillary. However, there are practical limits to this approach. As the capillary is made shorter, the surface area available for heat dissipation is decreased; on the other hand, more Joule heat is produced due to the reduced electric resistance of the capillary.

1.2.4.3 Resolution

Resolution R_s of two zones in capillary zone electrohporesis is given by (22):

$$R_s = \frac{1}{4}\left[\frac{(\mu + \mu_{eo})V}{2D}\right]^{\frac{1}{2}}\left[\frac{\mu_{ep1} - \mu_{ep2}}{\mu + \mu_{eo}}\right] \tag{1.10}$$

$$R_s = 0.177(\mu_{ep1} - \mu_{ep2})\sqrt{\frac{V_{ep}}{D(\mu + \mu_{eo})}} \tag{1.11}$$

where μ_{ep1} and μ_{ep2} are the electrophoretic mobilities of the two species and μ is their average mobility. From this equation, it is clear that resolution is poor if there is a large electroosmotic flow in the same direction as the electrophoretic migration. Resolution can be improved by suppressing the electroosmotic flow at the cost of a longer migration time.

1.2.5. Sample injection

Electrokinetic and hyrdrodynamic injection are best suited for reproducible delivery of nanoliters or even picoliters of sample into 25 μm to 75 μm internal diameter capillaries (28, 29). Several other injection techniques, such as a split injector (31), a rotary injector (32), and a micro injection system (3-34) have also been designed.

1.2.5.1 Electrokinetic injection

In electrokinetic injection, the anodic end of the capillary and the anode are placed into the sample vial together. An injection voltage (typically 2 kV – 10 kV) is applied briefly, causing electromigration of small plug of sample into the capillary. The capillary

and the anode are then placed into the buffer reservoir, and the separation voltage (typically 10 kV - 20 kV) is applied. The quantity of sample injected into the capillary, $Q_{injection}$ can be calculated (28)

$$Q_{injection} = \frac{(\mu_{ep} + \mu_{eo})\, V_{injection}\, \pi r^2\, t_{injection}\, C}{L} \qquad (1.12)$$

where $t_{injection}$ is the time of injection at injection voltage $V_{injection}$, r is the inner radius of the capillary, and C is the sample concentration. The amount of sample injected can also be determined by substituting equation 1.8 into equation 1.12.

$$Q_{injection} = \frac{L' \pi r^2\, C\, V_{injection}\, t_{injection}}{V_{ep}\, t_r} \qquad (1.13)$$

The drawback of electromigration injection is the two types of discrimination (27, 29) that result. The first one occurs as a result of the differences in mobility of the sample species. Charged species with higher mobility are introduced into the capillary faster and in larger quantities than species with lower mobility. The second type of discrimination is related to the differences in the conductivity between the sample and the buffer (29). Dasgupta and colleagues (35) attempted to use a small wire loop to reduce differential injection of species with different mobilities. They reported that the mobility induced bias is dramatically lowered. However, the injection device is very sophisticated and difficult to construct. Linhares and coworker (36) fabricated an on-column fracture for sample injection to reduce discriminative injection. In this method, an on-column fracture was made on the capillary. The fracture allows ions, but does not allow a significant quantity of buffer solution to pass through. During injection, a potential is applied between the fracture and the outlet of the capillary. Electroosmotic flow (EOF) pulls sample ions into

the capillary through the inlet of the capillary. The amount of sample introduced is proportional to the EOF. It is assumed that no electromigration of analytes occurs and introduction of sample is on longer biased by using the EOF as pump.

1.2.5.2 Hydrodynamic Injection

In hydrodynamic injection, the end of the capillary is placed into the sample reservoir, followed by lifting the sample reservoir to a specified height Δh above the level of the ground buffer reservoir (29). This height difference causes hydrostatic pressure, pushing the sample into the capillary without any discrimination for ionic components. The quantity of sample injected can be calculated by

$$Q_{injection} = \frac{\rho g \pi r^4 \Delta h C t_{injection}}{8 \eta L} \qquad (1.14)$$

where ρ is the solution density, g is the gravitational force constant, and η is the viscosity of the sample solution.

1.2.6. Detection in Capillary Zone Electrophoresis

Capillary zone electrophoresis is a powerful technique for the separation of biological macromolecules such as oligoneucleotides, proteins and DNA. One of the major limitations is the lack of sensitive detection. Several reviews have emphasized the necessity for enhanced detection (23, 24, 37, 38). Currently commercial CE instruments provide either UV/visible absorbance or fluorescence detection. UV-visible absorbance is the most popular on-column detection technique, although the detection sensitivity is rather poor (detection limit 10^{-5} ~ 10^{-7} M) due to the short optical pathlength. Several

attempts have been made to enhance sensitivity by increasing the optical path length (39-47). Sensitivity can be increased using a capillary of bigger internal diameter, but a bigger diameter also means more Joule heating, which is not good for efficient separation. "Bubble cells", a pipet-like structure made directly from capillary, offer longer path length with minimal loss of resolution when using a reduced detection slit width (39). Z-cells (a short section of bends in the capillary) offer a longer pathlength but cause a loss of separation efficiency (40-41). Also, the Z-cell structure is fragile. A Z-cell design is commercially available from LC Packings Inc. Rectangular capillaries give longer pathlength but higher Joule heating (42). Internal reflection cells offer longer pathlength by reflecting the light through the section of the capillary several times, but cause a loss in resolution (43-44).

Fluorescence detection is by far the most sensitive detection technique routinely used in CE. Chen and coworkers have reported the detection of 30 molecules of Rodamine using a green He-Ne laser (48) and the detection of 6 molecules of sulforhodamine 101 using a yellow He-Ne laser (49). Only a small number of chemicals are naturally fluorescent. For those non-fluorescent analytes, such as oligosaccharides (48-50), the primary amine group of amino acids (51-53), peptides (54), biological thiols (55), and phosphate containing compounds (56), precapillary or post-capillary chemical derivatization is required. Fluorescence derivatization sometimes results in poor yield and several impurities which can increase background. Other detection techniques include radioisotopes (57-58), Raman spectroscopy (59), mass spectrometry (60-64), conductivity (65-72), amperometry (73-88), thermoptical (89-91) and chemiluminescence (92-115).

Chemiluminescence (CL) detection is based on the reaction of the analyte with the CL reagent to produce light in the detection cell. Many post-column CL reactors have been successfully interfaced with CE capillaries. The coaxial CL flow cell is popular for CE detection in which the separation capillary is inserted into a reaction capillary held in position by a TEE connector (93). Since the CL signal is transient, mixing should take place in front of the collection optics. In a flow system like CE, the ideal CL-CE reactor should have no turbulence, and diffusion should be the dominant mixing mechanism. This requires the matching of the flow rate between the separation buffer and the CL reagents. If the CL reagent flow rate is too high, sample zone can be swept from the flow cell before the reaction is complete; if the flow rate is too low, band broadening will occur due to a long residence time in the flow cell (93). A sheath flow cell allows the CL reagents to carry the sample zone toward the detection window undisturbed, minimizing the turbulent flow which often occurs in conventional cross mixing.

Hara and colleagues reported the first peroxyoxalate CL reaction detection for CE (92, 94-97). However, the stability of peroxyoxalate CL reagents can be affected by the high electric field in CE. The low solubility and instability of oxalate derivatives in aqueous solution are another problem. The use of an organic solvent as the CE buffer affects the migration behavior of the analytes. Wu and Huie (98) overcame the problem of incompatibility between mixed aqueous-organic solvents and electrically driven separations by switching off the CE power supply at an appropriate time and connecting the CE capillary to a syringe pump to effect dynamic elution.

Ruberto and Grayeski (99-100) reported the acridinium CL reaction for CE detection using a post-column CL reactor. A detection limit of 650 attomoles of acridinium ester was reported. Separation produced ~ 4,000 theoretical plates.

In 1992, Dadoo and coworkers (101) reported a detection limit of 3 x 10^{-9} M for luminol and 7 x 10^{-9} M for N-(4-aminobutyl)-N-ethylisoluminol using the luminol CL reaction for CE detection with a coaxial CL reactor. The detection limits are about two or three orders of magnitude lower than UV detection. In this work, parabolic mirror was used to reflect the light generated from the CL reaction onto the PMT for high collection efficiency. Due to the turbulent mixing of the analyte with the CL reagent, separation efficiency was very poor (< 20,000 theoretical plate number). To simplify the instrument design, Dadoo and coworkers also developed an end-column CL detector in which the signal is generated at the capillary outlet (102). In this new design, the outlet end of the separation capillary is immersed into the buffer reservoir containing the CL reagent. The eluted analytes react with CL reagents in the buffer reservoir to produce light, and then the light is transported through a single fiber to a photomultiplier tube. The new design showed a less effective collection efficiency due to the small solid angle of the fiber optics for light collection. A detection limit of 2 x 10^{-8} M for luminol and 5 x 10^{-9} M for ATP was reported. Zhao and coworkers (103) separated the isoluminol thiocarbamyl derivatives of amino acids using a sheath flow cuvette and were able to improve the separation efficiency up to ~ 100,000 plate number although the complete separation of twenty isoluminol derivatized amino acids was not accomplished.

Huang and coworkers (104-106) applied the catalytic effect to detect transition metal ions in CE by a sample stacking injection. They claimed that mixing luminol in the

separation buffer rather than in the post-column CL reagents could significantly enhance the sensitivity of detection. The separation of metal ions is best preformed in acidic media to avoid hydrolysis in basic media. They claimed an average theoretical plate number of 460,000 for the separation of Co^{2+}, Cu^{2+}, Ni^{2+}, Fe^{3+} and Mn^{2+}, which is much higher than the common theoretical plate number with post-column detection in CE (~ 50,000). A post-column CL detector induces additional zone broadening due to the CL reaction. There are quite a few things that need to be questioned in their most recent article (106). For example, the workers were able to dissolve luminol to 1 mM in a buffer of pH 4.54. The same experiment was repeated here, but the solubility of luminol in the identical buffer was found to be less than 0.3 mM. Based on the electropherogram given in this paper (106), we calculated the theoretical plate number for each metal ion. Results indicate that the theoretical plate number is ~ 34,596 for Co^{2+}, 21,232 for Cu^{2+}, 213,444 for Ni^{2+}, and 150,544 for Fe^{3+} respectively. The average theoretical plate number is 104,954, much lower than the average theoretical plate number claimed. Huang and coworkers (106) also claimed the detection limits of 5.0×10^{-13} M for Co^{2+}, 1.0×10^{-10} M for Cu^{2+}, 5.0×10^{-9} M for Ni^{2+}, 5.0×10^{-8} M for Fe^{3+}, and 8.0×10^{-6} M for Mn^{2+}.

Indirect CL detection has also been used for the detection of species that produces interference or suppression to a CL reaction where the analytes are detected as an inverted peak. Liao and colleagues (110-111) applied indirect CL detection for five amino acids using a Cu^{2+}-catalyzed CL system. The formation of a Cu^{2+}-amino acid complex reduced the catalytic activity of Cu(II) considerably, producing a negative peak. Indirect CL detection can be applied to more species although it is less sensitive than direct CL detection.

Several reviews have also covered the use of chemiluminescence as a method of detection (116-120). The previously described CE systems with CL detection are bulky and complicated. Campana and coworkers, (117) who presented the most recent review on the application of chemiluminescence to capillary electrophoresis in 1997 suggested, "Future advances should focus on developing new detectors that are instrumentally simpler than current ones". Chapter 2 describes the construction of the miniaturized chemiluminescence detector. The CL detector is mounted on the side of a high voltage Plexiglas box so that the whole system is a single unit, unlike those used in previous work in which the CL detector is separated from the CE system. Chapter 3 describes the characterization of the miniaturized CE-CL detector. The major problem is previous work in which the CL detector is separated from the CE system. Chapter 3 describes the characterization of the miniaturized CE-CL detector. The major problem is the strong adsorption of metal ions to the surface of the fused silica capillary. Chapter 4 describes the construction of an automatic sample injection system for CE. This new injection system is characterized in chapter 5. Chapter 6 summarizes briefly two parts of the work (chemiluminescence detection and the automatic sample injection system for CE) and draws some important conclusions. Chapter 7 describes the future work for CL detection for CE and the automatic sample injection system in which I suggest the adoption of a linear motion control system for more precise sample injection.

List of References

1. Ingle, J. D. Jr. and Crouch, S. R., *Spectrochemical Analysis*, Prentice Hall, Englewood Cliffs, New Jersey, **1988**, p 479-485.
2. Birks, John W, *Chemiluminescence and Photochemical Reaction Detection in Chromatography*, VCH Publishers Inc., **1989**, p99.
3. Nieman, T. A., *Luminescence Techniques in Chemical and Biological Analysis, Practical Spectroscopy Series, Vol. 12*, Marcel Dekker, New York, 1991, pp523.
4. Burr, John G, *Chemiluminescence and Bioluminescence*, Marcel Dekker Inc., New York, **1985**, p 470.
5. Seitz, W. R., *CRC Crit. Rev. Anal. Chem.*, **1981**, *13*, 1-58.
6. Seitz, W. R. and Neary, M. P., *Contemp. Topics Anal. Clin. Chem.*, **1977**, *1*, 49-125.
7. Isacsson, U. and Wettermark, G., *Anal. Chim., Acta.*, **1974**, *68*, 339-362.
8. Seitz, W. R., and Hercules, D. M, *Chemiluminescence and Bioluminescence*, Plenum, New York, **1973**, p427-449.
9. Babko, A. K and Lukovskaya, N. M. *Zh. Anal. Khim.*, **1962**, *17*, 50.
10. Babko, A. K. and Lukovskaya , N. M. *Zavod. Lab.*, **1963**, *29*, 404.
11. Babko, A. K. and Dubovenko, L. I. *Zh. Anal. Khim.*, **1964**, *200*, 428.
12. Babko, A. K. and Kalinichenko, I. E. *Ukr. Khim. Zh.*, **1965**, *31*, 1316.
13. Seitz, W. R.; Suydam W. W.; Hercules, D. M. *Anal. Chem.*, **1972**, *44*, 957-963.
14. Seitz, W. R., and Hercules, D. M., *Anal. Chem.*, **1972**, *44*, 2143-2149.
15. Neary, M. P., Seitz, W. R., and Hercules, D. M., *Analytical Letters*, **1974**, **7**, 583-590.

16. Delumyea, R. and Hartkopf, A. V., *Anal. Chem.*, **1976**, *48*, 1402-1405

17. Tiselius, A. *Trans. Faraday Soc.*, **1937**, *33*, 524.

18. Hjerten, S. *Chromatogr. Rev.*, **1967**, *9*, 122-219.

19. Virtanen, R. *Acta Polytech. Scand*, **1974**, *123*, 1.

20. Mikkers, F. E. P.; Everaerts, F. M.; Verheggan, Th. P. E. M. *J. Chromatogr.*, **1979**, *169*, 11.

21. Mikkers, F. E. P.; Everaerts, F. M.; Verheggen, Th. P. E. M. *J. Chromatogr.*, **1979**, *169*, 1.

22. Jorgenson, J. W.; Lukacs, K. D. *Anal. Chem.*, **1981**, *53*, 1298.

23. Kuhr, W. G., *Anal. Chem.*, **1990**, *62*, 403R-414R.

24. Kuhr, W. G.; Monnig, C. A. *Anal. Chem.*, **1992**, *64*, 389R-407R.

25. Clarie, R. L. S., *Anal. Chem.*, **1996**, 68, 569-586R

26. Beale, Stephen C., *Anal. Chem.*, **1998**, *70*, 279R-300R.

27. Li, S.F.Y. *Capillary Electrophoresis-Principles, Practice and Applications; Journal of Chromatography Library, Vol. 52;* Elsevier: Amsterdam, 1992; pp31-53.

28. Lukacs, K. D.; Jorgenson, J. W.; *J. High Res. Chromatogr. Commun.*, **1985**, *8*, 407.

29. Huang, X.; Gordon, M. J.; Zare, R. N. *Anal. Chem.* **1988**, *60*, 375-377.

30. Rose, D. J.; Jorgenson, J. W. *Anal. Chem.*, **1988**, *60*, 642.

31. Deml, M.; Foret, F.; Bocek, P. *J. Chromatogr.* **1985**, *320*, 159.

32 Tsuda, T.; Mizuno, T.; Akiyama, J. *Anal. Chem.* **1987**, *59*, 799.

33 Wallingford, R. A.; Ewing, A. G. *Anal. Chem.* **1988**, *60*, 1972.

34. Wallingford, R. A.; Ewing, A. G. *Anal. Chem.* **1987**, *59*, 678.

35. Dasgupta, P. K.; Surowiec, Kazimierz. *Anal. Chem.* **1996**, *68*, 4291-4299.

36. Linhares, M. C.; Kissenger, P. T. *Anal. Chem.* **1991**, *63*, 2076-2078.

37. Goodall, D. M.; Lloyd, D. K.; Williams, S. J. *LC-GC* **1990**, *8*, 788-799.

38. Novotony, M. V.; Kobb, K. A.; Liu, J. *J. Electrophoresis*, **1990**, *11*, 735-749.

39. Heiger, D. N., *"High Performance Capillary Electrophoresis", an introduction.* Hewlett Packard, Waldbronn, Germany, 1992, p.101

40. Chervet, J. P.; Van-Soest, R. E. J.; Ursem, M. *J liq. Chromatogr.* **1991**, *543*, 439.

41. Moring, S. E.; Reel, R. T.; Van-Soest, R. E. J., *Anal. Chem.* **1993**, *65*, 3454.

42. Tsuda, T; Sweedler, R. N.; Zare, R. N. *Anal. Chem.* **1990**, *62*, 2149.

43 Wang, T.; Hartwick, A. *Anal. Chem.* **1992**, *64*, 1745.

44. Wang, T.; Aiken, J. H. Huie, C. W.; Hartwick, R. A. *Anal. Chem.* **1991**, *63*, 1372.32.

45. Djordjevic, N. M.; Widder, M.; Widder, M.; Kuhn, R. *J. High Resolut. Chromatogr.* **1997**, *20*, 189-192.

46. Delonge, T.; Fouckhardt, H. J. *J. Chromatogr., A* **1995**, *716*, 135-139.

47. Djordjevic, N. M.; Ryan, K. *J. liq. Chromatogr. Relat. Technol.* **1996**, *19*, 201-206.

48. Chen, D. Y.; Dovichi, N. J. *J. Chromatogr., B: Biomed. Appl. Chem.* **1994**, 657, 265-9.

49. Chen, D. Y.; Adelhelm, K.; Cheng, X. L.; Dovichi, N. J. *Analyst* **1994**, *119*, 349-352.

50 Chen, F.-T. A.; Evangelista, R. A. *Anal. Biochem.* **1995**, *230*, 273-280.

51 Lada, M. W.; Kennedy, R. T. *Anal. Chem.* **1996**, *68*, 2790-2797.

52. Engstroem, A.; Anderson, P. E.; Josefsson, B.; Pfeffer, W. D. *Anal. Chem.* **1995,** *67*, 3018-3-22.

53 Chen, P.; Novotny, M. V. *Anal. Chem.* **1997**, *69*, 2806-2811.

54 Beijersten, I.; Westerlund, D. *J. Chromatogr., A* **1995**, *716*, 389-399.

55 Orwar, O.; Fishman, H. A.; Ziv, N. E.; Scheller, R. H.; Zare, R. N. *Anal. Chem.* **1995**, *67*, 4261-4268.

56 Wang, P.; Giese, R. W. *Anal. Biochem.* **1995**, *230*, 329-332.

57. Tracht, S. E.; Cruz, L.; Stobba-Wiley: C. M.; Sweedler, J. V. *Anal. Chem.* **1996**, *68,* 3922-3927.

58. Klunder, G. L.; Andrews, J. E., Jr.; Grant, P. M.; Anderson, B. D.; Russo, R. E. *Anal. Chem.* **1997**, *69*, 2988-2993.

59. Walker, P. A., III.; Kowalchyk, W. K.; Morris, M. D. Anal. Chem. 1995, 67, 4255-4260.

60. Ramsey, R. S.; Mcluckey, S. A. *J. Microcolumn Sep.* **1995**, *7*, 461-469.

61. Mazereeuw, M.; Hofte, A. J. P.; Tjaden, U. R.; van der Greef, *J. Rapid Commun. Mass Spectrom.* **1997**, *11*, 981-986.

62. Cao, P.; Moini, M. *J. Am. Soc. Mass Spectrom.* **1997**, *8*, 561-564.

63. Severs, J. C.; Smith, R. D. *Anal. Chem.* **1997**, *69*, 2154-2158.

64. Lamoree, M. H.; Tjaden, U. R.; van der greef, J. *J. Chromatogr., A* **1997**, *777*, 31-39.

65. Huang, X.; Pang, T-K J; Gordon, M. J.; Zare, R.. N. *Anal. Chem.* **1987**, *59*, 2747.

66. Huang, X.; Luckey, J. A.; Gordon, M. J.; Zare, R. N. *Anal. Chem.* **1989**, *61*, 766.

67. Huang, X. H.; Zare, R. N. *Anal. Chem.* **1991**, *63*, 2193-2196.

68. Zemann, A. J.; Schnell, Erhard; Volgger, Dietmar; bonn, G. K. Anal. Chem. **1998**, *70*, 563-567.

69. Mayrhofer, K.; Zemann, A. J.; Schnell, Erhard; Bonn, G. K. Anal. Chem. **1999**, *71*, 3828 – 3833.

70. Mueller, D.; Jelinek, I.; Opekar, F.; Stulik, K.; Electrophoresis **1996**, *8*, 722-725.

71. Harrold, M.; Stillan, J.; Bao, L.; Rocklin, R.; Avdalovic, N. J. *Chromatogr., A* **1995**, *717*, 371-383.

72. Haber, C.; Jone, W. R.; Soglia, J.; Surve, M. A.; McGlynn, M.; Caplan, A.; Reineck, J. R.; Krstanovic, C. J. *Capillary Electrophor.* **1996**, *3*, 1-11.

73. Weber, P. L.; Lunte, S. M. *Electrophoresis* **1996**, *17*, 302-309.

74. Wen, J.; Cassidy, R. M.; *Anal. Chem.* **1996**, *68*, 1047-1053.

75. He, P.; Ye, J.; Fang, Y.; Suzuki, I.; Osa, T. *Anal. Chim. Acta* **1997**, *337*, 217-223.

76. Swanek, F. D.; Chen, G.; Ewing, A. G. *Anal. Chem.* **1996**, *68*, 3912-3916.

77. Lin, H.; Xu, D.-K.; Chen, H.-Y. *J. Chromatogr., A* **1997**, *760*, 227-233.

78. Liu, J.; Zhou, W.; You, T.; Li, F.; Wang, E.; Dong, S. *Anal. Chem.* **1996**, *68*, 3350-3353.

79. Jin, W.; Weng, Q.; Wu, J. *Anal. Chim. Acta* **1997**, *342*, 67-74.

80. You, T.; Wu, M.; Wang, E. Anal Lett. **1997**, 30, 1025-1036.

81. Jin, W.; Weng, Q.; Wu, J. Anal. Lett. **1997**, *30*, 753-769.

82. Hu, S.; Wang, Z.-L.; Li, P.-B.; Cheng, J.-K. *Anal. Chem.* **1997**, *69*, 264-267.

83. Matysik, F.-M. *J. Chromatogr., A* **1996**, *742*, 229-234.

84. Park, S.; Lunte, C. E. *Anal. Chem.* **1995**, *67*, 4366-4370.

85. Zhong, M.; Zhou, J.; Lunte, S. M.; Zhao, G.; Giolando, D. M.; Kirchholl, J. R. *Anal. Chem.* **1996**, *68*, 203-207.

86. Voegel, P. D.; Zhou, W.; Baldwin, R. P. *Anal. Chem.* **1997**, *69*, 951-957.

87. Fermier, A. M.; Gostkowski, M. L.; Colon, L. A. *Anal. Chem.* **1996**, *68*, 1661-1664.

88. Zhong, M.; Lunte, S. M. *Anal. Chem.* **1996**, *68*, 2488-2493.

89. Waldron, K. C.; Li, J. J. *J. Chromatogr,, B: Biomed. Appl.* **1996**, *683*, 47-54.

90. Seidel, B. S. Steinle, E.; Faubel, W.; Ache, H. J. *Proc. SPIE-int. Soc. Opt. Eng.* **1996**, *2836*, 283-292.

91. Ren, J.; Li, B.; Deng, Y.; Cheng, J. *Talanta* **1995**, *42*, 1891-1895.

92. Hara, T.; Okamura, S.; Kato, J.; Yokogi, J.; Nakajima, R. *Anal. Sci.* **1991**, *7*, 261-264.

93. Rose, D. J. and Jorgenson , J. W. *J. Chromatogr.*, **1988**, *447*, 117.

94. Hara, T.; Kayama, S.; Nashida, H.; Nakajima, R. *Anal. Sci.* **1994**, *10*, 223-25.

95. Hara, T.; Kayama, S.; Nashida, H.; Nakajima, R. *Anal. Sci.* **1994**, *10*, 823-25.

96. Tsukagoshi, K.; Tanaka, A.; Nakajima, R.; Hara, T. *Anal. Sci.* **1996**, *12*, 525-28.

97. Tsukagoshi, K.; Akasaka, H.; Nakajima, R.; Hara, T. *Chem. Lett.* **1996**, 467-468.

98. Wu, N.; huie, C. W. *J. Chromatogr.* **1993**, *634*, 309-15.

99. Ruberto, M. A.; Grayeski, M. L. *Anal. Chem.* **1992**, *64*, 2758-62.

100. Ruberto, Michael A. and Grayeski, M. L. *J. Microcol.* **1994**, *Sep. 6*, 545-550.

101. Dadoo, R.; Colon, L. A.; Zare, R. N. *J. High Resolution Chromatography*, **1992**, *15*, 133.

102. Dadoo, R.; Seto, A. G.; Colon, Luis A.; Zare, R. Z. *Anal. Chem.*, **1994**, *66*, 303.

103. Zhao, J. Y.; Labba, J.; Dovichi, N. J. *J. of Microcolumn Separation*, **1993,** *5*, 331.

104. Huang, b.; Li, J., and Cheng, K., "Highly Sensitive Chemiluminescence Detection for Capillary Ion Analysis". Sepu, 1995, 13, 430.

105. Huang, B.; Li, J. J.; Cheng, J. K. *Chemical Journal of Chinese Universities*, **1996**, *17*, 528-530.

106. Huang, Bo; Li, Jian-jun; Zhang, Le; Cheng, Jie-ke, *Anal Chem.*, **1996**, 68, 2366-2369.

107. Dasgupta, P. K.; Genfa, Z.; Li, J.; Boring, C. B.;Jambunathan, S., and Al-Horr, R., *Anal. Chem.*, **1999**, 71, 1400.

108. Tsukagoshi, K.; Fujimura, S. and Nakajima, R. *Anal. Chem.*, **1997**, 13, 279.

109. Lee, Y.-T, and Whang, C.-W. *J. Chromatogr., A*, **1997**, 771, 379.

110. Liao, S.-Y., and Whang, C.-T., *J. High. Resolut. Chromatogr.*, **1995**, 18, 667.

111. Liao, S.-Y., and Whang, C.- Y., *J. Chromatogr.*, **1996**, 736, 247.

112. Hara, T.; Yokogi, J.; Okamura, S. *J. Chromatography*, 1993, **A652**, 361.

113. Gilman, S. D.; Silverman, C. E.; Ewing, A. G. *J. of Mirocolumn Separation,* **1994**, 6, 97.

114. Hara, T.; Nishida, H.; Kayama, S.; Nakajima, R. *Bull. Chem. SOC. Japan,* **1994**, *67*,1193.

115. Gilman, S. D.; Silverman, C. E.; Ewing, A.G. *J. Microcolumn Separation*, **1994**, *6*, 97.

116. Baeyens, W.R.G.; Ling, B. L.; Imai, K.; Calokerino, A.C.; Schulman, S.G. *J. Microcolumn Separation*, **1994**, *6*, 195.

117. Garcia Campana, Anna M; Baeyens, W. R.G. ; Zhao, Y. N. *Anal. Chem.* **1997**, 83A.

118. Sanders, M. G.; Andrew, K. N., and Worsford, P. J., "Trends in Chemiluminescence Detection for Liquid Separation, *Anal. Commun.*, **1997**, *34*, 13.

119. Baeyens, W. R. G.; Schuman, S. G.; Calokerinos, A. C.; Zhao, Y., Garcia Compana, A. M.; Nakasima, K., and De Keuleleire, D., *J. Pharm. Biomed. Anal.*, **1998**, 17, 941.

120. Soper, S. A.; Warner, I. M., and McGown, L. B., *Anal. Chem.*, **1998**, 70, 477R.

Chapter 2

Construction of a Miniaturized Post-Column Chemiluminescence Detector for Capillary Electrophoresis

Chemiluminescence (CL) has been applied as a sensitive means of detection in capillary electrophoresis (1-23) since the early 90's. As discussed in this chapter, most CE-CL systems use a post-column sheath flow cell for the detection. These CL detectors are usually enclosed in a large, dark box. The box is bulky, heavy, and inconvenient for transportation. It is not convenient for adjustment on the bench-top since the chemiluminescence detector and the CE system are not held together. Furthermore, since only one end of the reaction capillary is held by a TEE connector, the reaction capillary may be tilted slightly to a different angle after another installation, which can affect the solid angle for light collection and cause a variation in detection sensitivity. A large dark-box with many joint edges may increase the chances of room-light leakage which can significantly increase the background noise level.

In this chapter, some major design considerations are listed for chemiluminescence detection in CE. The source of noise and factors affecting collection efficiency are also discussed. Finally, the collection efficiency of the miniaturized CL detector is calculated based on the solid angle from the light source, the chemiluminescence reactor (24). Our goal was to construct a miniaturized CE-CL system with low noise, but high collection efficiency.

2.1 Design Considerations for Chemiluminescence (CL) Detector

The design considerations for the CL detector are listed in figure 2.1.

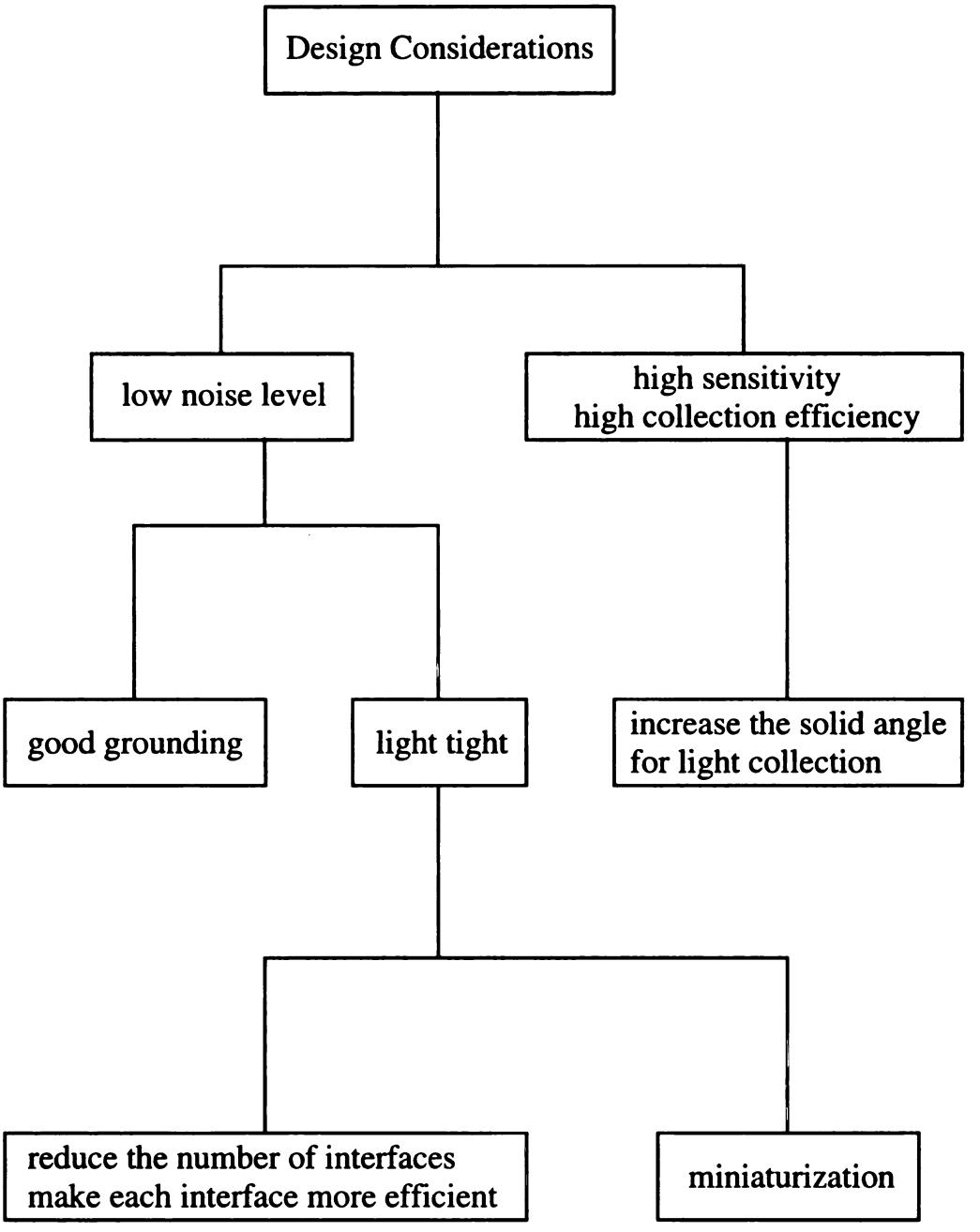

Figure 2.1 Design considerations for chemiluminescence detector

2.2 Construction of the Miniaturized CE-CL Detector

2.2.1 Outer Body of the CL Detector

The detector shown in figure 2.2a & b consists of three parts. The left part in figure 2.2a is used to hold the body to the CE high voltage box. It also allows for visual inspection of the capillary. The central part was used to fix the separation and reaction capillaries. The right part was used to mount the photomultiplier tube. The hole on the right part is carefully machined to fit the PMT power supply socket; a good fit efficiently blocks room light. Since the PMT casing diameter is bigger than this hole, the PMT casing further block the room light. A ½"-20 hole is drilled on the central part to allow the mounting of a front-coated mirror which serves to reflect the light back to the PMT tube for enhancement of collection efficiency.

2.2.2 Etching of the Separation Capillary

A Bunsen burner is used to burn off the polyimide coating about 5 cm from the tips of twenty 50 μm i.d. x 363 μm o.d. x 51 cm or 50 μm i.d. x 363 μm o.d. x 41 cm long fused-silica capillaries (Polymicro Technologies, Inc., product number TSP050375). The tips were dipped into the liquid wax of a burning candle for sealing. This coating-removed segment of the capillary was then carefully immersed into a 49 % HF solution inside a fumehood for 72 minutes exactly; the etching rate is ≈ 2.86 μm / min. The rate of etching was found to be constant during the etching process. The residual HF from the etched portion was rinsed off with distilled water. The outside diameter of the etched segment was 116.8 μm, measured by a micrometer. The capillary tip was trimmed with a capillary cutter so that the overall length of capillary is 40 cm or 50 cm.

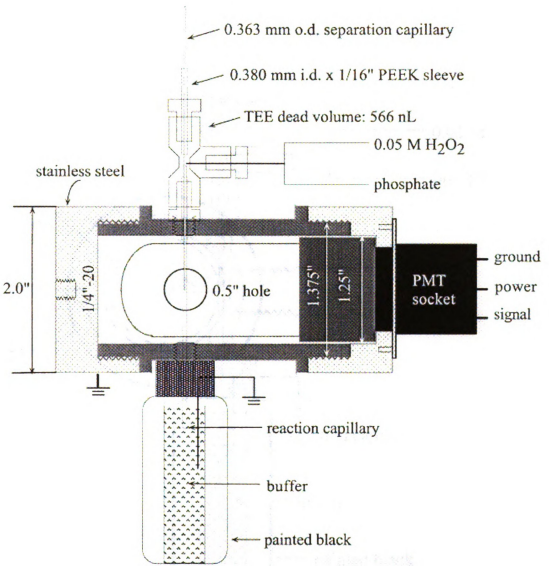

Figure 2.2a Front view: miniaturized post-column chemiluminescence detector in capillary electrophoresis

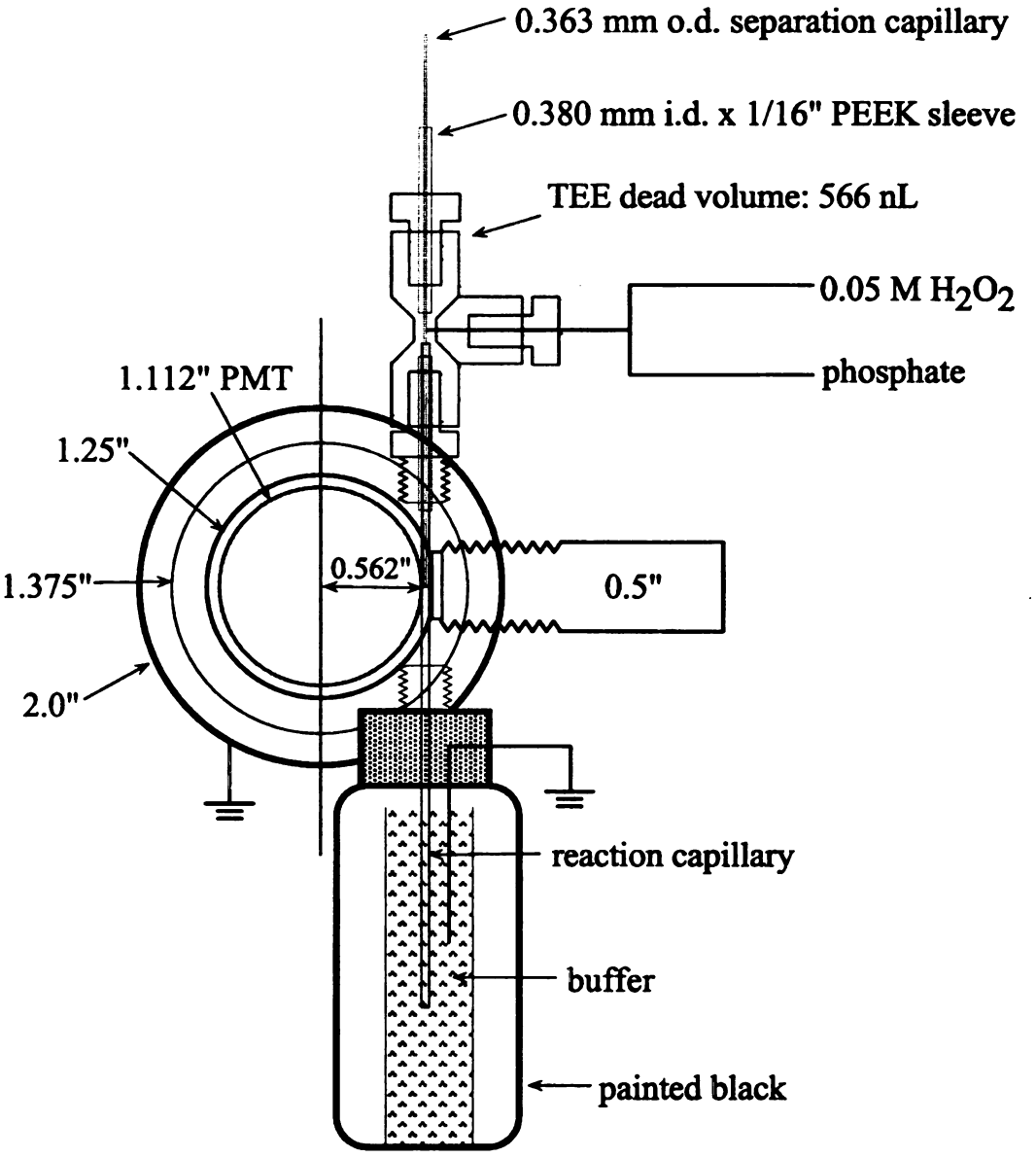

Figure 2.2b Side view: miniaturized post-column chemiluminescence detector in capillary electrophoresis

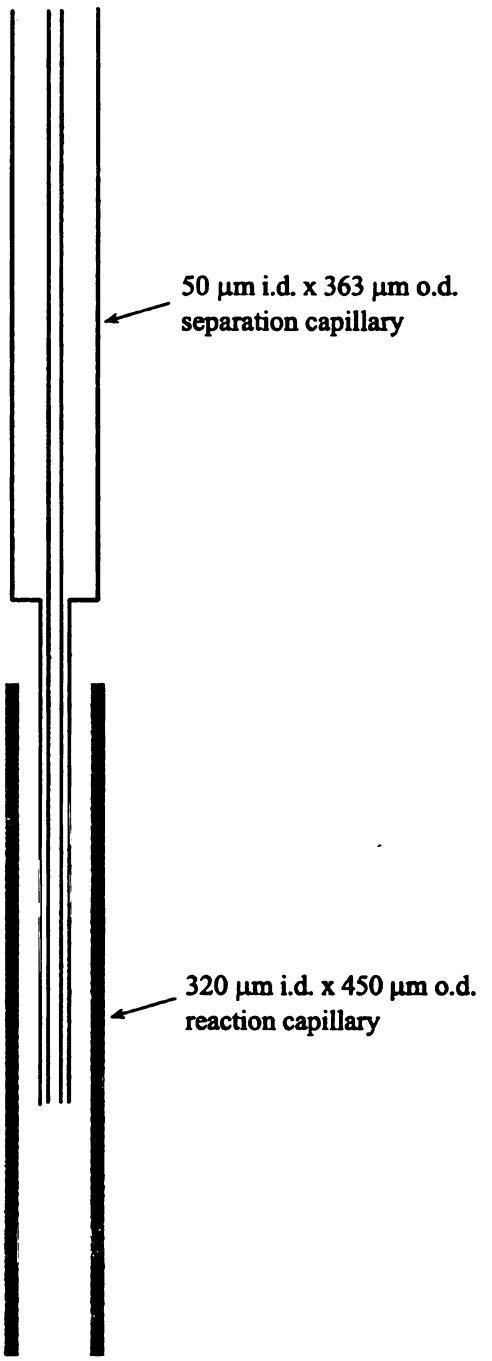

Figure 2.2c Detailed view of the flow cell in miniaturized CL detector in CE

2.2.3 Reaction Capillary

A 320 μm i.d. x 435 μm o.d. x 8 cm (Polymicro Technologies, Inc., product number TSP320450) capillary was chosen as the reaction capillary to fit with the etched segment of the separation capillary. A Bunsen burner was used to burn off the polyimide coating about 3 cm from one end for a length of 2 cm to make a window for CL detection.

2.2.4. Installation of the Miniaturized Chemiluminescence Detector

2.2.4.1 Installation of Chemiluminescence Flow Cell

A ferrule (Upchurch Scientific, product number F142) was pushed onto the cavity of a screw (Upchurch Scientific, product number F300). A 500 μm i.d. x 1/16" o.d. PEEK sleeve (Upchurch Scienticfic, product number F230) was then pushed through the ferrule and tightened against a TEE connector (Upchurch Scientific, product number F727) to be locked. The screw was set loosely on the TEE connector. The unetched end of the separation capillary was inserted through the PEEK sleeve into the TEE connector. The capillary was then pulled carefully until the beginning of the etched segment could be seen from the side-arm of the TEE connector. A screw with ferrule-locked PEEK sleeve was then inserted into the separation capillary and fastened onto the TEE connector to hold the separation capillary in place. The next part turned out to be the most challenging work for the overall installation process. Extreme care was required to insert the reaction capillary into the etched segment of the separation capillary through the PEEK sleeve. Finally the reaction capillary was tightened to the TEE connector.

2.2.4.2 Installation of CL Flow Cell to CL Outer Body

The PMT was mounted onto the right part in figure 2.2a. The right part is then mounted to the central part in figure 2.2a. The interface of the CL flow cell described in section 2.2.4.1 to the CL outer body is tricky. First, the outer body must be laid on a bench-top, without using a hand to hold it since it can be broken easily. Secondly, the

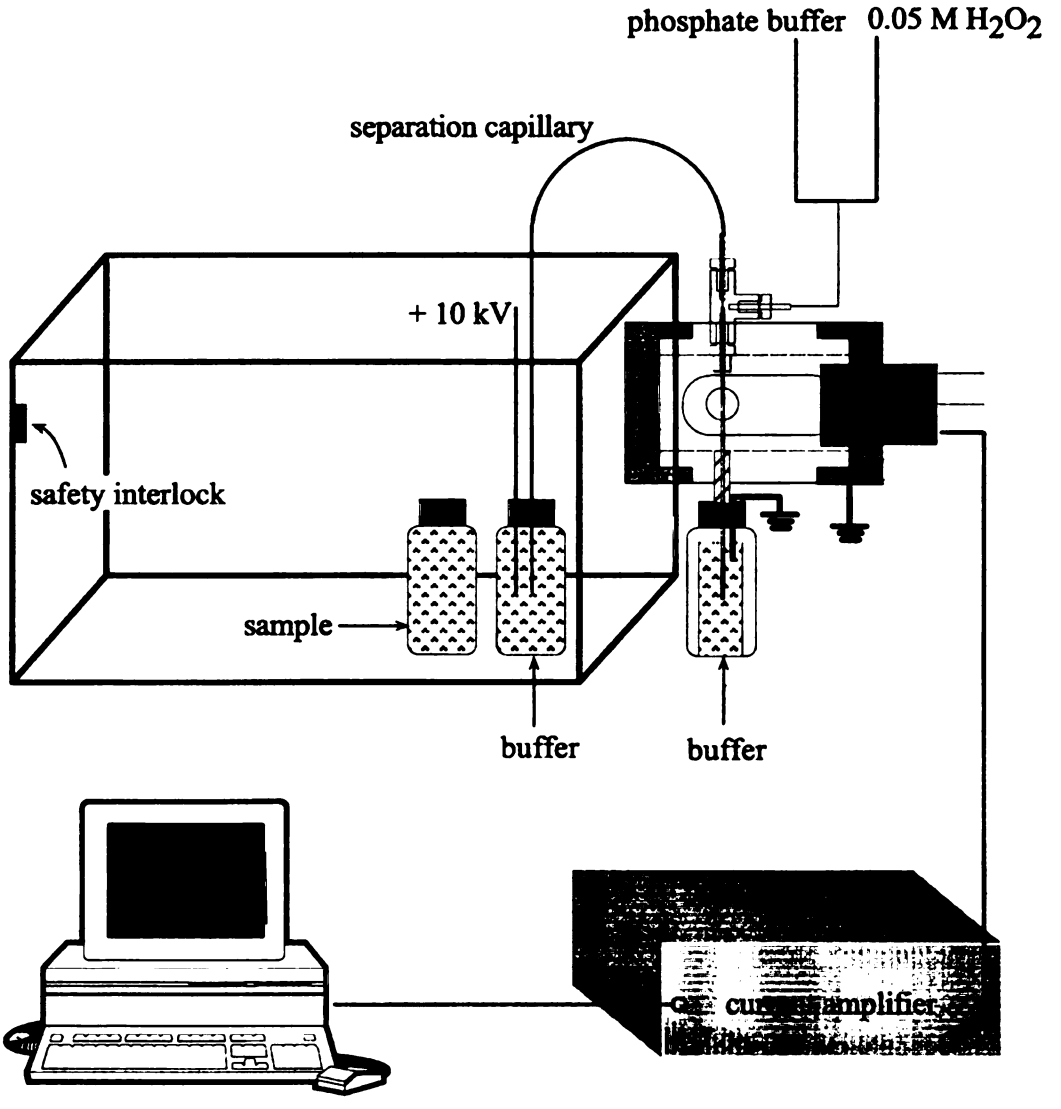

Figure 2.3 Instrumental set-up for the miniaturized post-column CE-CL detection

reaction capillary was inserted through the two ¼" holes on the top and bottom of the outer body carefully. Then the cap for the ground buffer reservoir was inserted into the reaction capillary and tightened to the outer body. The front-coated mirror was mounted to the ½"-20 hole on the outer body until it just touched the reaction capillary. Finally, the left part in figure 2.2a was mounted onto the rest of the outer body, and the whole installation process was complete after it is screwed onto the high voltage box. For an experienced person, this process takes about 20 minutes.

2.3 Instrumentation for Chemiluminescence Detection in Capillary Electrophoresis

The instrumental set-up for the miniaturized post-column CE-CL detector is shown in figure 2.3. The output cord of the high voltage power supply (Bertan Associates, Inc., Syosset, New York, U.S.A., Model 205 A-10P) was inserted through the top of the Plexiglas into the buffer reservoir. The power supply was set at 10 kV for all the electrokinetic injections and separations. The light generated in the chemiluminescence reaction was detected by a PMT (Hamamatsu, 1P28A), powered by a High Voltage Power Supply (Heath model EU-42A, Benton Harbor, MI) at 800 V at all times. Photocurrent from the PMT is amplified by a current amplifier (model 427A, Keithley Instruments Inc., Cleveland, Ohio). The response time of the amplifier was set to 3 ms at an amplification of 10^8 V/A for all the electrophoretic operations. Finally, the amplifier output was recorded by a microcomputer (33MHz, 486, Gateway, Inc., North Sioux, SD 57049) through a data acquisition board (National Instruments, Austin, TX) at a sampling rate of 1000 points/s.

The instrumentation for CL detection is very simple, just a sample cell, PMT, and data acquisition system. Since there is no light source required, a wavelength selection device is not necessary. The CL signal is often very weak, so efficient light collection is critical. The sample cell is placed as close to the detector as possible. A front-coated plane mirror is glued on the ½"-20 threaded rod and then carefully adjusted into the reaction capillary until a soft touch is felt. The front-coated mirror reflects light more efficiently than a back-coated mirror in this application.

2.4 Electrical Noise

The sources of noise were not clearly understood early in this research. Our second version of the CL detector was made of black Delrin (26), which picks up a significant amount of electrical noise associated with the power lines due to the poor shielding (see figure 2.4). To study the source of this noise, an oscilloscope was used to monitor the output from the current amplifier. Surprisingly, there was a large AC noise of ~ 60 Hz. The p-p amplitude of this AC noise was about 0.66 V, making it the dominant source of noise in the CL detection. However, if the black Delrin body was covered with grounded aluminum foil, this power line noise was eliminated. We postulated that the PMT tube and housing is not only a good detector for light, but also a good antenna for receiving all sorts of electrical interference. A poorly grounded CL detector body can pick up a significant amount of electrical noise associated with the power lines. A stainless steel body was used for the final version of the CL detector. The ground buffer reservoir was glued with metal tape to remove the electrical interference as well. This modification to the early CE-CL detector turned out to be efficient in shielding the ubiquitous AC

electrical interference from the power lines. A BNC coaxial cable was used to isolate the electrical noise during the signal transport.

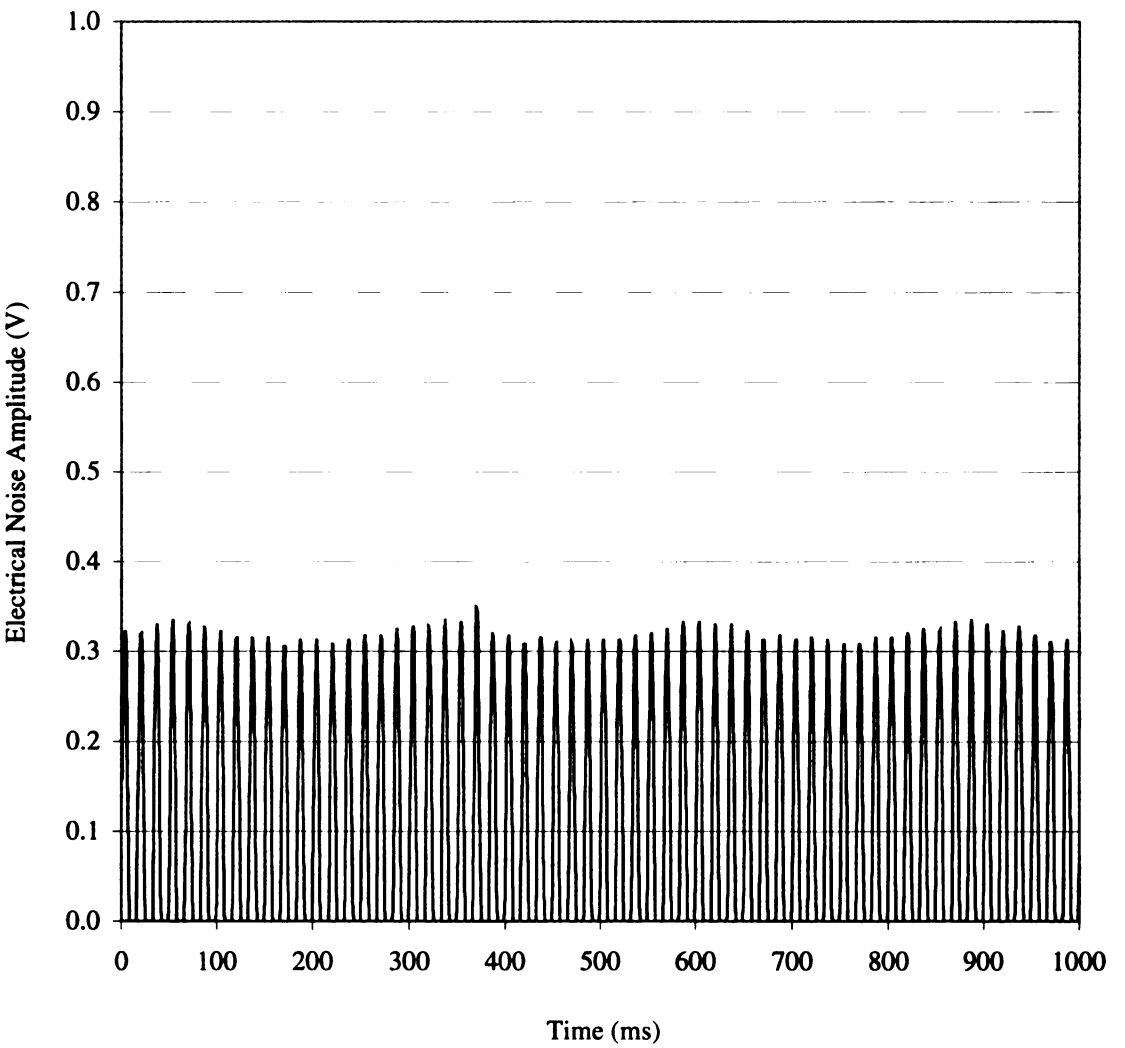

Figure 2.4 Electrical noise of the miniaturized chemiluminescence detector made of black Delrin without proper grounding. PMT power supply voltage: 800V; amplifier: 10^8 V/A; sampling rate: 1000 points/s.

2.5 Noise Level of the Miniaturized CL Detector and the Conventional CL Detector

The leakage of room light into the CL detector increases the noise level dramatically, but can be reduced by minimizing the number of joint interfaces while making each interface more light-tight. In the first version of the CL detector (25), we enclosed the PMT in a large dark box (10" x 10" x 18"), which showed a serious leakage of room light through the front door. We then explored the construction of the miniaturized chemiluminescence detector using black Delrin (26) and stainless steel (27) as materials for the outer casing.

The miniaturized CL detector solved many problems of the traditional chemiluminescence detector. The noise levels between the miniaturized and the traditional CL detector are compared in figure 2.5. The miniaturized CL detector reduced the average noise level by a factor of 20 compared to the traditional dark-box CL detector. The p-p amplitude of the miniaturized CL detector is also much lower than that of the traditional CL detector. The lower trace in figure 2.5 is the noise of the miniaturized CL detector (average noise level is 0.0044 V). The upper trace is the noise of the conventional CL detector (average noise level is 0.0885 V). Clearly, the miniaturized CL detector is considerably more light tight than the conventional CL detector. I believe the major source of light leakage in the conventional detector is from the door. In the miniaturized CL detector, the "door" does not exist. The only possibility of light leakage is through the separation capillary; experimental results show little difference of background signal when there is light or no light in the room.

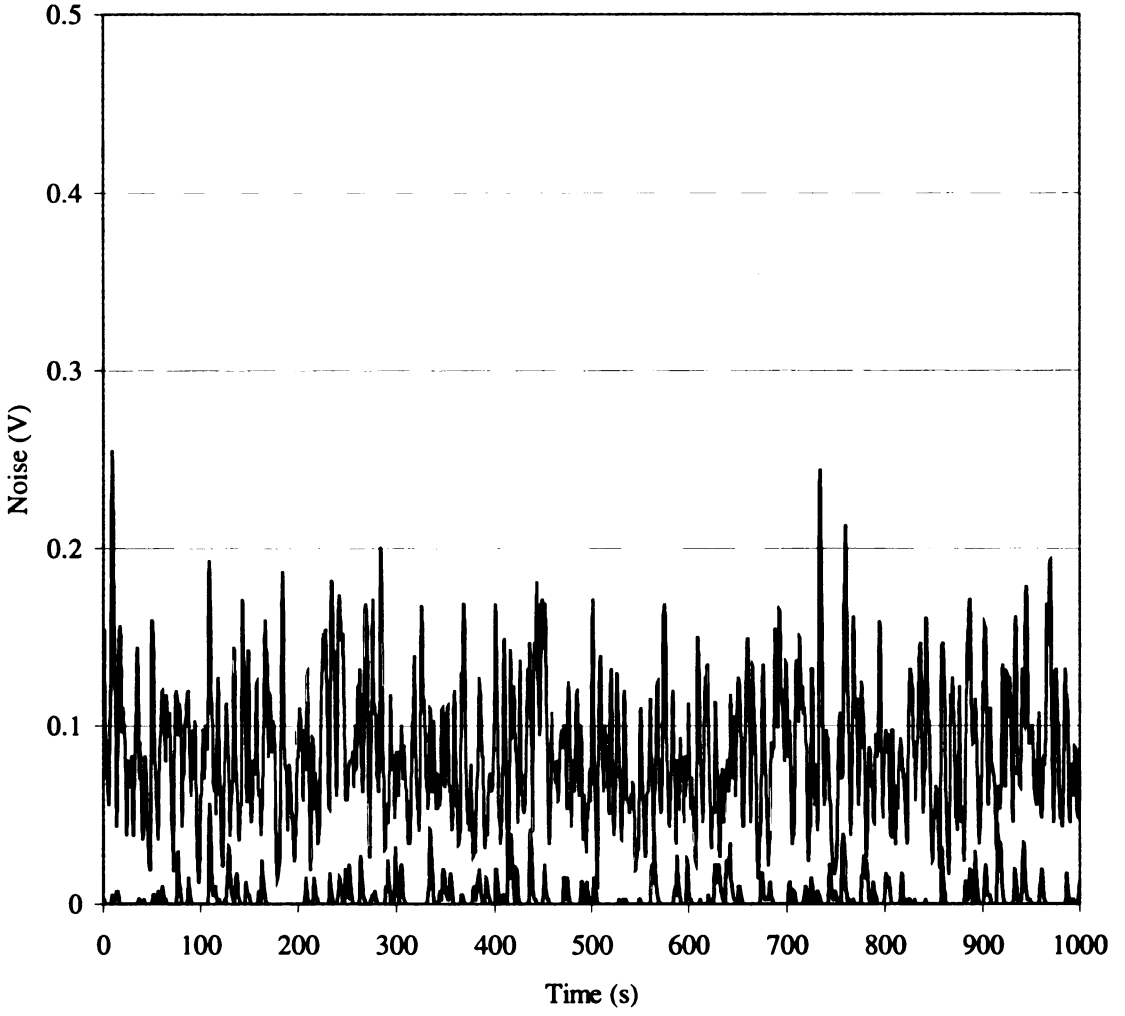

Figure 2.5 Comparison of noise level between the miniaturized CL (lower trace) and conventional CL detector (upper trace) in capillary electrophoresis. PMT power supply: 800 V; amplifier: 10^8 V/A; sampling rate: 1000 points/s.

2.6 Factors Affecting the Collection Efficiency

Our second version of CL detector was made of black Delrin. With this material, the interior wall can absorb some of the chemiluminescence emission. Ideally, all the light generated from the chemiluminescence reaction should go to the PMT and the rest should be reflected back to the PMT for higher collection efficiency. To improve the reflection of light, we replaced the black Delrin with machined stainless steel. The latter material, when grounded properly, is very efficient in shielding against electrical interference from nearby sources.

The high collection efficiency can be achieved by increasing the solid angle for light collection. Collection efficiency, in terms of solid angle, is defined as the amount of light reaching the optical element (28):

$$\Omega = \frac{A}{S^2} \tag{2.1}$$

Here A is the effective or limiting area of the optical element as determined either by the element itself or by an aperture stop, and S is its distance from the source. In the present CL detector, A is the sensing area of the photocathode, and S is its distance from the tip of the separation capillary. Equation 2.1 indicates that the solid angle can be increased by placing a lens of high numerical aperture between the PMT and the reaction capillary or by reducing the distance from the PMT to the reaction capillary. However, there is little space inside the miniaturized CL detector for inserting a lens. On the other hand, the lens needs a support, making the internal configuration of the CL detector more sophisticated. It is better to place the reaction capillary close to the PMT. With the above-mentioned concepts, a miniaturized CL detector was constructed as shown in figure 2.2a and figure 2.2b.

2.7 Collection Efficiency of the Miniaturized CL Detector

When the sample zone exits the separation capillary, the chemiluminescence reaction starts immediately. The emitted light is collected by the PMT in the miniaturized CL detector. It is assumed that the sample zone (~ 2 mm long) is a point source. A screen in front of the photocathode is internally built to scatter light and enhance its collection. Light reaching the screen is reflected to the photocathode. By calculating the solid angle of the sample zone to the screen, the collection efficiency of the miniaturized CL detector can be calculated. Figure 2.6 is the schematic diagram of the inner configuration of the CL detector. The screen surface is divided into four equal parts as labeled in figure 2.6. Area A is further divided into two parts, area A_I and area A_{II}. Ω_I and Ω_{II} denote the solid angles of area A_I and area A_{II} respectively. Since the solid angle of the four equal parts is identical, the overall solid angle, Ω, spanned by the rectangular stray screen can be calculated as

$$\Omega = 4(\Omega_I + \Omega_{II}) \tag{2.2}$$

Ω_I can be represented as a two dimensional integral over the surface area of A_I:

$$\begin{aligned} \Omega_I &= \iint_{AI} d\Omega = \iint_{AI} \sin\theta \quad d\theta\, d\phi \\ &= \int_0^{\phi_0} d\phi \quad \int_0^{\theta_I} \sin\theta \quad d\theta \\ &= \int_0^{\phi_0} d\phi \quad [1-\cos\theta_I] \end{aligned} \tag{2.3}$$

Here the upper limit ϕ_0 of the ϕ integration and the upper limit θ_I of the θ integration are defined in figure 2.6. The solid angle Ω_{II} can be calculated in the same way.

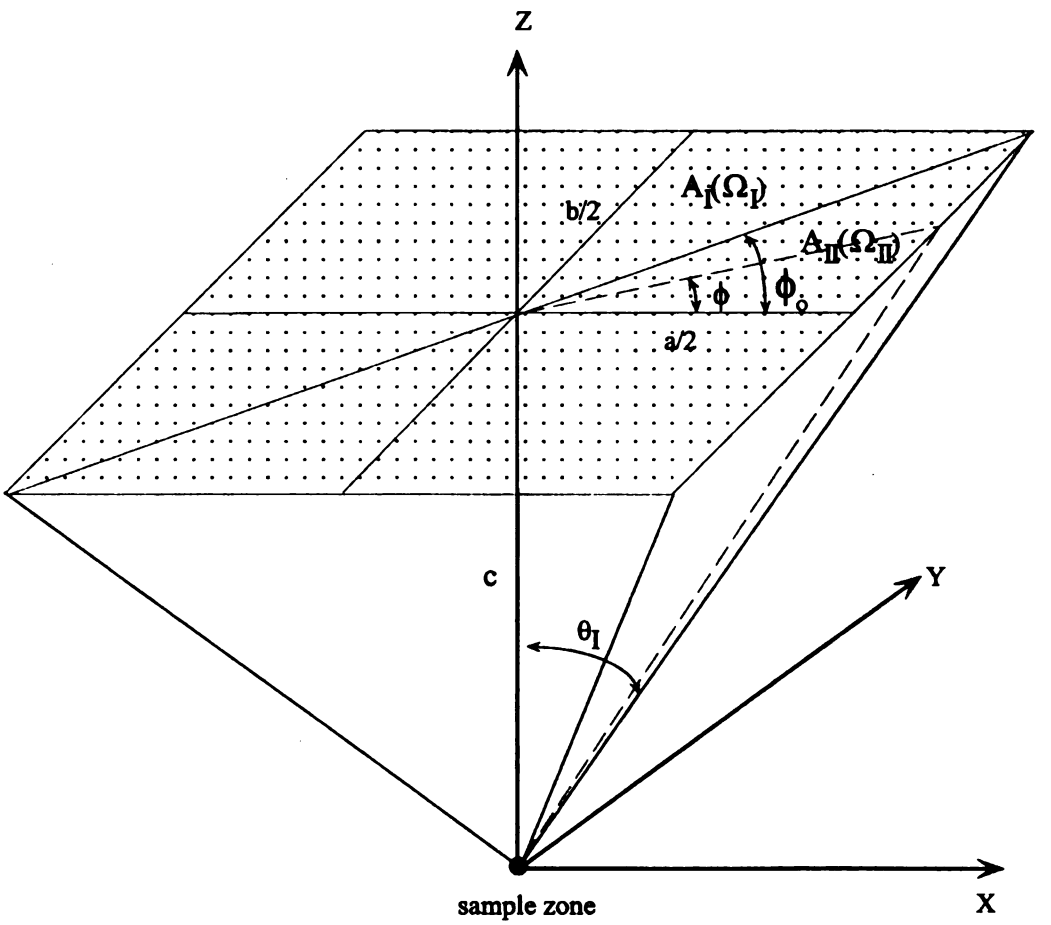

Figure 2.6 Three dimensional diagram for the calculation of solid angle
a is the length of PMT window, 25 mm; b is the width of the PMT window, 12 mm. c is the distance from stray screen to the reaction capillary, 4 mm.

$$\Omega_{II} = \iint_{II} d\Omega = \iint_{II} \sin\theta \, d\theta \, d\phi$$

$$= \int_{\phi_0}^{\frac{\pi}{2}} d\phi \int_{0}^{\theta_{II}} \sin\theta \, d\theta \qquad (2.4)$$

$$= \int_{\phi_0}^{\frac{\pi}{2}} d\phi \left[1 - \cos\theta_{II}\right]$$

The integration limits involved in equation 2.3 and 2.4 can be evaluated as:

$$\phi_0 = \tan^{-1}\left(\frac{b}{a}\right) \qquad (2.5a)$$

$$\theta_I = \tan^{-1}\left(\frac{a}{2c\cos\phi}\right) \qquad (2.5b)$$

$$\theta_{II} = \tan^{-1}\left(\frac{b}{2c\sin\phi}\right) \qquad (2.5c)$$

Substituting expressions 2.3 - 2.5 into expression 2.2, we have

$$\Omega = 4\left\{\int_{0}^{\phi_0} d\phi \left[1 - \cos\theta_I\right] + \int_{\phi_0}^{\frac{\pi}{2}} d\phi \left[1 - \cos\theta_{II}\right]\right\} \qquad (2.6)$$

Since $$\tan\theta_I = \frac{a}{2c\cos\phi} \qquad (2.7)$$

$$\cos\theta_I = \frac{1}{\sqrt{1 + \tan^2\theta_I}} \qquad (2.8)$$

Based on the same strategy, we can derive

$$\cos\theta_{II} = \frac{1}{\sqrt{1 + \tan^2\theta_{II}}} \qquad (2.9)$$

Substituting equation 2.8 and 2.9 into equation 2.6, we have

$$\Omega = 4\left\{\int_0^{\tan^{-1}\left(\frac{b}{a}\right)} d\phi \left[1 - \frac{1}{\sqrt{1+\left(\frac{a}{2c\cos\phi}\right)^2}}\right] + \int_{\tan^{-1}\left(\frac{b}{a}\right)}^{\frac{\pi}{2}} d\phi \left[1 - \frac{1}{\sqrt{1+\left(\frac{b}{2c\sin\phi}\right)}}\right]\right\}$$

With a = 12 mm; b = 25 mm and c = 4 mm, the solid angle Ω was calculated to be 3.66 steradians, and the collection efficiency was thus found to be:

$$\eta = \frac{\Omega}{4\pi} = 0.29(29\%)$$

The reflection plane mirror (10 mm diameter) was placed very close to the separation capillary. The inner wall of the stainless steel detection chamber was carefully machined to be smooth. If we assume the chemiluminescence toward the mirror is totally reflected back to the PMT photocathode, the total collection efficiency of the miniaturized chemiluminescence detector is doubled to 58%.

2.8 Conclusion

In this work, a miniaturized chemiluminescence detector was designed for capillary zone electrophoresis. This detector significantly reduces the electrical noise and leakage of room light, and gives a collection efficiency of ≈ 58%.

List of reference

1. Hara, T.; Kayama, S.; Nashida, H.; Nakajima, R. *Anal. Sci.* **1994**, *10*, 223-25.
2. Hara, T.; Kayama, S.; Nashida, H.; Nakajima, R. *Anal. Sci.* **1994**, *10*, 823-25.
3. Tsukagoshi, K.; Tanaka, A.; Nakajima, R.; Hara, T. *Anal. Sci.* **1996**, *12*, 525-28.
4. Tsukagoshi, K.; Akasaka, H.; Nakajima, R.; Hara, T. *Chem. Lett.* **1996**, 467-468.
5. Wu, N.; huie, C. W. *J. Chromatogr.* **1993**, *634*, 309-15.
6. Ruberto, M. A.; Grayeski, M. L. *Anal. Chem.* **1992**, *64*, 2758-62.
7. Ruberto, M. A.; Grayeski, M. L. *J. Microcol.* **1994**, Sep. *6*, 545-550.
8. Dadoo, R.; Colon, L. A.; Zare, R. N. *J. High Resolution Chromatography*, **1992**, *15*, 133.
9. Dadoo , R.; Seto, A. G.; Colon, L. A.; Zare, R. N.; *Anal. Chem.*, **1994**, *66*, 303.
10. Zhao, J. Y.; Labba, J.; Dovichi, N. J. *J. of Microcolumn Separation*, **1993**, *5*, 331.
11. Huang, B.; Li, J., and Cheng, K. Sepu, 1995, *13*, 430.
12. Huang, B.; Li, J. J.; Cheng, J. K. *Chemical Journal of Chinese Universities*, **1996**, *17*, 528-530.
13. Huang, Bo; Li, Jian-jun; Zhang, Le; Cheng, Jie-ke, *Anal Chem.*, **1996**, *68*, 2366-2369.
14. Dasgupta, P. K.; Genfa, Z.; Li, J.; Boring, C. B.;Jambunathan, S., and Al-Horr, R., *Anal. Chem.*, **1999**, *71*, 1400.
15. Tsukagoshi, K.; Fujimura, S. and Nakajima, R. *Anal. Chem.*, **1997**, *13*, 279.
16. Lee, Y.-T.; Whang, C.-W. *J. Chromatogr., A*, **1997**, *771*, 379.
17. Liao, S.-Y.; Whang, C.-T., *J. High. Resolut. Chromatogr.*, **1995**, *18*, 667.
18. Liao, S.-Y.; Whang, C.- Y., *J. Chromatogr.*, **1996**, *736*, 247.

19. Hara, T.; Yokogi, J. ; Okamura, S. *J. Chromatography*, **1993**, *A652*, 361.

20. Gilman, S. D.; Silverman, C. E.; Ewing, A. G. *J. of Mirocolumn Separation*, **1994**, *6*, 97.

21. Hara, T.; Nishida, H.; Kayama, S.; Nakajima, R. *Bull. Chem. SOC. Japan*, **1994**, *67*,1193.

22. Gilman, S. D.; Silverman, C. E.; Ewing, A.G. *J. Microcolumn Separation*, **1994**, *6*, 97.

23. Baeyens, W.R.G.; Ling, B. L.; Imai, K.; Calokerino, A.C.; Schulman, S.G. *J. Microcolumn Separation*, **1994**, *6*, 195.

24. Ingle, J. D.; Crouch, S. R., *Spectrochemical Analysis*, Prentice Hall, Englewood Cliffs, New Jersey, **1988**, p 479-485.

25. Peng, C. H.; Crouch, S. R., "High Sensitivity Post-Column Chemiluminescence Detection in Capillary Zone Electrophoresis", presented at the ANACHEM/SAS Meeting, October 2, **1996**, Dearborn, Michigan.

26. Peng, C. H.; Crouch, S. R., "Miniaturized Post-Column Chemiluminescence Detector in Capillary Zone Electrophoresis", presented at the ANACHEM/SAS Meeting, Nov. 3, **1997**, Dearborn, Michigan.

27. Peng, C. H.; Crouch, S. R. "Miniaturized post-column chemiluminescence detector in capillary zone electrophoresis". Manuscript submitted.

28. Ingle, J. D.; Crouch, S. R., *Spectrochemical Analysis*, Prentice Hall, Englewood Cliffs, New Jersey, **1988**, p 53.

Chapter 3

Detection of Transition Metal Ions Using Miniaturized Chemiluminescence Detector in Capillary Zone Electrophoresis

Chemiluminescence (CL) has been used as a sensitive method of detection in capillary electrophoresis (CE) since the early 90's when Hara *et al.*(1) and Dadoo *et al.*(2) reported their pioneering work. Luminol is the most popular CL reagent in CL detection. Detection of metal ions in CE has been explored extensively using several kinds of detection as described in chapter 1. In this work, metals are separated by CE and detected by chemiluminescence because they catalyze the luminol/H_2O_2 chemiluminescence. The reaction scheme of luminol/H_2O_2 chemiluminescence is described in chapter 1.

This chapter describes the separation of several transition metal cations. The importance of daily capillary conditioning is emphasized. It was found that a regular conditioning procedure in CE (3), is not enough for the separation of transition metal ions. Because of this, we developed a special conditioning procedure that involves 1 hour of rinsing with 0.1 M NaOH and 12 hours of rinsing with 0.1 M HCl, based on the work of Lu and Cassidy (4).

The lifetime of luminol/H_2O_2 chemiluminescence at different pH values was measured to aid in the pH optimization of the post-column CL reagents. Some important factors such as the pH of the separation buffer, the buffer composition and adsorption are discussed. Ten consecutive injections gives a reproducibility of 8 - 18% under various conditions (in term of RSD for peak height), which is poorer than that for on-column detection (about 2 - 10%) (3, 5).

3.1. Preparation of Stock Solutions

3.1.1 Preparation of 0.010 M Luminol Stock Solution (pH = 12.00)

Weigh accurately 1.7716 g (0.010 mole) 3-Aminophthalhydrazide (luminol) (Aldrich Chem. Co., product # 12,307-2) and dissolve in a 1000 mL beaker. About 990 mL of deionized distilled water is added to the beaker. Lumniol tends to form small chunks in water; the ultrasonic bath is turned on to crack these small chunks. The solubility of luminol is very low in acidic solutions but much higher in basic solutions. A 5 M NaOH solution is added to adjust the luminol solution to pH 12.00. The luminol solution is then filtered through a 0.45 μm pore size membrane filter (Millipore Inc.). Finally, the luminol solution is diluted to 1000 mL with deionized distilled water and transfered into a 1L glass bottle. The bottle cap must be tightened to prevent the CO_2 from entering. Introduction of CO_2 can change the pH of the luminol stock solution dramatically over long periods of time. Finally, the luminol solution is stored in the refrigerator. The pH of the luminol solution was found to be stable for at least one year.

3.1.2 Preparation of 0.050 M H_2O_2

Pipet 491 μL of 30.9 % H_2O_2 (density 1.12 g/mL, J. T. Baker, product # 2186-01) into a 100 mL volumetric flask, and dilute to the mark with deionized, distilled water. All 0.050 M H_2O_2 solutions are prepared daily following this procedure.

3.1.3 Preparation of Separation Buffer (0.01 M acetic acid, 2 x 10^{-4} M luminol)

Pipet 1 mL of 1 M acetic acid, various amounts of 2-Hydroxyisobutyric acid (HIBA) (Aldrich Chem. Co., product # 32,359-4) if needed, and 2 mL of 0.010 M luminol stock

solution, then dilute to 100 mL. The pH of the buffer is adjusted to the desired value with 2 M or 5 M NaOH. The buffer solution is stored in refrigerator since the luminol solution is not stable at room temperature.

3.1.4 Preparation of Sample Stock Solution

Metal solutions were prepared from metal nitrate salts, $Co(NO_3)_2 \cdot 6H_2O$ (Spectrum Quality Inc.), $Cu(NO_3)_2 \cdot 2.5\ H_2O$ (J. T. Baker Inc.), $Cr(NO_3)_3 \cdot 9H_2O$ (Spectrum Quality Inc.) without further purification. All sample solutions at different concentrations were serially diluted daily and stored in plastic bottles.

3.2 Instrumentation

3.2.1 Instrumentation for Lifetime Measurement

The experimental set-up for measuring the CL lifetime is shown in figure 3.1. The light generated by the chemiluminescence reaction is detected by the PMT (Hamamatsu, 1P28A PMT Photomultiplier tube) placed about 1 cm in front of a 1 mL glass vial. The PMT is powered at 600 V (Heath Power Supply, model EU-42A). The PMT photocurrent is amplified by a current amplifier and then recorded by a computer at a sampling rate of 1000 points/s.

A solution of H_2O_2 (200 µL of 0.025 M, various pH values) was injected into a 20 µL solution of separation buffer (0.01 M acetic acid and 3×10^{-4} M luminol, pH = 4.65). The pH of the mixed solution remained unchanged due to the large volume of H_2O_2. For precise CL measurement, an automatic syringe is often employed to achieve a more reproducible injection speed and volume (6). Ideally, the mixing process should be fast

enough that the emission vs. time curve is affected solely by the rate of chemiluminescence reaction rather than by the rate of reagent mixing.

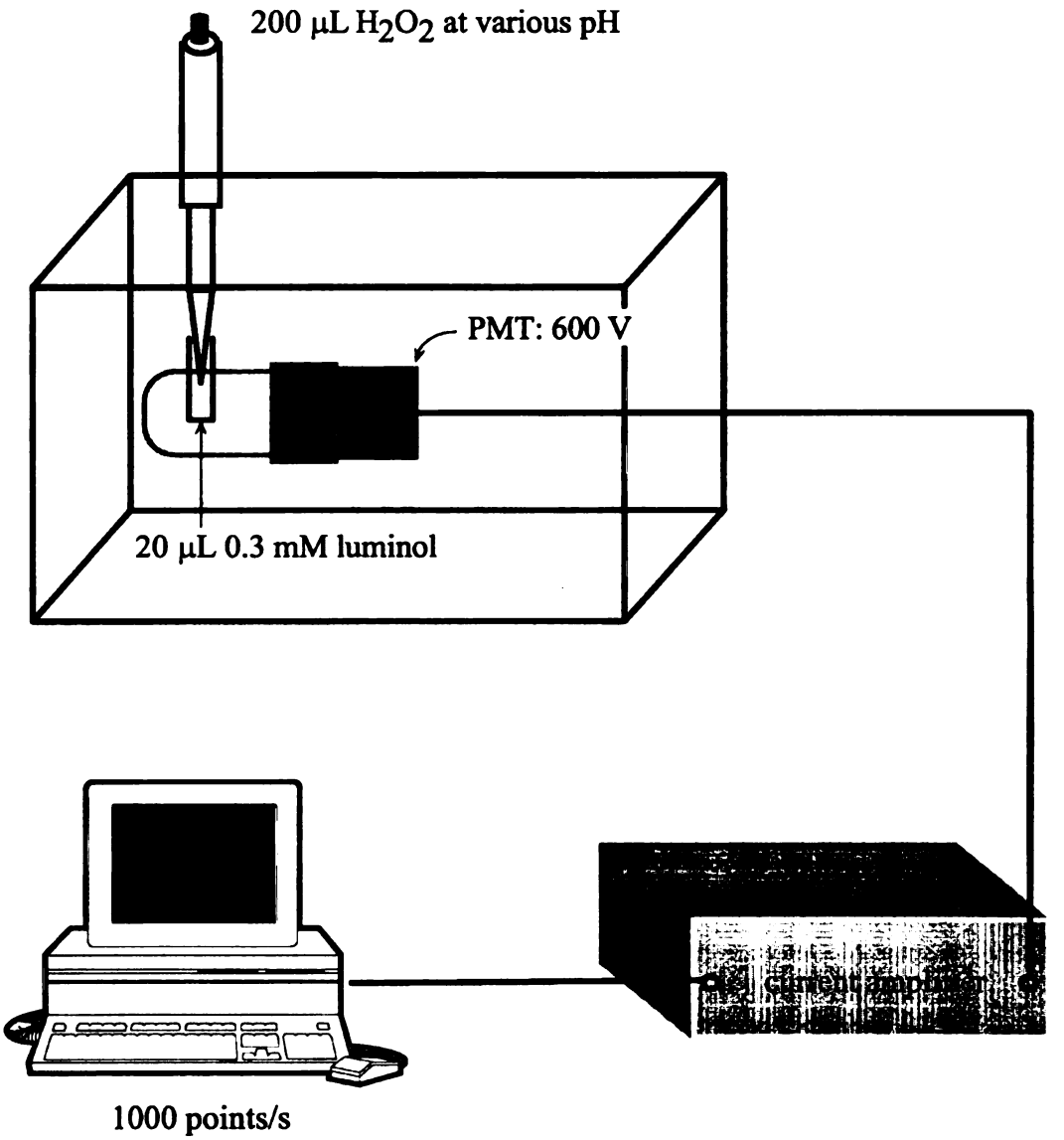

Figure 3.1 Instrument for lifetime measurement of luminol-H_2O_2 chemiluminescence
Amplifier setting: 10^8 V/A; rise time: 0.1 ms; sampling rate: 1000 points/s

3.2.2 Instrumentation for Electrophoretic Separation

The instrumentation used for CE separation is described in chapter 2.

3.3 Procedures

3.3.1 Capillary Conditioning

Regular conditioning for fused silica capillaries was done by flushing the capillary with 0.1 M NaOH for about one-half hour, and then with 0.1 M HCl for another one-half hour. However, this is not enough for the separation of transition metal ions due to their strong adsorption to the capillary wall. Thus, we developed a special conditioning procedure. The capillary was first flushed with 0.1 M NaOH for 1 hour at a flow rate of 10 μL/min, then flushed overnight with 0.1 M HCl at a flow rate of 3 μL/min. The capillary must be conditioned by this procedure after each working day or the reproducibility of the peaks can be very poor. Figure 3.2a and figure 3.2b show the Electropherograms of the first run and the ninth run of 1.0×10^{-8} M Co^{2+}, 1.0×10^{-6} M Cr^{3+}, 1.0×10^{-6} M Cu^{2+} under identical conditions. The first run shows a higher peak but a longer migration time. The peak area and migration time for the same sample under the same separation conditions decreases during a series of electrophoresis runs. This may result from the strong adsorption of the transition metal cations to the capillary walls (4). During the electrophoretic runs, the active sites on the capillary wall are continuously covered by the transition metal cations, which can slow down the electroosmotic flow and reduce the amount of sample injected into the separation capillary. This explains the decreased peak height during the separation of the same sample under identical

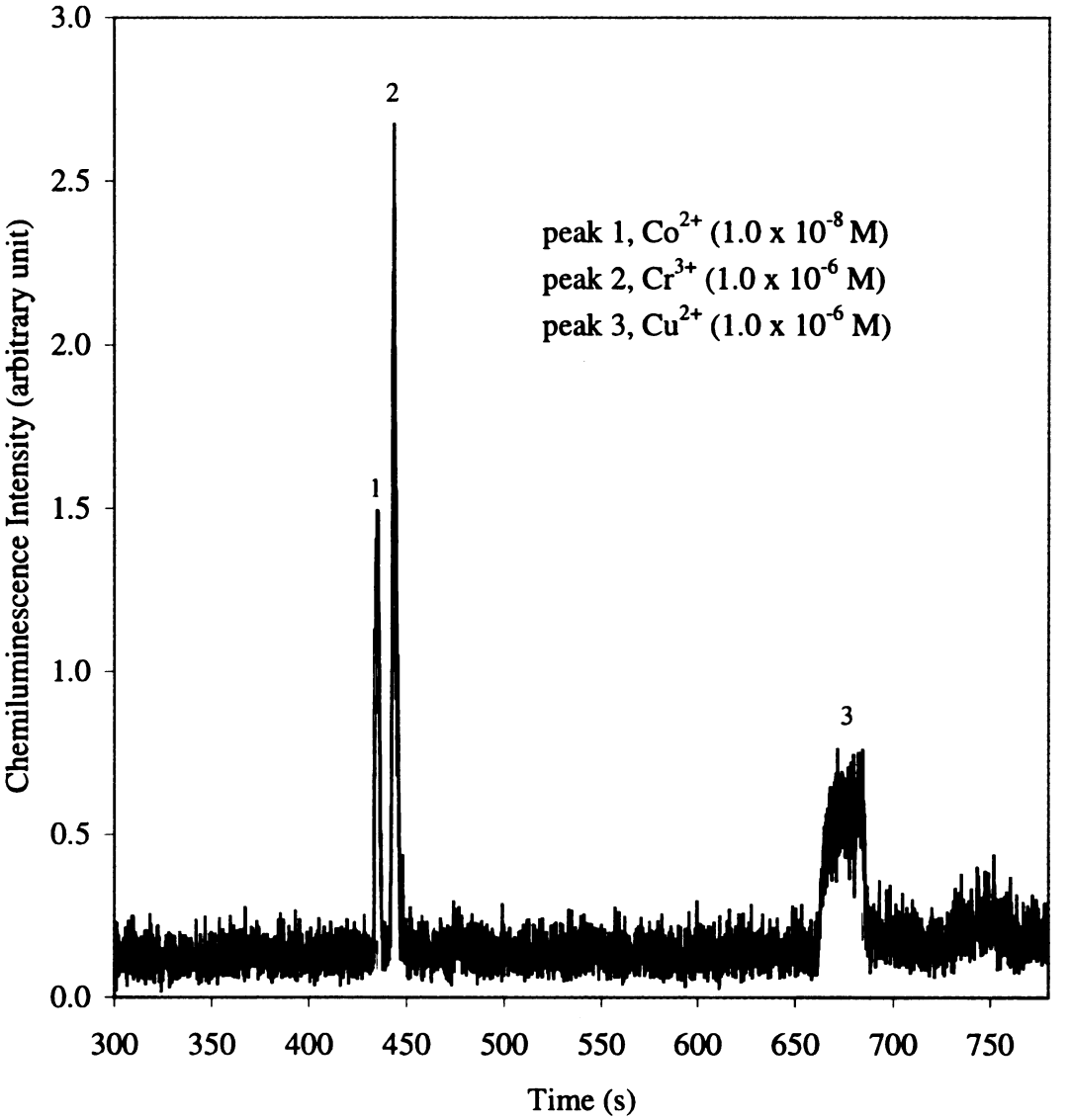

Figure 3.2a Electropherogram of the first run of 1.0 x 10^{-8} M Co^{2+}, 1.0 x 10^{-6} M Cr^{3+}, 1.0 x 10^{-6} M Cu^{2+}.
Sample: 1.0 x 10^{-8} M Co^{2+}, 1.0 x 10^{-6} M Cr^{3+}, 1.0 x 10^{-6} M Cu^{2+} in deionized distilled water; buffer: 2.0 x 10^{-4} M luminol, 0.01 M NaAc/HAc, 0.005 M HIBA, pH = 3.53; post-column CL reagent: 0.05 M H_2O_2, 0.1 M phosphate, pH = 12.49; flow rate: 6 μL/min; electrophoretic voltage: 10 kV; injection voltage: 10 kV; injection time: 10 s; fused silica capillary: 50 μm x 363 μm o.d. x 50 cm.

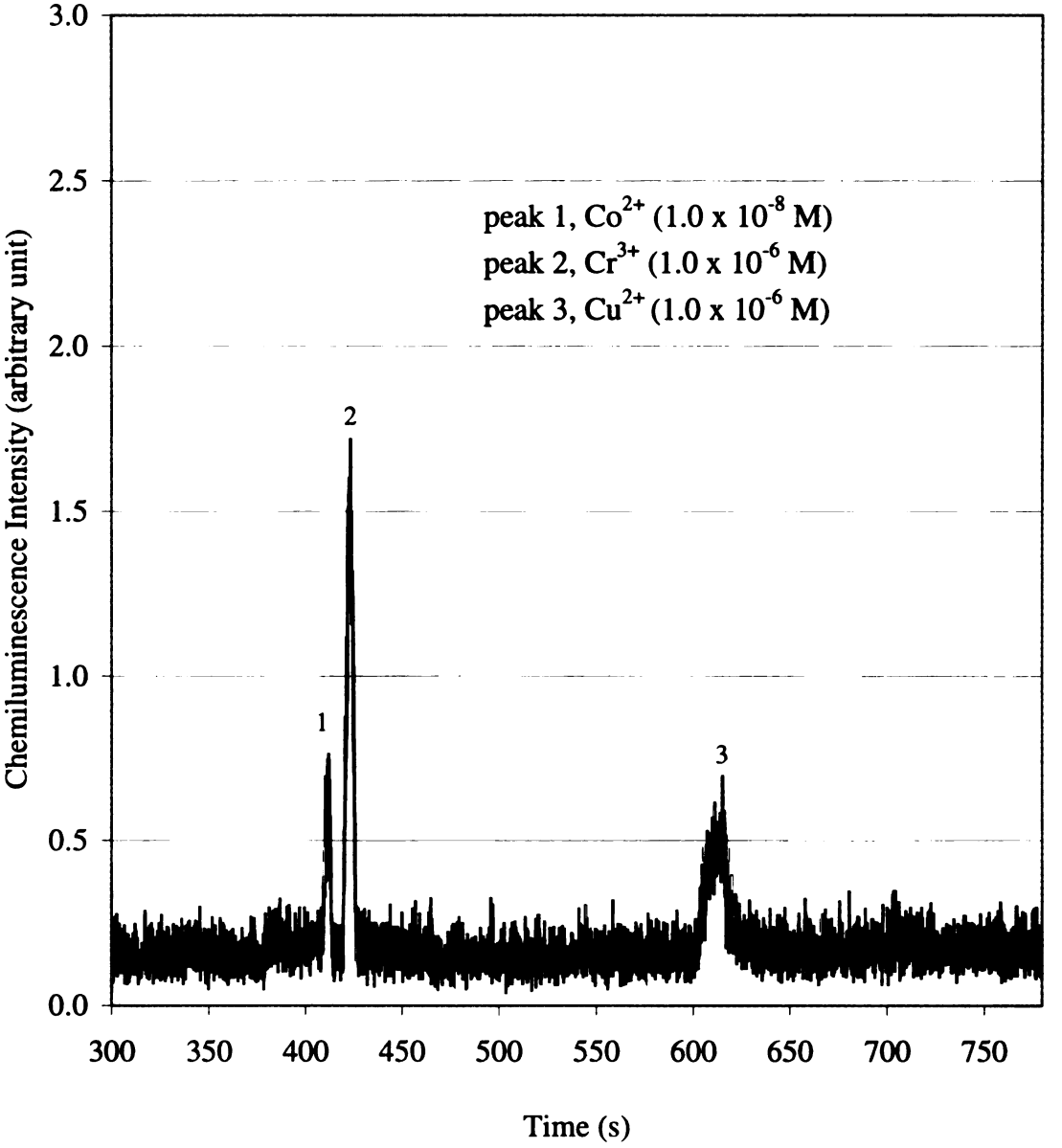

Figure 3.2b Electropherogram of the ninth run of 1.0 x 10^{-8} M Co^{2+}, 1.0 x 10^{-6} M Cr^{3+}, 1.0 x 10^{-6} M Cu^{2+}.
Sample: 1.0 x 10^{-8} M Co^{2+}, 1.0 x 10^{-6} M Cr^{3+}, 1.0 x 10^{-6} M Cu^{2+} in deionized distilled water; buffer: 2.0 x 10^{-4} M luminol, 0.01 M NaAc/HAc, 0.005 M HIBA, pH = 3.53; post-column CL reagent: 0.05 M H_2O_2, 0.1 M phosphate, pH = 12.49; flow rate: 6 µL/min; electrophoretic voltage: 10 kV; injection voltage: 10 kV; injection time: 10 s; fused silica capillary: 50 µm x 363 µm o.d. x 50 cm.

conditions as shown in figures 3.2a and figure 3.2b. Most likely, the migration time decreases because the capillary wall becomes less negatively charged due to the accumulation of the cations. This reduces the adsorption of metal cations to some extent and allows the sample zones to migrate faster than in the early runs. The increase in the electrophoretic is larger than the decrease in the electroosmotic flow, making the overall rate of electrophoretic flow faster. The exact mechanism for the adsorption of metals was not studied in this work, but experimental results show that strict conditioning is crucial in order to achieve reproducible separation of transition metal cations.

3.3.2 Sample Injection

Electrokinetic injection was used for all the CE separations in this chapter. The capillary and the Pt electrode were placed into the sample solution, and a 10 kV injection voltage was applied for 5 - 10 seconds. Then the capillary is placed into the buffer, solution and electrophoresis begun.

3.4 Results and Discussion

3.4.1 Lifetime and Intensity of Luminol-H_2O_2 Chemiluminescence at Various pH values

Figure 3.3 indicates the lifetime of chemiluminescence is less than 60 ms between pH 12.50 and 13.00. The chemiluminescence reaches a maximum at pH 12.50. The CL emission is finished within 300 ms under any solution pH as shown in figure 3.3. For CL detection of CE separations, it is important to calculate how long the sample zone is observed by the PMT. The linear flow rate of the CL reagents is 1.24 mm/s, given the volume flow rate of the post-column CL reagent (6 μL/min) and the internal diameter of

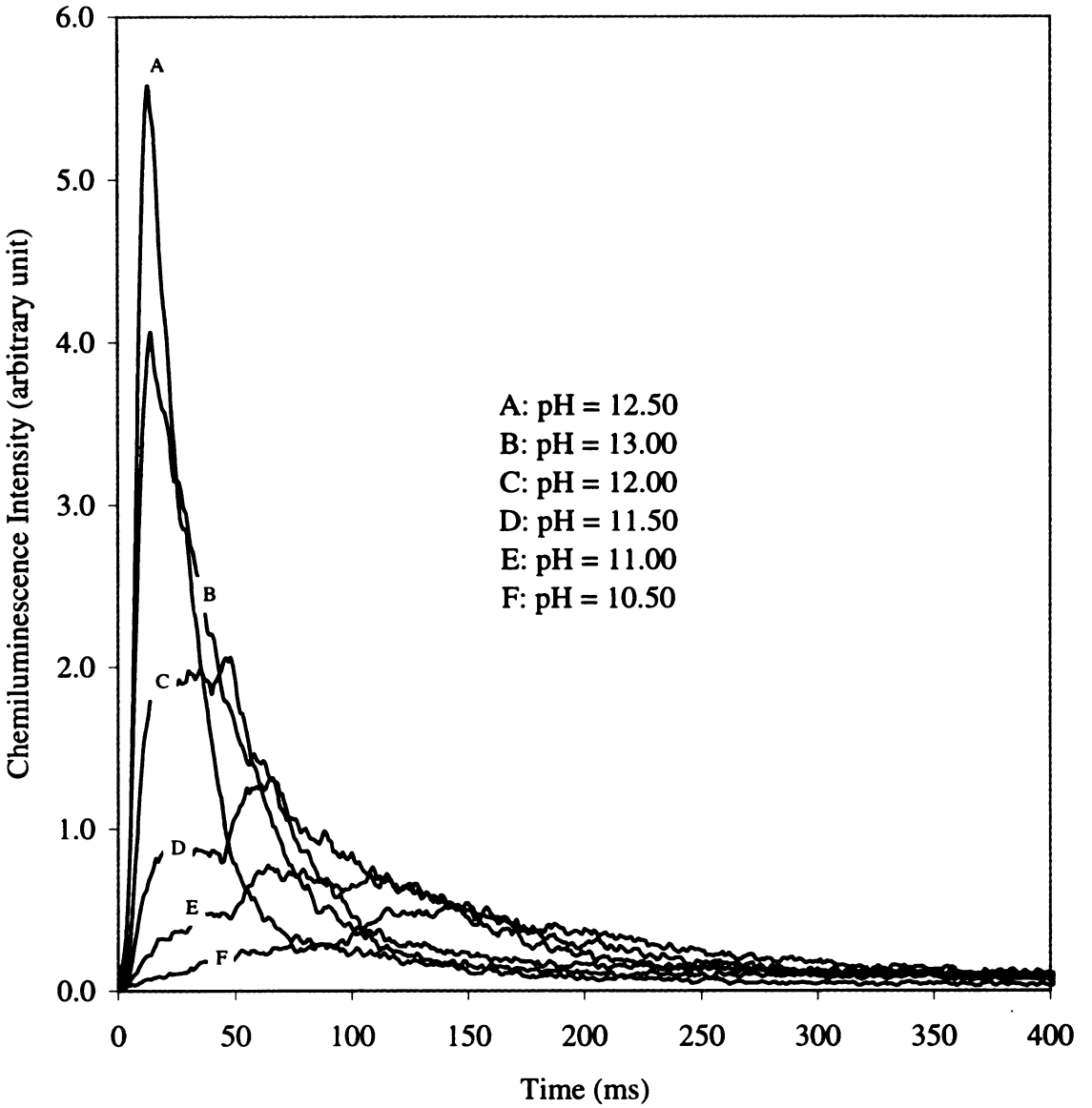

Figure 3.3 Lifetime of luminol-H_2O_2 chemiluminescence at various pH values PMT power supply: 600 V; Amplifier: 10^8 V/A; sampling rate: 1000 points/s

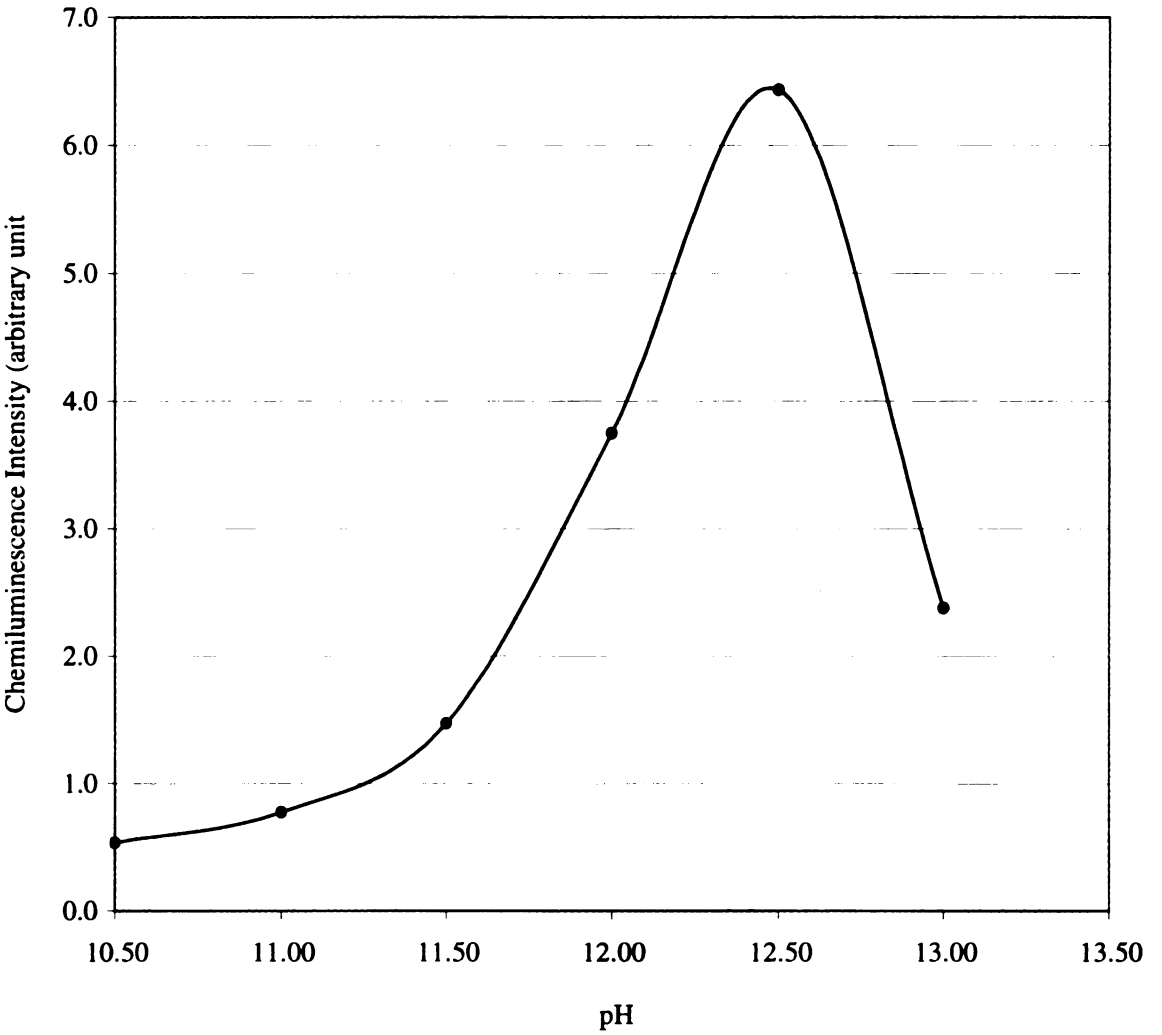

Figure 3.4 Intensity of luminol-H_2O_2 chemiluminescence at various pH values
PMT power supply: 600 V; Amplifier: 10^8 V/A; sampling rate: 1000 points/s
Reagent A: 200 µL 0.025 M H_2O_2 at various pH ---> Reagent B: 20 µL of 3.0 x 10^{-4} M luminol, 0.01 M NaAc/HAc, pH: 4.65

the reaction capillary (320 μm i.d.). The exposure time of the sample zone in front of the PMT is approximately 3 seconds; this is sufficient for completion of the CL reaction catalyzed by the transition metal ions.

The maximum emission at various pH values is shown in figure 3.4. The CL emission increases with rising pH, and reaches a maximum at pH 12.50, and decreases in more basic solutions.3.4.2 Selection of Mixing Mode

For the separation of transition metal ions in CE, there are three possible modes of mixing, as described in figure 3.5, figure 3.6 and figure 3.7. These are studied in order to select an optimum mode. The transition metal ions are best separated in acidic media, but detection is best performed in basic media as shown in figure 3.4.

3.4.2.1 Mixing Mode 1: Mix H_2O_2 in Separation Buffer

In mode 1 as shown in figure 3.5, 0.05 M H_2O_2 is added into the separation buffer (0.01 M NaAc/HAc, pH = 4.50). This mode of mixing produces severe decomposition of H_2O_2. The Pt electrode turned out to be a good catalyst for the decomposition of H_2O_2, which generates bubbles around the Pt electrode surface. These bubbles frequently disrupt the high electric field. Decomposition of H_2O_2 is much faster when the 10 kV high voltage is applied across the separation capillary. Routine electrophoresis is not feasible with this mixing mode. Therefore, we gave up this mode of mixing early in this work.

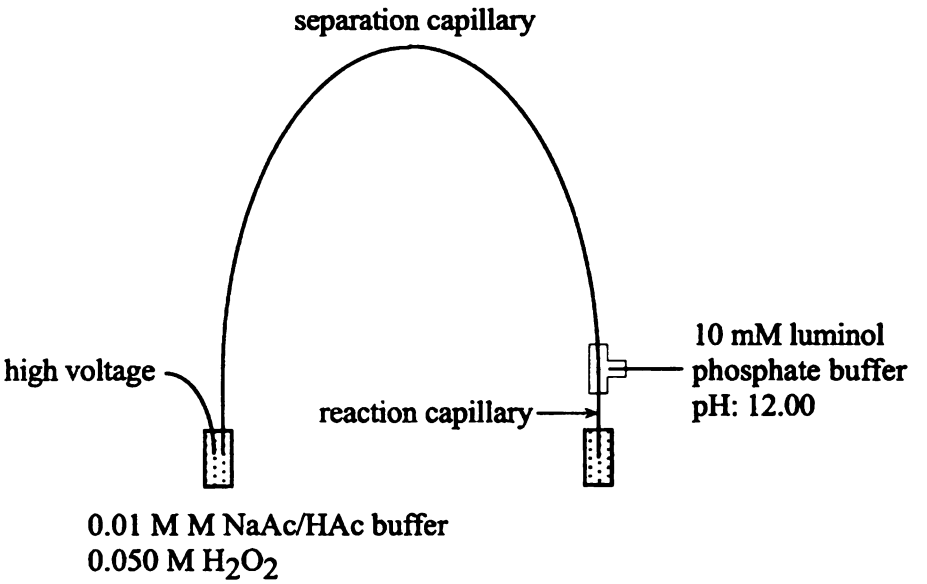

Figure 3.5 Mixing mode 1 for chemiluminescence detection in capillary electrophoresis

3.4.2.2 Mixing Mode 2: Mixing Luminol with H_2O_2 as Post-column CL Reagents

In mode 2 as shown in figure 3.6, 0.05 M H_2O_2 is mixed online with an equal amount of 0.01 M luminol using a syringe pump (Harvard Apparatus, model 22). The lifetime of the luminol/H_2O_2 chemiluminescence is less than 400 ms at any pH value as shown in figure 3.3. It takes about 30 minutes for the merged stream of CL reagents to reach the post-column flow cell for detection, thus significant amount of luminol/H_2O_2 chemiluminescence can occur within the Teflon tube and the mixing TEE before the separated metals can catalyze the luminol/H_2O_2 chemiluminescence. The experimental result showed poor sensitivity. The detection limit for cobalt, which has the greatest catalytic effect on the luminol/H_2O_2 chemiluminescence is about 10^{-6} M. Mode 2 did not demonstrate the high sensitivity of chemiluminescence detection. Consequently, no further effort was attempted for mixing mode 2.

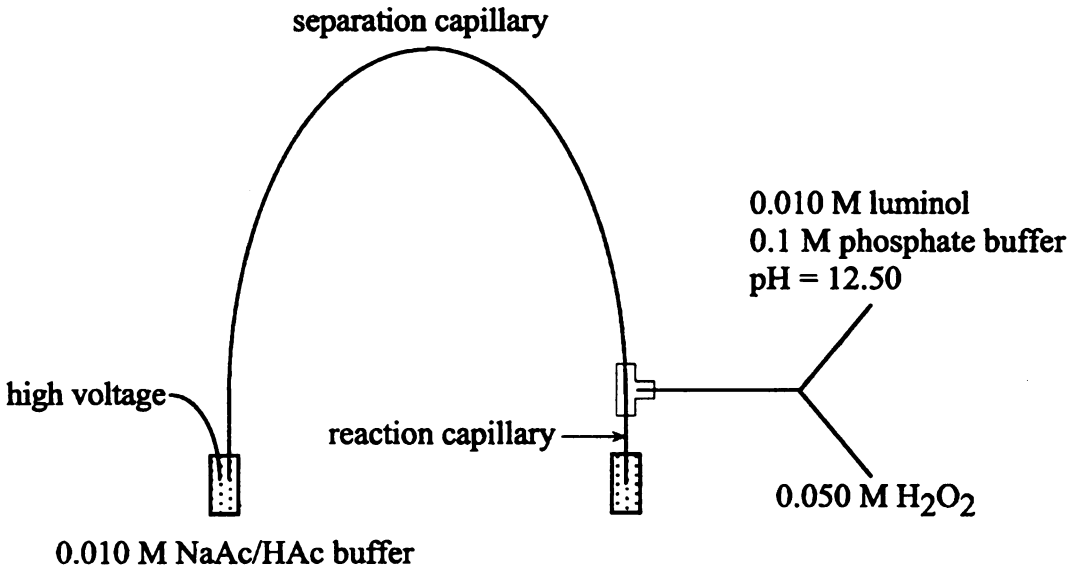

Figure 3.6 Mixing mode 2 for chemiluminescence detection in capillary electrophoresis

3.4.2.3. Mixing Mode 3: Luminol in the Separation Buffer

In mode 3 as shown in figure 3.7, luminol is added into the separation buffer. peroxide and phosphate buffer are mixed from two independent streams and merged as one stream flowing down the TEE connector to react with the eluted transition metal ions. Unfortunately, the solubility of luminol is poor at the low pH necessary for good separation of the transition metal ions. A solubility test for luminol in the buffer at different pH values was done and is listed in Table 3.1. The buffer containing 3.0×10^{-4} M luminol is not stable in the pH 3.50 - 5.00 range. The buffer containing 0.01 M acetic acid and 2.0×10^{-4} M luminol did not show a luminol precipitate at pH 3.50 - 5.00 one month after preparation and was chosen for all the CE separations. The sensitivity of this mode is much higher than that of mixing mode 1 and mixing mode 2.

Table 3.1 Solubility of luminol in buffers of different pH values

Buffer	pH = 3.50	pH = 4.50	pH = 5.00
0.01 M acetic acid, 1.0×10^{-4} M luminol	soluble	soluble	soluble
0.01 M acetic acid, 2.0×10^{-4} M luminol	soluble	soluble	soluble
0.01 M acetic acid, 3.0×10^{-4} M luminol	precipitate	precipitate	precipitate in one or two hours

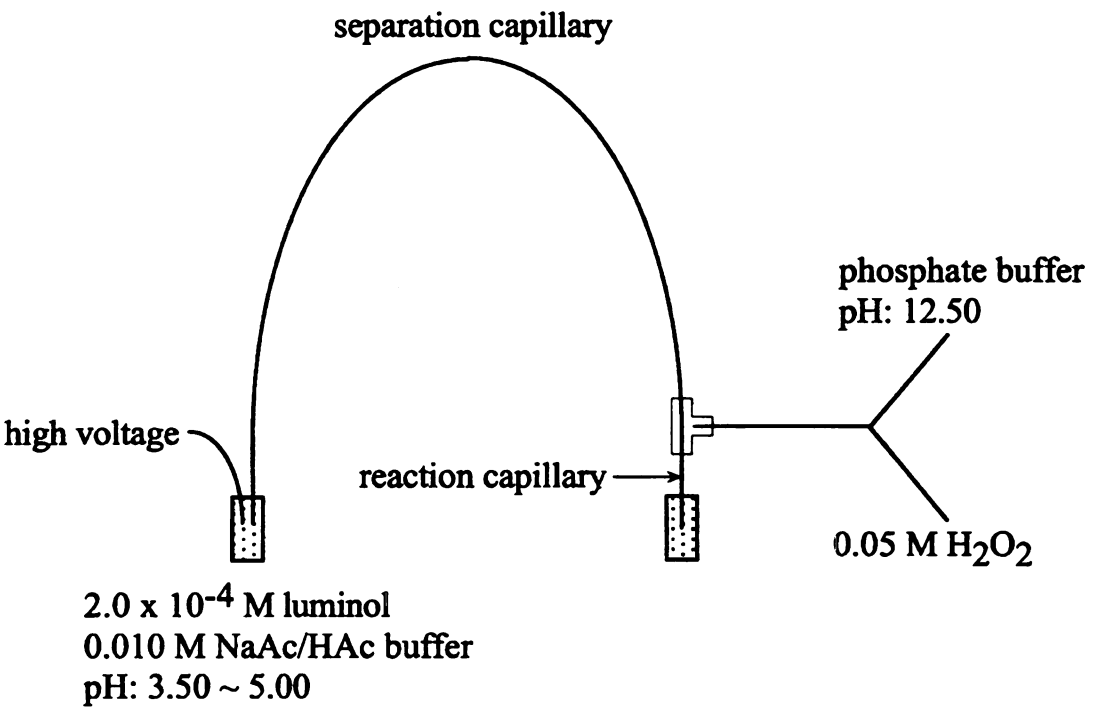

Figure 3.7 Mixing mode 3: luminol in the separation buffer

3.4.3 Optimization of pH for Post-Column Chemiluminescence Detection

The luminol CL reaction is optimized at alkaline conditions, depending upon the catalyst. The transition metal ions are best separated by CE at low pH. Consequently, a post-column pH change is required when applying the luminol CL reaction for detection in CE. Generally, the mixing process reduces the number of theoretical plates (7). A smaller internal diameter capillary enhances the separation efficiency, and allows easier and faster pH switching. In our work, a 50 μm i.d. fused silica capillary was selected for all the electrophoretic operations; a 320 μm i.d. x 435 μm o.d. fused silica capillary was chosen as the reaction capillary. The volume flow rate of the CL reagents is about 41 times that of the separation capillary under the same linear flow rate. Considering the strong buffer capacity of the post-column CL reagents, it should be possible to switch rapidly to the more basic pH.

In a flow system like CE with CL detection, the post-column pH switching occurs through diffusion. When the sample zone exit the separation capillary, the pH of the zone is quickly raised toward that of the post-column CL reagents. The rate of this pH ramping is determined by many factors such as the pH, the buffer capacity and viscosity of both the separation buffer and post-column CL reagent. For a rapid pH switching, a low concentration of separation buffer and a CL reagent with high buffer capacity is essential. Only a few sample injections were performed each day for the freshly conditioned capillary due to the limited loading capacity of the fused silica capillary. An ideal buffer should have strong buffer capacity and should not interact with the sample.

In the detection of transition metals in CE, one of the most important factors is the pH of the post-column CL reagents. The post-column CL reagent comes from two separate

streams of 0.05 M H_2O_2 and phosphate buffer. The H_2O_2 and the basic phosphate should be mixed on-line with the phosphate buffer (pH 11.50 ~ 13.00) to reach the optimum pH range for post-column CL detection, since H_2O_2 decomposes slowly in alkaline solution. Figure 3.8 shows the various combinations and the resulting pH of the mixtures.

The peak heights for 1.0 x10^{-8} M Co^{2+} from three electrokinetic injections are plotted versus pH in figure 3.9. As the buffer solution exits the separation capillary, there is a large pH change from pH 4.06 toward that of the post-column CL reagents. The peak height increases with rising pH of the post-column CL reagent, since the pH of the sample zone has not reached the optimized pH value (~12.5) for maximum chemiluminescence emission.

The peak heights for Co^{2+} and Cr^{3+} from three electrokinetic injections are plotted versus pH in figures 3.10 and 3.11 respectively. The pH (4.74) of the separation buffer shown in figure 3.10 and 3.11 is higher than that of the buffer in figure 3.9 (pH 4.06). The buffer capacity of the post-column CL reagents is also higher due to the higher concentration of phosphate (0.1 M), and thus gives a more basic pH after switching. The optimized pH for maximum chemiluminescence is reached earlier in figure 3.10 than in figure 3.9. This explains the bending of the curve in figure 3.10.

Figures 3.10 and 3.11 show similar trends for Co^{2+} and Cr^{3+}. The highest sensitivity is achieved around pH 12.00 for both Co^{2+} and Cr^{3+}. The optimized pH for the post column CL detection of Co^{2+} and Cr^{3+} is somewhere between 12.00 and 13.00. If more pH values were selected for pH optimization, the peak height v.s. pH may give a sharper maximum and allow a more precise choice of pH.

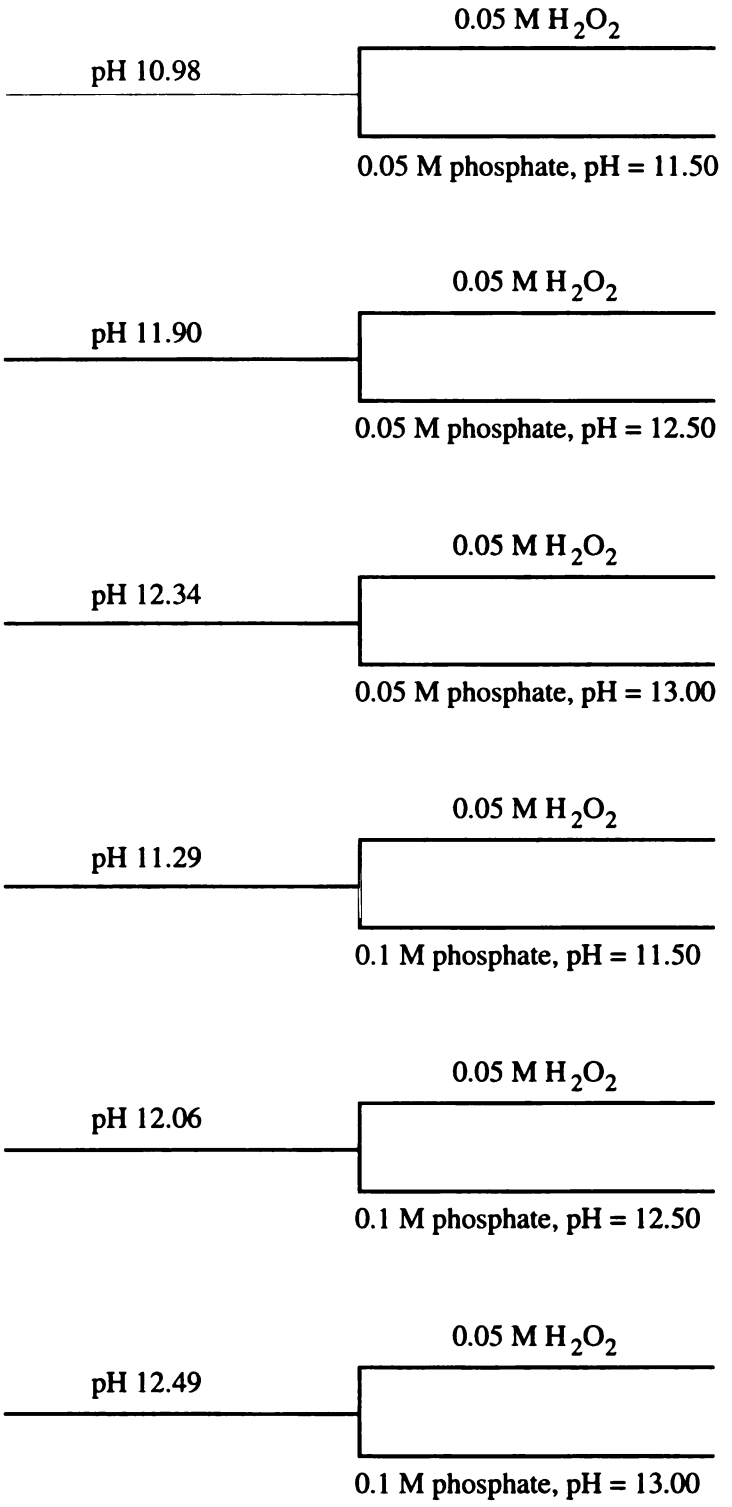

Figure 3.8 Final pH value of the post-column CL reagents

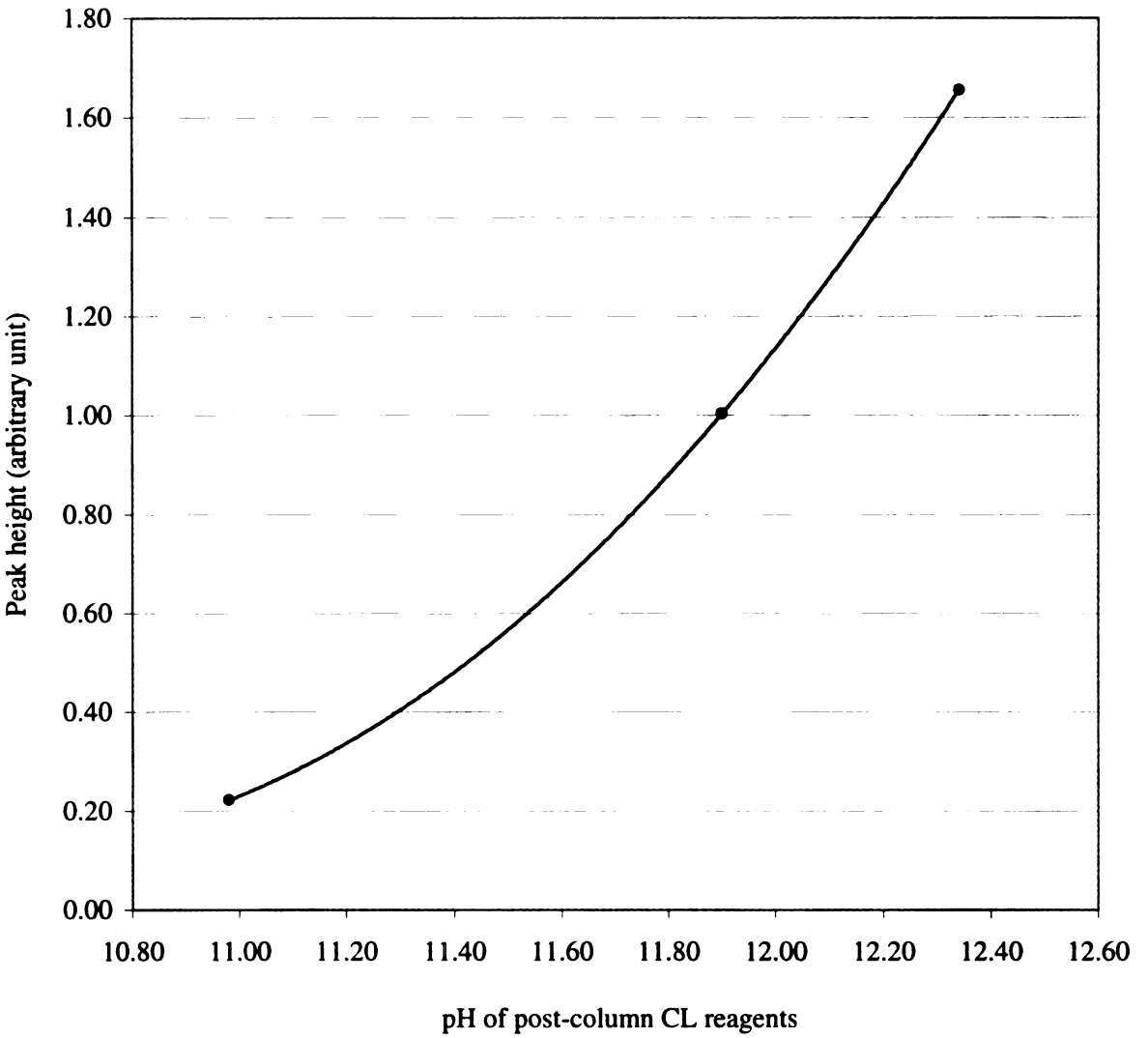

Figure 3.9 Peak height of 1.0 x 10^{-8} M Co^{2+} at various pH values of CL reagent. Sample: 1.0 x 10^{-8} M Co^{2+} in deionized distilled water; separation buffer: 2 x 10^{-4} M luminol, 0.010 M NaAc/HAc, pH: 4.06; post-column CL reagents: 0.025 M H_2O_2, 0.025 M phosphate, pH = 10.98, 11.90, 12.34; flow rate: 6 µL /s; electrophoretic current: 0.8 µA; PMT voltage: 800 V; amplifier: 10^8 V/A; amplifier rise time: 3 ms; separation voltage: 10 kV; sample injection: 10 s at 10 kV; separation capillary: 50 µm i.d. 363 µm o.d. x 50 cm long.

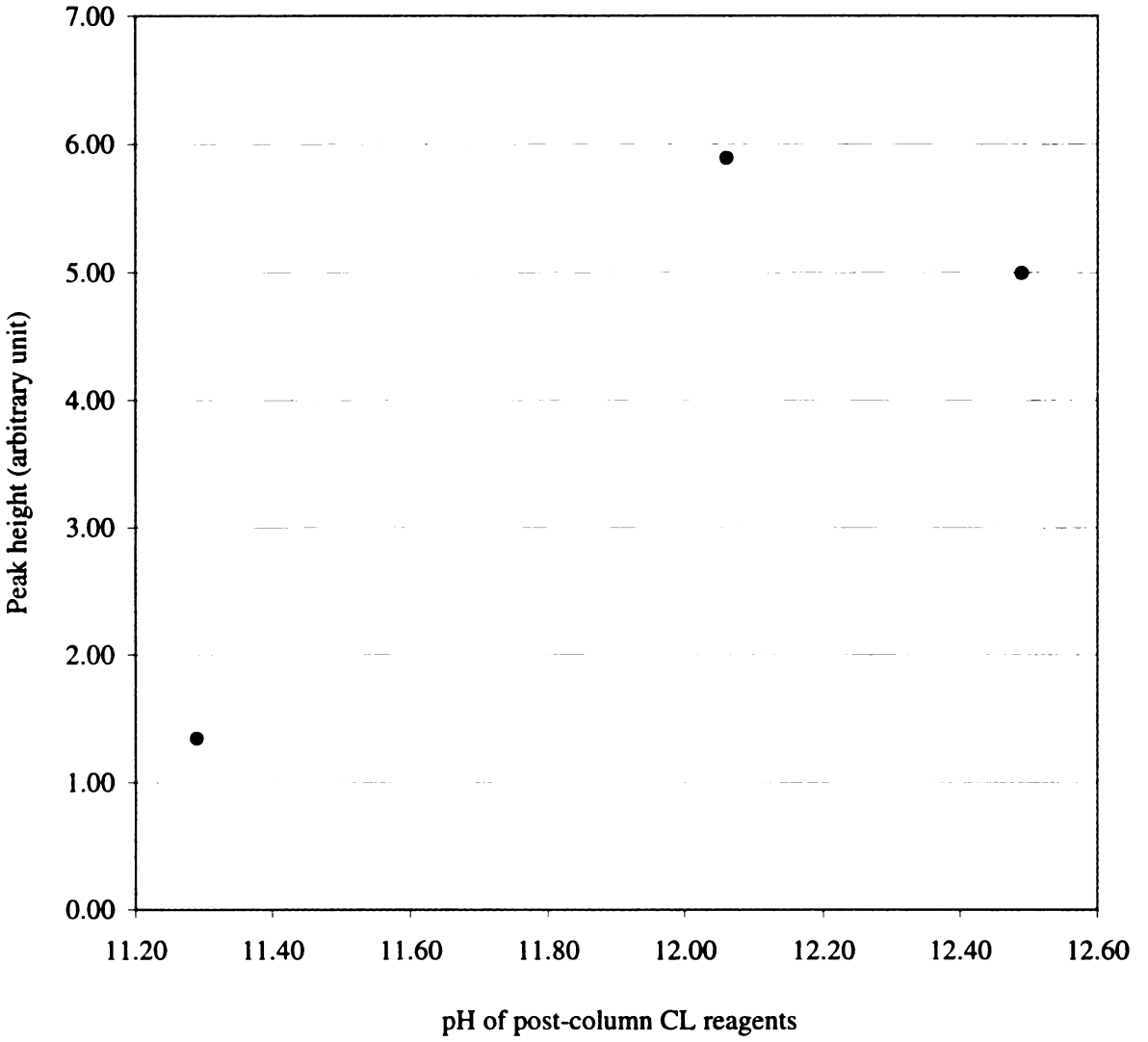

Figure 3.10 Peak height of 1.0 x 10^{-9} M Co^{2+} at various pH values of CL reagent. Sample: 1.0 x 10^{-9} M Co^{2+} and 5.0 x 10^{-7} M Cr^{3+} in deionized distilled water; separation buffer: 2 x 10^{-4} M luminol, 0.010 M NaAc/HAc, pH: 4.74; post-column CL reagents: 0.025 M H_2O_2, 0.050 M phosphate, pH = 11.29, 12.06, 12.49; flow rate: 6 µL /s; electrophoretic current: 2.2 µA; PMT voltage: 800 V; amplifier: 10^8 V/A; amplifier rise time: 3 ms; separation voltage: 10 kV; sample injection: 10 s at 10 kV; separation capillary: 50 µm i.d. 363 µm o.d. x 40 cm long.

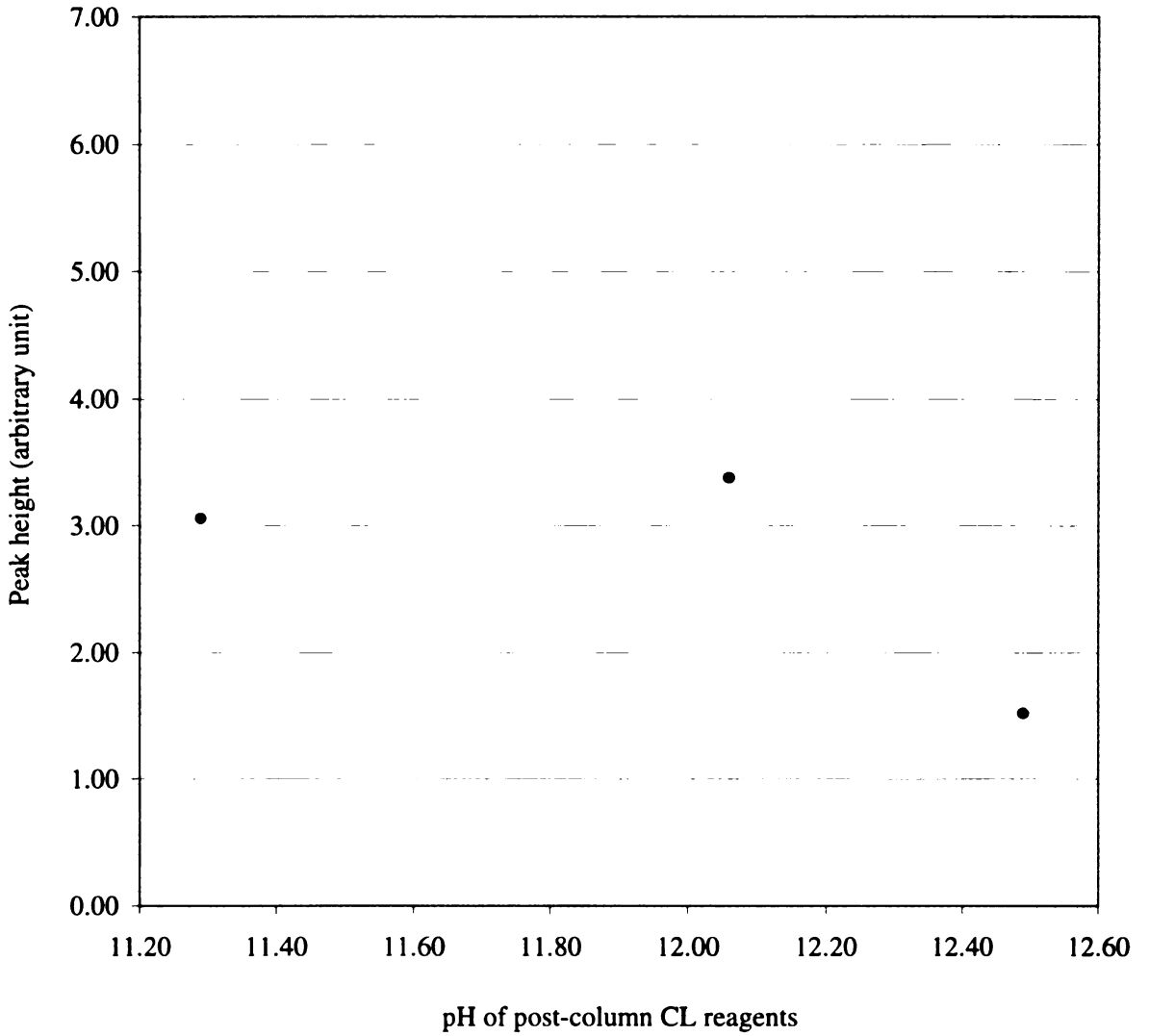

Figure 3.11 Peak height of 5.0 x 10^{-7} M Cr^{3+} at various pH values of CL reagent
Sample: 1.0 x 10^{-9} M Co^{2+} and 5.0 x 10^{-7} M Cr^{3+} in deionized distilled water; separation buffer: 2 x 10^{-4} M luminol, 0.010 M NaAc/HAc, pH: 4.74; post-column CL reagents: 0.025 M H_2O_2, 0.050 M phosphate, pH = 11.29, 12.06, 12.49; flow rate: 6 µL /s; electrophoretic current: 2.2 µA; PMT voltage: 800 V; amplifier: 10^8 V/A; amplifier rise time: 3 ms; separation voltage: 10 kV; sample injection: 10 s at 10 kV; separation capillary: 50 µm i.d. 363 µm o.d. x 40 cm long.

3.4.4 Optimization of Separation Buffer pH

The selectivity of the metal ion separation can be predicted from the equivalent ionic conductivities (8), λ_i, which are directly related to the mobilities, μ_i, of the ions:

$$\mu_i = \lambda_i / F \qquad (3.1)$$

where F is the Faraday constant. The velocity of migration for a certain ion V_{app} is given by:

$$V_{app} = (\mu_i + \mu_{EOF}) E \qquad (3.2)$$

Here μ_i is the electrophoretic mobility of the ion, μ_{EOF} is the electroosmotic flow mobility and E is the electric field. Based on the mobility of Co^{2+}(5.7×10^{-4} m^2/Vs), Cr^{3+}(6.9×10^{-4} m^2/Vs), and Cu^{2+}(5.6×10^{-4} m^2/Vs), the predicted elution order should be Cr^{3+} ---> Co^{2+} ---> Cu^{2+}. However, the observed elution order was Co^{2+} ---> Cr^{3+} ---> Cu^{2+}, due to the adsorption of Cr^{3+} to the capillary wall and to complexation of the metals by the buffer anions. Group IA metal ions like Li^+, Na^+, K^+ and Rb^+, exhibit no signs of adsorption, so their peak profiles are always fronting (9).

Adsorption of transition metal ions to the capillary wall is one of the most difficult problems. Although there are several ways to minimize adsorption, such as lowering the pH of the buffer, and addition of α-hydroxyisobutyric acid (HIBA) into the buffer. None of these is a perfect solution. The best way is to use a coated fused silica capillary. Actually we have explored this idea, but the result was not very successful due to our inability to make an inert coating. Coated capillaries are discussed further in chapter 6.

It is very important to establish the optimum pH for the separation buffer in CE since pH affects the electroosmotic flow rate and the number of surface negative charges dramatically as described in chapter 1. Maintenance of a constant pH is essential for

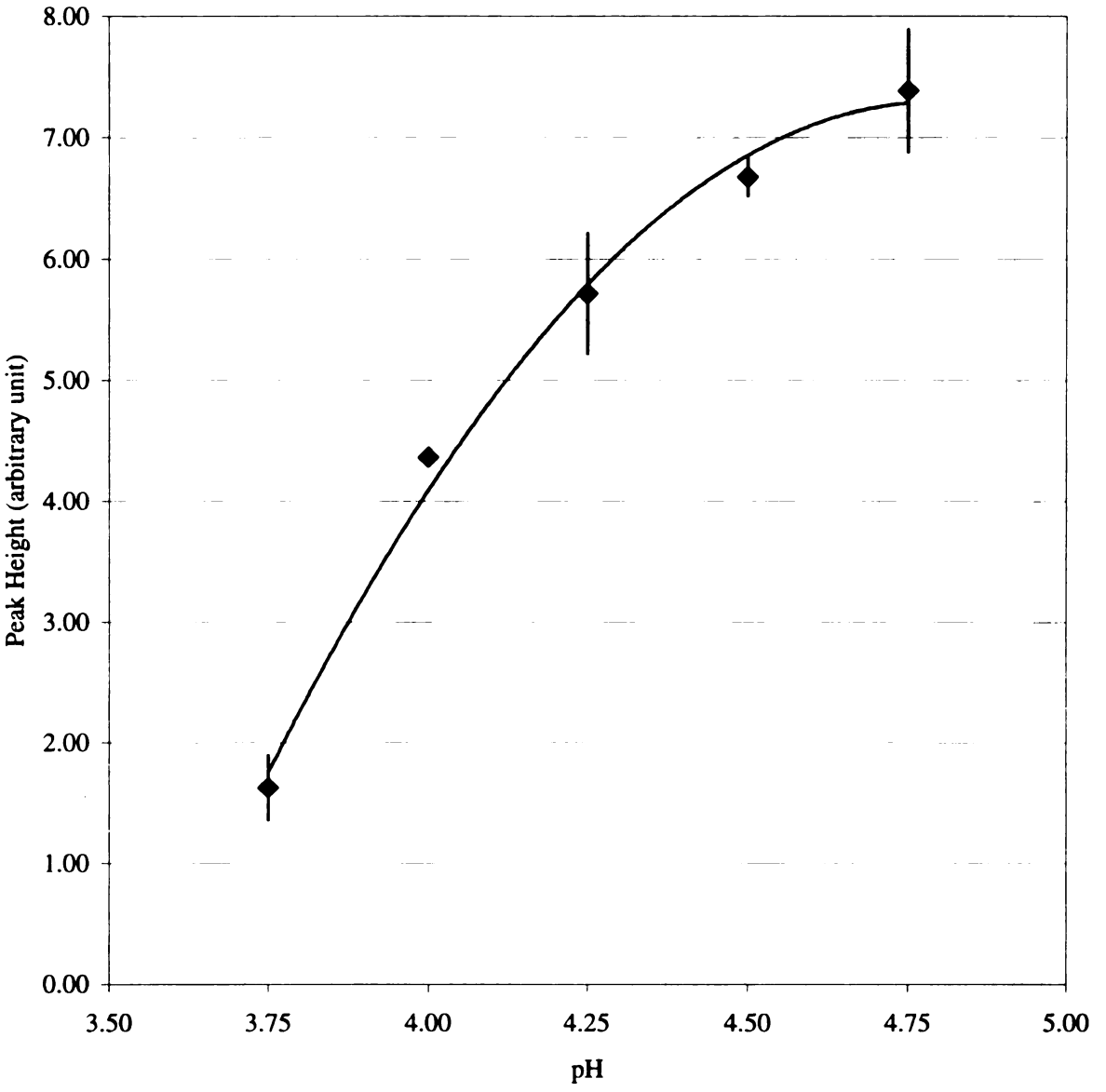

Figure 3.12 Peak height of 1.0×10^{-8} M Co^{2+} at various separation buffer pH values buffer: 2.0×10^{-4} M luminol, 0.01 M NaAc/HAc; post-column CL reagent: 0.05 M H_2O_2, 0.1 M phosphate, final pH = 12.49; flow rate: 6 µL/min; electrophoretic voltage: 10 kV; injection voltage: 10 kV; injection time: 10 s; capillary: 50 µm x 363 µm o.d. x 40 cm.

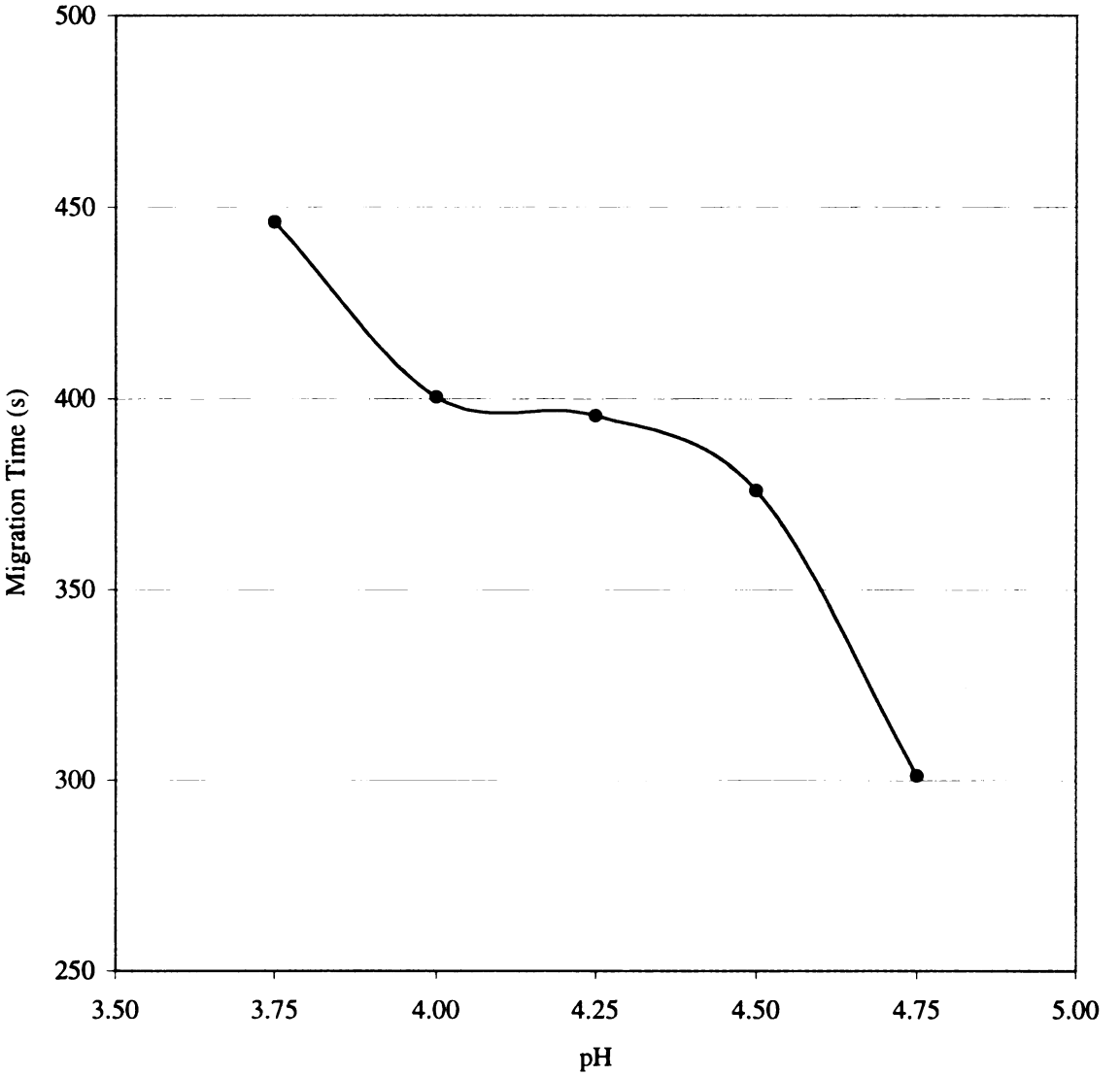

Figure 3.13 Migration time of 1.0×10^{-8} M Co^{2+} at various separation pH values buffer: 2.0×10^{-4} M luminol, 0.01 M NaAc/HAc; post-column CL reagent: 0.05 M H_2O_2, 0.1 M phosphate, final pH = 12.49; flow rate: 6 µL/min; electrophoretic voltage: 10 kV; injection voltage: 10 kV; injection time: 10 s; capillary: 50 µm x 363 µm o.d. x 40 cm.

assuring reproducible migration times. This is particularly important for the separation of transition metal ions since most of the transition metal ions undergo hydrolysis at pH values greater than 5 (10, 11). Transition metal ions show an increasing adsorption to the inner wall of the capillary at higher pH; therefore, their separation is accomplished in acidic solution (pH< 5) (12).

Figure 3.12 shows the peak height of 1.0 x 10^{-8} M Co^{2+} at various separation pH values. Note that the peak height increases with increasing buffer pH. With higher buffer pH, post-column pH switching can be accomplished faster; therefore, more light is generated within the time of CL detection (2s ~ 3s). Figure 3.13 shows the migration time of the sample zone at various buffer pH values. The migration time is decreased at higher pH due to the increased electroosmotic flow rate.

3.4.5 Signal Enhancement by Complexation

The adsorption of transition metals to the capillary wall is one of the major factors that affect migration time, peak height, etc. Even at pH values lower than 4, adsorption cannot be ignored, particularly at high metal ion concentrations. Certain applications (e.g., separation of transition metal cations), require the addition of a weak complexing agent such as hydroxyisobutric acid (HIBA) (13, 14), citric acid (15) or lactic acid (16) to the background electrolyte in order to provide greater differences in mobility.

We studied the stability of the buffer containing 2 x 10^{-4} M luminol and various amounts of HIBA. The results shown in table 3.2 indicate that the buffer (pH = 3.80) with 0.006 - 0.010 M HIBA showed poor stability. The precipitation of luminol in the buffer causes a day-to-day signal variation.

Table 3.2 Stability of the buffers containing various amount of HIBA at pH 3.80

Buffer	Preparation date	Date of luminol precipitation	Stability period
2×10^{-4} M luminol, 0.010 M NaAc/HAc 0 HIBA	11/1/1999	not seen	> 1 month
2×10^{-4} M luminol, 0.010 M NaAc/HAc 0.002 M HIBA	11/1/1999	not seen	> 1month
2×10^{-4} M luminol, 0.010 M NaAc/HAc 0.004 M HIBA	11/1/1999	not seen	> 1 month
2×10^{-4} M luminol, 0.010 M NaAc/HAc 0.006 M HIBA	11/1/1999	11/4/1999	< 3 days
2×10^{-4} M luminol, 0.010 M NaAc/HAc 0.008 M HIBA	11/1/1999	11/2/1999	< 1day
2×10^{-4} M luminol, 0.010 M NaAc/HAc 0.01 M HIBA	11/1/1999	11/2/1999	< 1 day

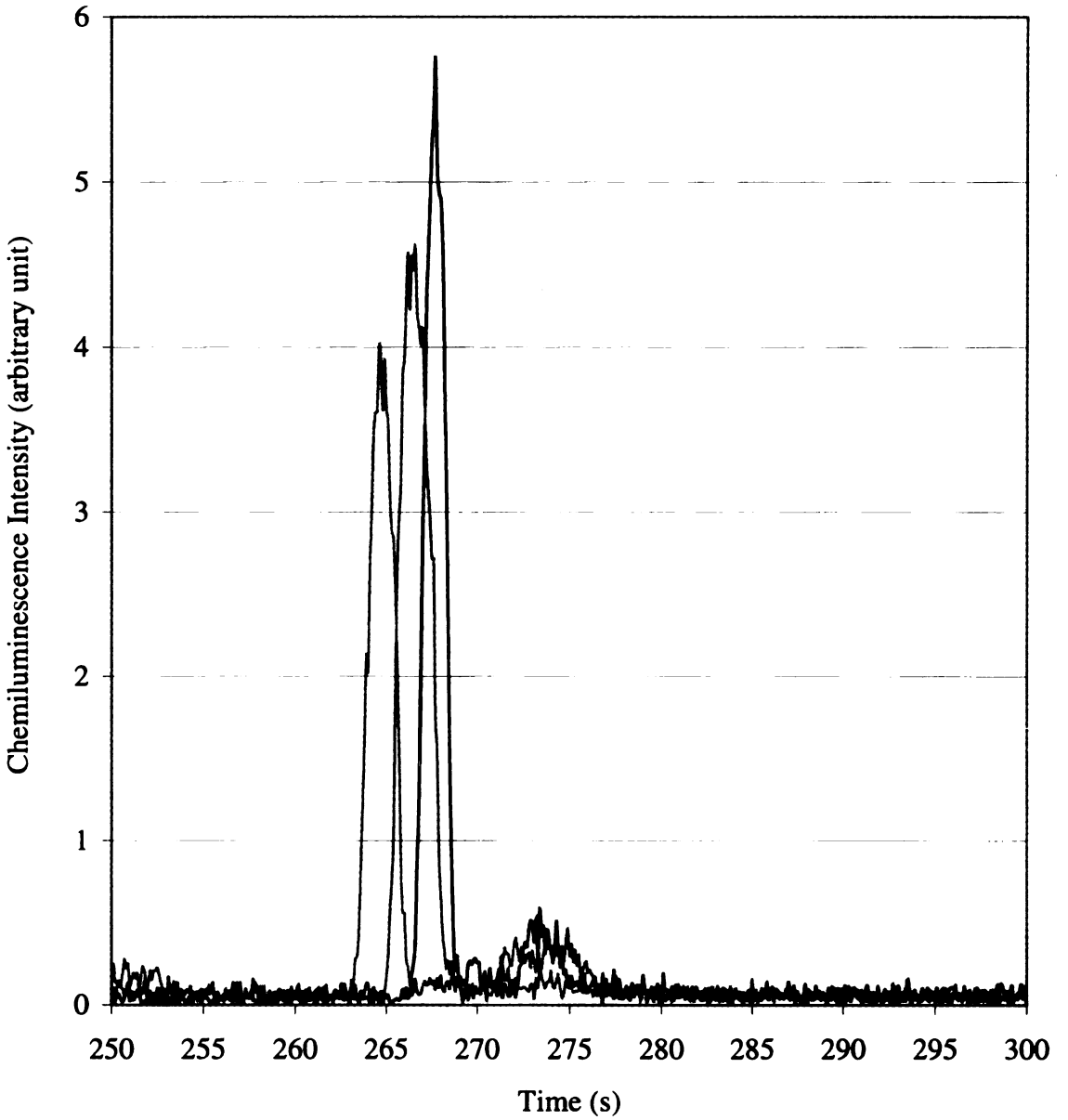

Figure 3.14 Peak height and migration time of Co^{2+}(1.0 x 10^{-8} M), 0.000 M HIBA buffer: 2.0 x 10^{-4} M luminol, 0.01 M NaAc/HAc, 0.000 M HIBA, separation pH = 3.78; post-column CL reagent: 0.05 M H_2O_2, 0.1 M phosphate, pH = 12.49; flow rate: 6 µL/min; electrophoretic voltage: 10 kV; injection voltage: 10 kV; injection time: 10 s; capillary: 50 µm x 363 µm o.d. x 40 cm.

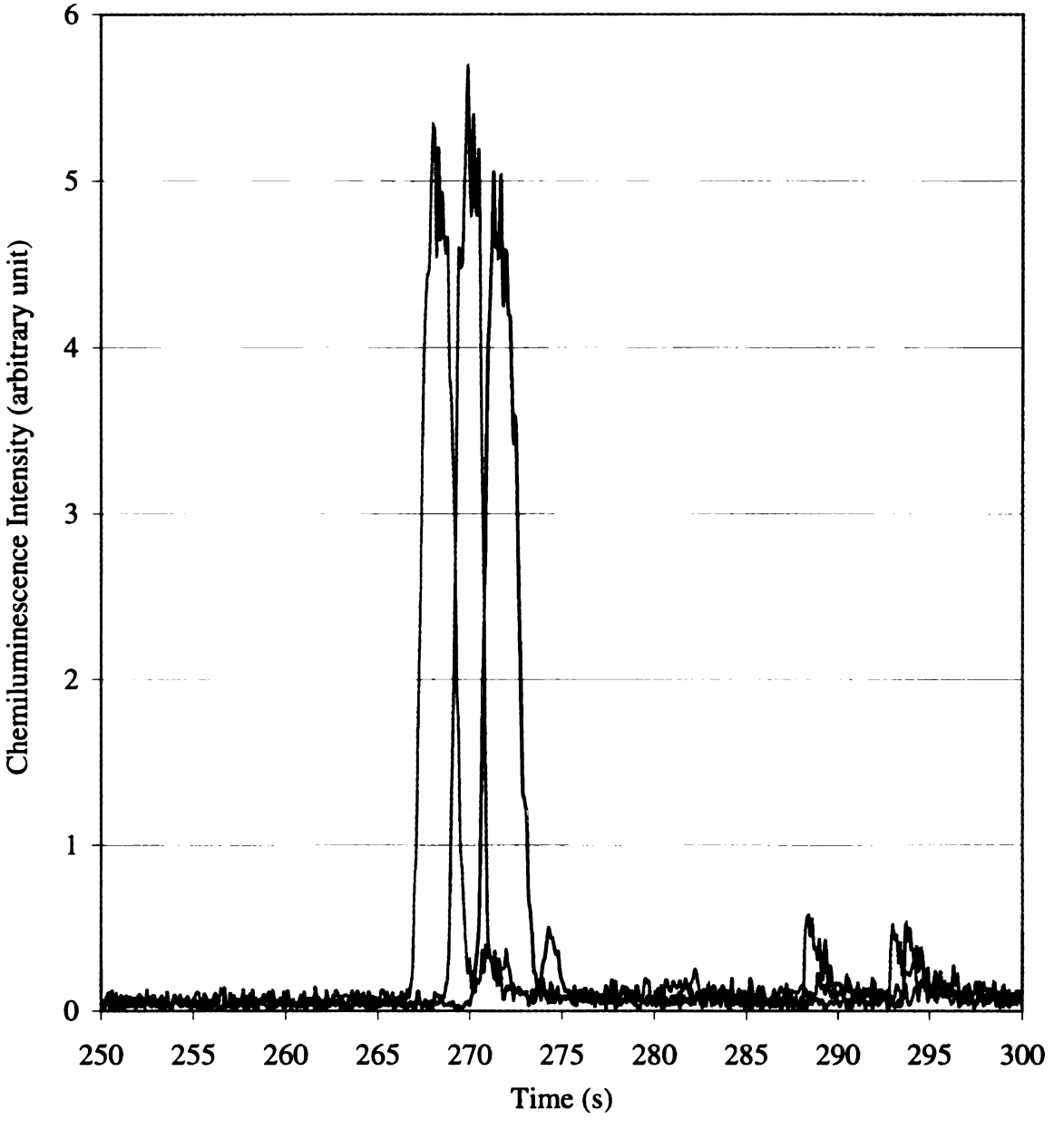

Figure 3.15 Peak height and migration time of Co^{2+} (1.0×10^{-8} M) with 0.002 M HIBA buffer: 2.0×10^{-4} M luminol, 0.01 M NaAc/HAc, 0.002 M HIBA, separation pH = 3.79; post-column CL reagent: 0.05 M H_2O_2, 0.1 M phosphate, pH = 12.49; flow rate: 6 μL/min; electrophoretic voltage: 10 kV; injection voltage: 10 kV; injection time: 10 s; capillary: 50 μm x 363 μm o.d. x 40 cm.

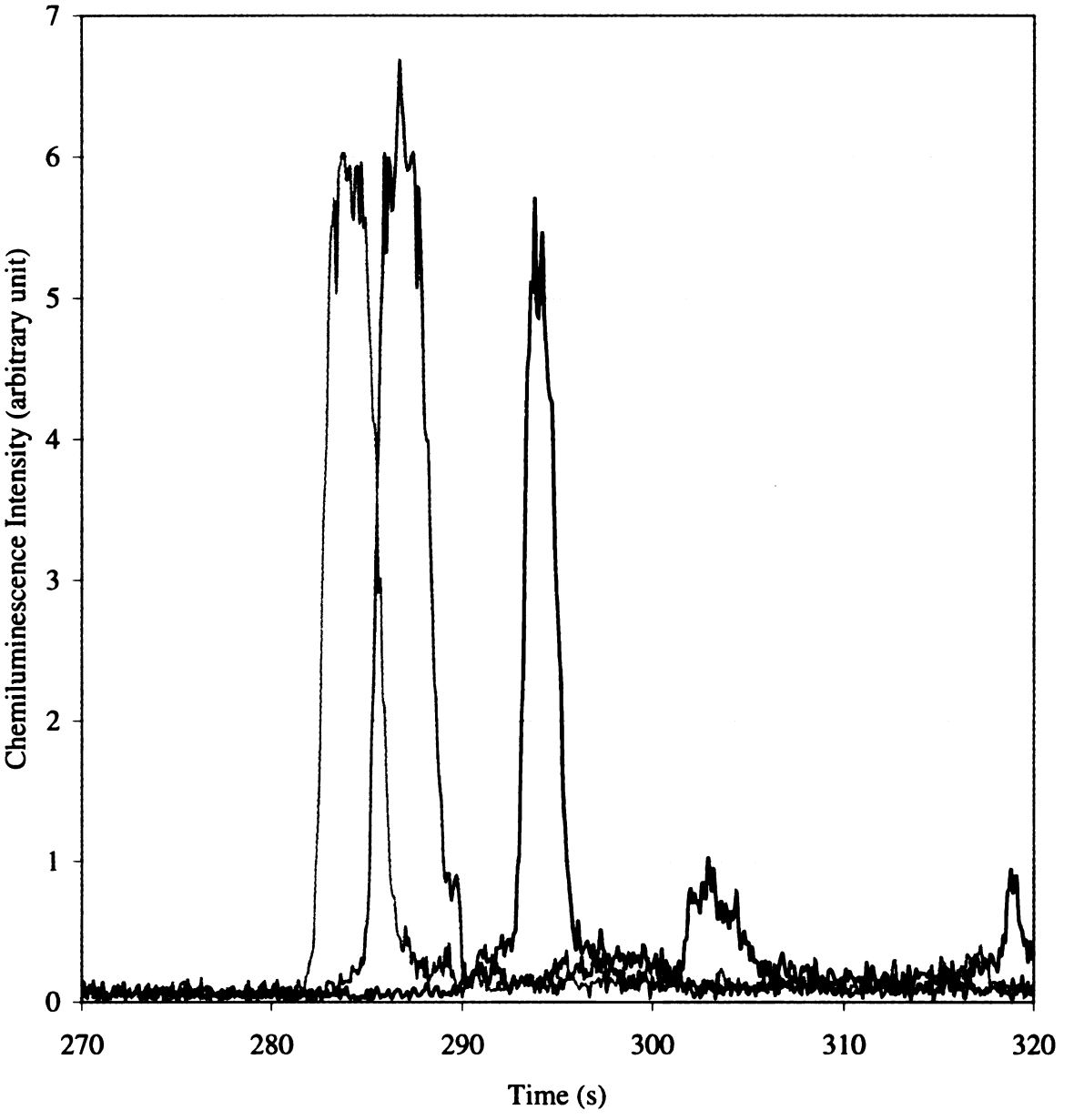

Figure 3.16 Peak height and migration time of Co^{2+} (1.0×10^{-8} M) at 0.004 M HIBA buffer: 2.0×10^{-4} M luminol, 0.01 M NaAc/HAc, 0.004 M HIBA, separation pH = 3.80; post-column CL reagent: 0.05 M H_2O_2, 0.1 M phosphate, pH = 12.49; flow rate: 6 μL/min; electrophoretic voltage: 10 kV; injection voltage: 10 kV; injection time: 10 s; capillary: 50 μm x 363 μm o.d. x 40 cm.

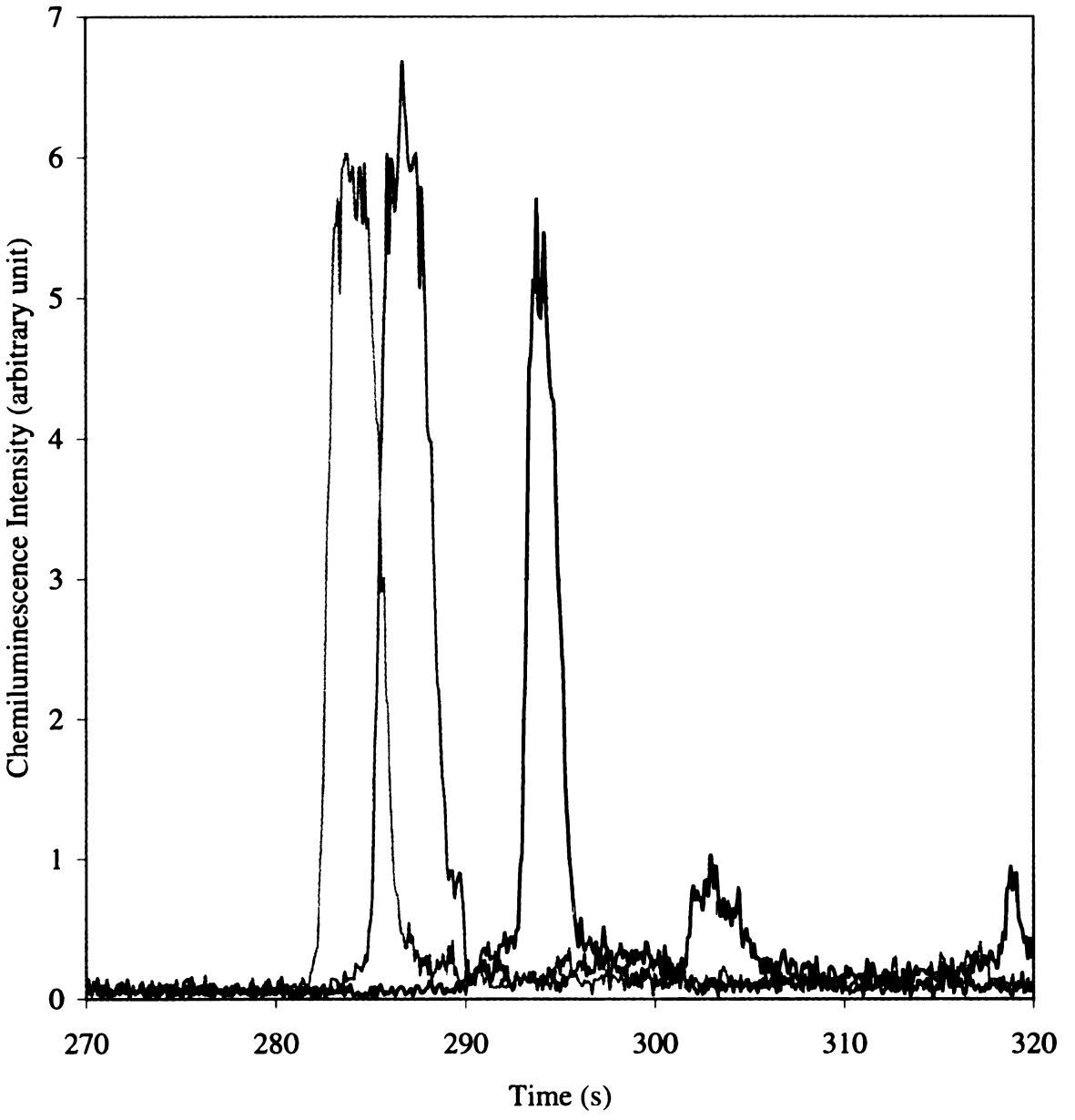

Figure 3.17 Peak height and migration time of Co^{2+} (1.0×10^{-8} M) at 0.006 M HIBA buffer: 2.0×10^{-4} M luminol, 0.01 M NaAc/HAc, 0.006 M HIBA, separation pH = 3.78; post-column CL reagent: 0.05 M H_2O_2, 0.1 M phosphate, pH = 12.49; flow rate: 6 μL/min; electrophoretic voltage: 10 kV; injection voltage: 10 kV; injection time: 10 s; capillary: 50 μm x 363 μm o.d. x 40 cm.

The apparent mobilities of metal ions are affected by the complexation of the metal cations and HIBA. The effect of HIBA on the migration time and peak height was investigated with a buffer (0.01 M NAc/HAc, 2 x 10^{-4} M luminol at pH 3.80) containing various amounts of HIBA. As the HIBA concentration is increased, the apparent mobilities of the metal ions are decreased, which leads to a longer migration time as shown in figure 3.14 - figure 3.17. The peak widths are also increased due to the longer time for diffusion and the distribution of mobilities due to the differing degrees of complexation. The peak height increases with increasing HIBA in the buffer. At high concentrations of HIBA (0.006 M), the peak height decreases due to the inhibition of chemiluminescence as the result of the strong complexation of the metal cations and HIBA.

HIBA can form a weak complex with the transition metal ions, which reduces the adsorption of metal ions to the inner wall of the capillary. However, can formation of the complex affect the chemiluminescence detection reaction?

The interaction between the metal ion, M^{z+}, and the complexing agent, $HIBA^-$, is expressed by the following equilibrium equation (17):

$$M^{z+} + nHIBA^- \rightleftharpoons [M(HIBA)_n]^{z-n} \qquad (3.3)$$

$$K = \frac{[M(HIBA)_n]^{z-n}}{[M^{z+}]\,[HIBA^-]^n} \qquad (3.4)$$

Here K is the stability constant, and n is the number of ligands. The total concentration of metal ion, $[M^+]_T$, is expressed by:

$$[M^{z+}]_T = [M^{z+}] + [M(HIBA)]^{z-1} + [M(HIBA)_2]^{z-2} + \ldots\ldots + [M(HIBA)_n]^{z-n} \qquad (3.5)$$

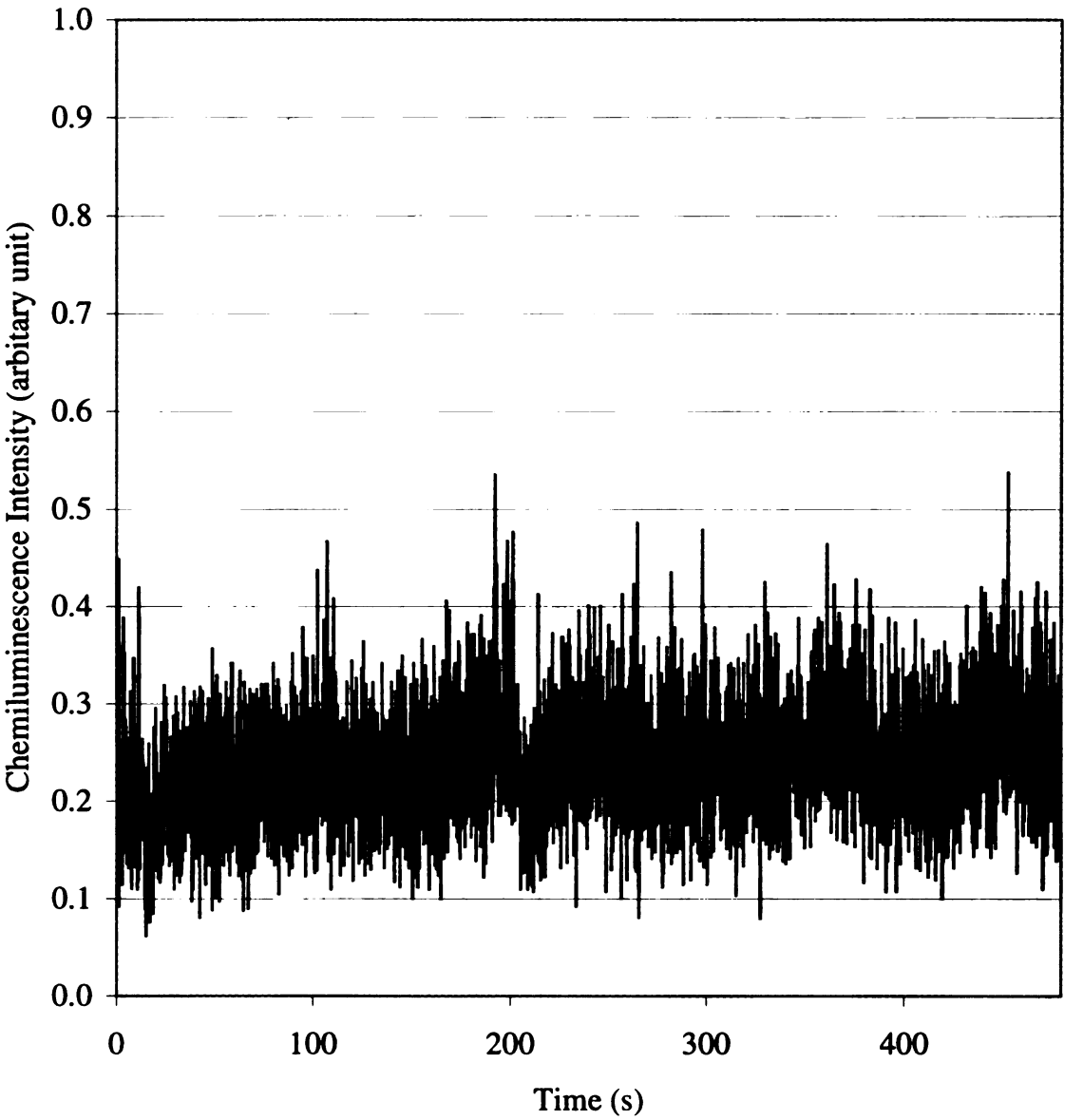

Figure 3.18 Background signal of the buffer containing zero HIBA, pH = 4.00. Buffer: 2.0 x 10^{-4} M luminol, 1.0 x 10^{-8} M Co^{2+}, 0.01 M NaAc/HAc, 0 mM HIBA, pH: 4.00; post-column CL reagents: 0.025 M H_2O_2, 0.050 M phosphate, pH = 13.00; CL reagent flow rate: 6 μL /s; electrophoretic current: 1.2 μA; PMT voltage: 800 V; amplifier: 10^8 V/A; amplifier rise time: 3 ms; separation voltage: 10 kV.

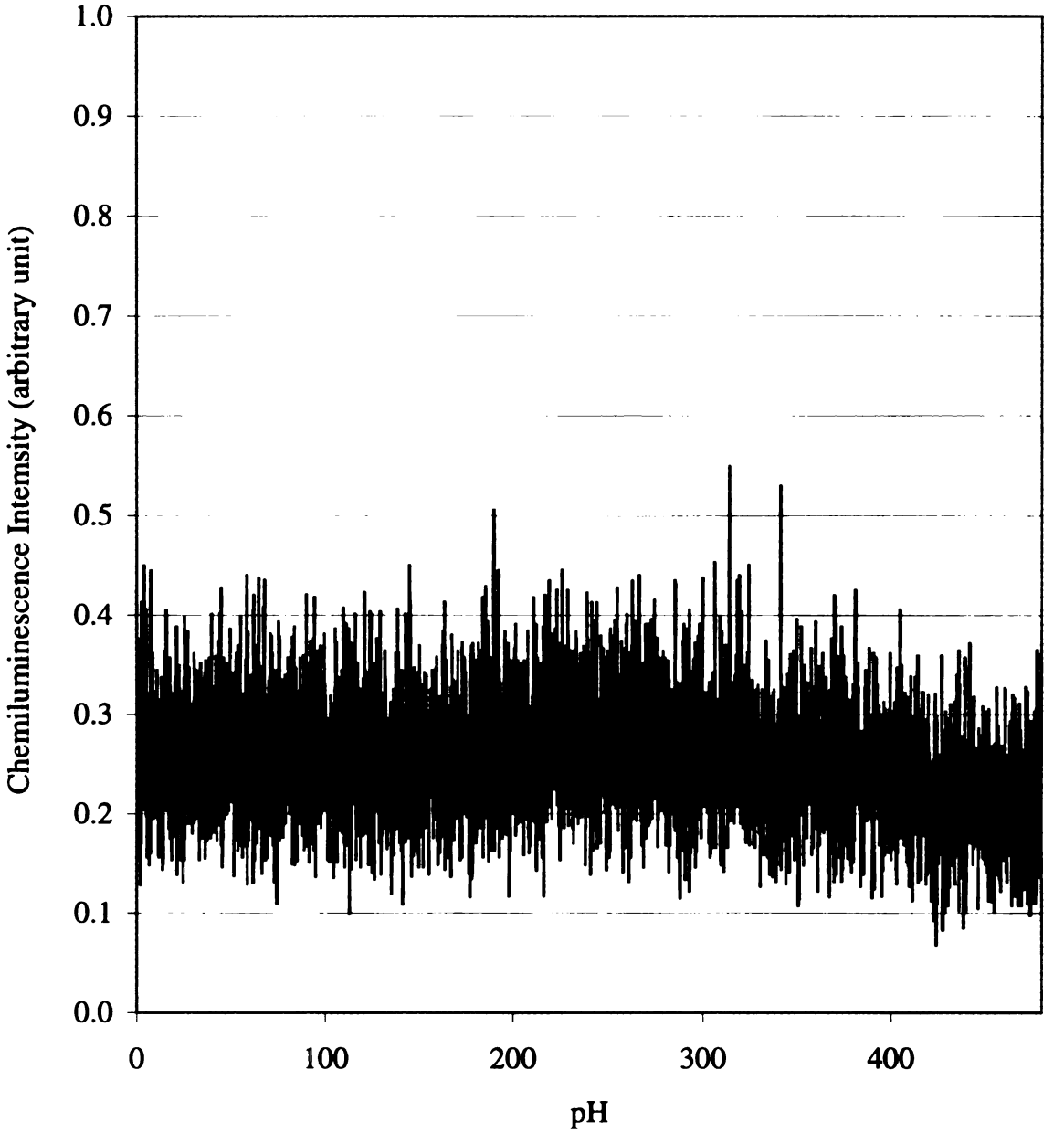

Figure 3.19. Background signal of the buffer containing 0.004 M HIBA, pH = 4.00. Buffer: 2.0 x 10^{-4} M luminol, 1.0 x 10^{-8} M Co^{2+}, 0.01 M NaAc/HAc, 0.004 M HIBA, pH: 4.00; post-column CL reagents: 0.025 M H_2O_2, 0.050 M phosphate, pH = 13.00; CL reagent flow rate: 6 μL/s; electrophoretic current: 1.2 μA; PMT voltage: 800 V; amplifier: 10^8 V/A; amplifier rise time: 3 ms; separation voltage: 10 kV.

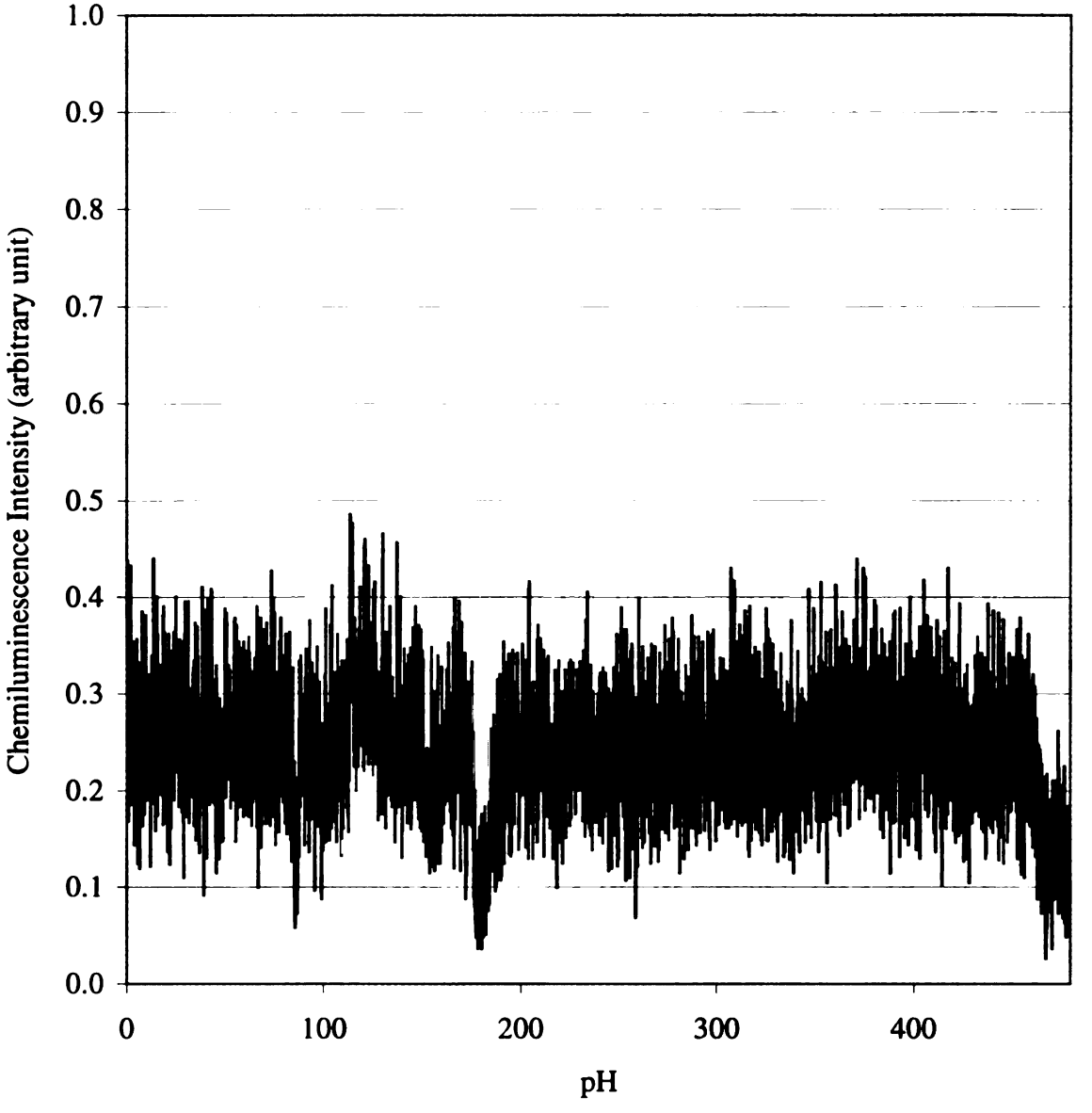

Figure 3.20 Background signal of the buffer containing 8mM HIBA, pH = 4.00
Buffer: 2.0 x 10^{-4} M luminol, 1.0 x 10^{-8} M Co^{2+}, 0.01 M NaAc/HAc, 8 mM HIBA, pH: 4.00; post-column CL reagents: 0.025 M H_2O_2, 0.050 M phosphate, pH = 13.00; CL reagent flow rate: 6 μL/s; electrophoretic current: 2.3 μA; PMT voltage: 800 V; amplifier: 10^8 V/A; amplifier rise time: 3 ms; separation voltage: 10 kV.

HIBA acts as a carrier for the metal ions, and thus reduces the adsorption of metal ions to the capillary wall.

The apparent mobilties of the metal ions are the sum of the mobilities of free metal and each complex:

$$\mu_{app} = \alpha \mu_{M^{z+}} + \beta \mu_{HIBA^{z-1}} + ... + \mu_{EOF} \qquad (3.6)$$

Here α, β are the mole fractions of each species containing the metal ion, and μ_{EOF} is the electroosmotic flow mobility. The uncomplexed metal ions have a higher mobility than the background electrolyte and the peaks show various degrees of fronting (18, 19). The complexed cations possess lower apparent mobilities, which more closely match the mobility of the electrolyte. The peak shapes in Figure 3.14, therefore, exhibit better peak symmetry.

A static test was done to study if the metal-HIBA complex can affect post-column chemiluminescence. A separation buffer of 2 x 10^{-4} M luminol, 1.0 x 10^{-8} M Co^{2+}, 0.01 M acetic acid buffer with different amounts of HIBA was prepared. Under 10 kV high voltage, the Co^{2+}-HIBA complex in the separation buffer migrates toward the ground buffer end. No significant difference in background signal can be seen as shown in figure 3.18 - figure 3.20. This indicates that the metal-HIBA complexes can release the free metal ions quickly upon mixing with the post-column CL reagents.

3.4.6 Effect of pH on Sensitivity for Buffers with HIBA

The effect of buffer pH on peak height and migration time of Co^{2+} is shown in figure 3.21 and figure 3.22. As the buffer pH is increased from 3.50 to 4.00, migration times decrease due to the increased electroosmotic flow; the peak height increases significantly

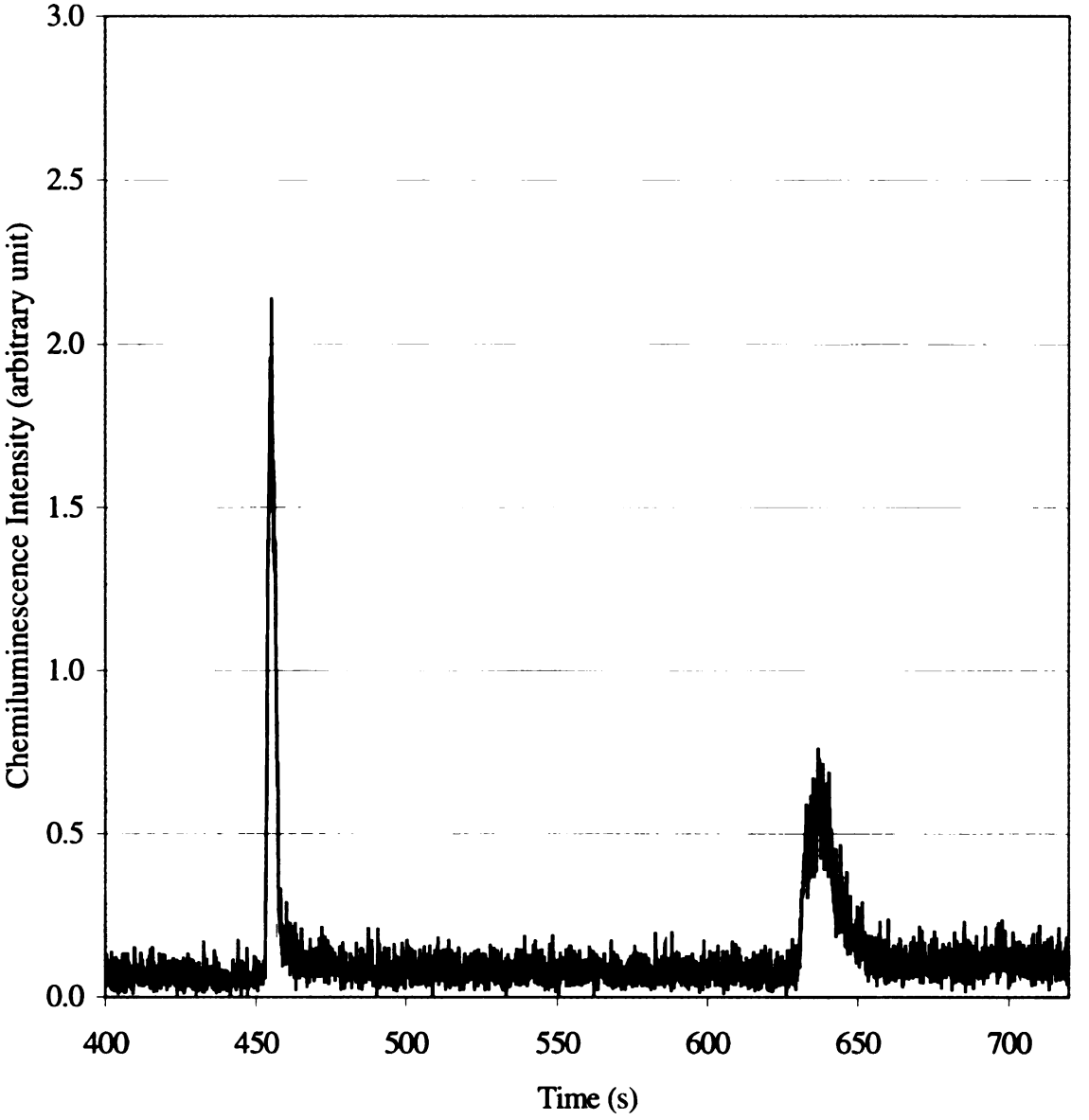

Figure 3.21 Migration time and sensitivity of Co^{2+} for buffer with 5 mM HIBA, **pH 3.50** Sample: 1.0 x 10^{-8} M Co^{2+}, 5.0 x 10^{-7} M Cu^{2+}; buffer: 2.0 x 10^{-4} M luminol, 0.01 M NaAc/HAc, 0.005 M HIBA, pH = 3.50 post-column CL reagent: 0.05 M H_2O_2, 0.1 M phosphate, pH = 12.49; flow rate: 6 µL/min; electrophoretic voltage: 10 kV; injection voltage: 10 kV; injection time: 10 s; capillary: 50 µm x 363 µm o.d. x 50 cm.

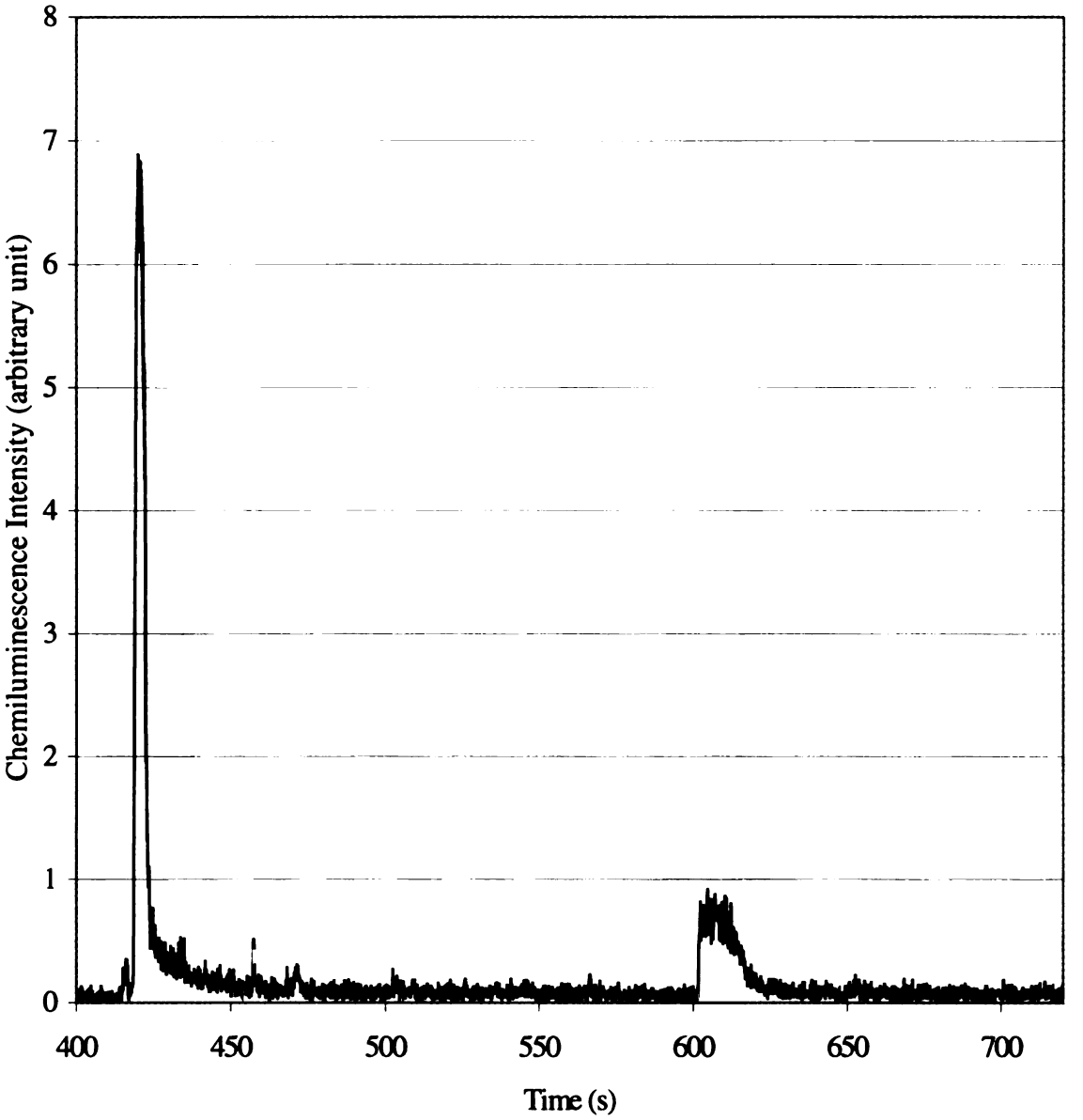

Figure 3.22 Peak height and migration time of Co^{2+} for buffer with 5 mM HIBA, pH 4.00
Sample: 1.0 x 10^{-8} M Co^{2+}, 5.0 x 10^{-7} M Cu^{2+}; buffer: 2.0 x 10^{-4} M luminol, 0.01 M NaAc/HAc, 0.005 M HIBA, pH = 4.00; post-column CL reagent: 0.05 M H_2O_2, 0.1 M phosphate, pH = 12.49; flow rate: 6 μL/min; electrophoretic voltage: 10 kV; injection voltage: 10 kV; injection time: 10 s; capillary: 50 μm x 363 μm o.d. x 50 cm.

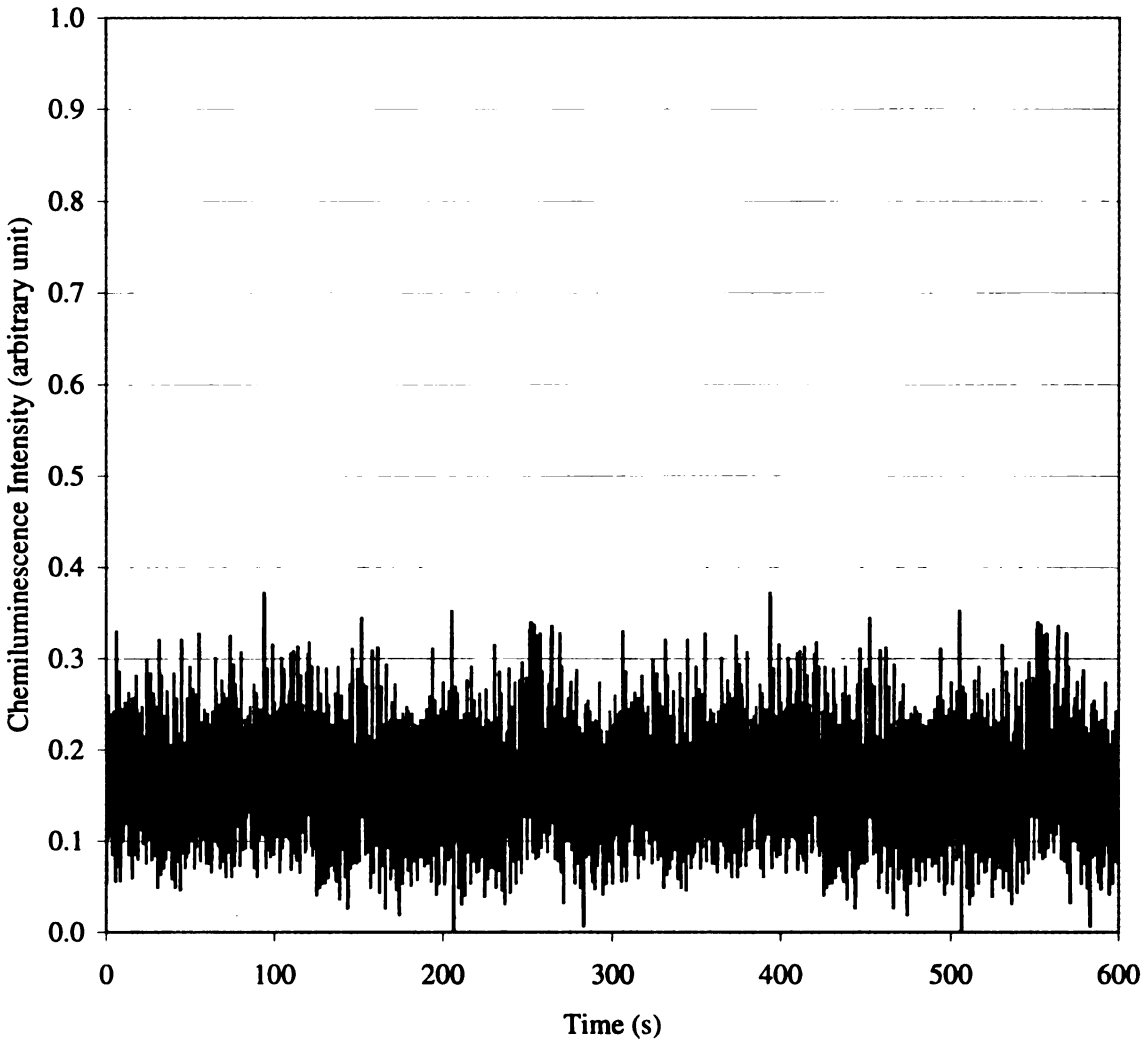

Figure 3.23 Effect of pH (3.85) on the background signal
Buffer: 2.0 x 10^{-4} M luminol, 1.0 x 10^{-8} M Co^{2+}, 0.01 M NaAc/HAc, 0.004 M HIBA, pH 3.85; post-column CL reagents: 0.025 M H_2O_2, 0.050 M phosphate, pH = 13.00; CL reagent flow rate: 6 μL /s; electrophoretic current: 1.2 μA; PMT voltage: 800 V; amplifier: 10^8 V/A; amplifier rise time: 3 ms; separation voltage: 10 kV; capillary: 50 μm x 363 μm o.d. x 40 cm long.

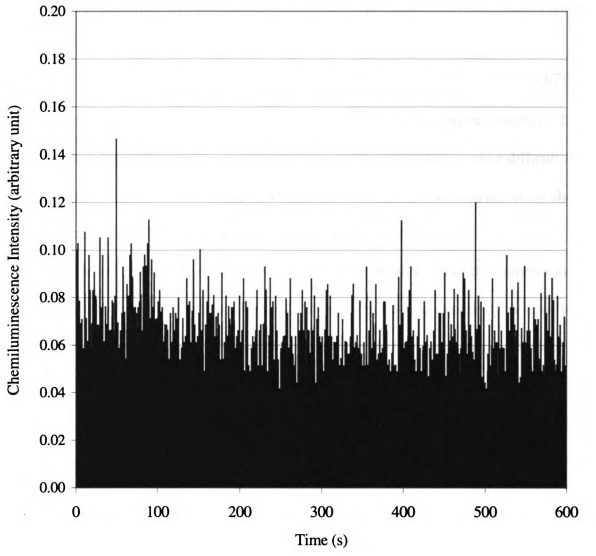

Figure 3.24 Effect of pH (4.10) on the background signal
Buffer: 2.0 x 10^{-4} M luminol, 1.0 x 10^{-8} M Co^{2+}, 0.01 M NaAc/HAc, 0.004 M HIBA, pH 4.10; post-column CL reagents: 0.025 M H_2O_2, 0.050 M phosphate, pH = 13.00; CL reagent flow rate: 6 μL /s; electrophoretic current: 2.0 μA; PMT voltage: 800 V; amplifier: 10^8 V/A; amplifier rise time: 3 ms; separation voltage: 10 kV; capillary: 50 μm x 363 μm o.d. x 40 cm long.

for Co^{2+}. However, no peak can be detected at pH 4.25. Why? As the buffer pH increases, the mole fraction of A^- increases (pKa of HIBA = 3.79)(20) as illustrated by equation 3.7:

$$HA \rightleftharpoons H^+ + A^- \qquad (3.7)$$

This reduces the mole fraction of free metal ions by forming more complex. The increased stability of the metal-complex at higher buffer pH makes it more difficult for the post-column CL reaction to compete for the metal ions from the complex in the short period of time (about 3 s) available; therefore, no peaks can be detected.

The pH affects both the electroosmotic flow and the equilibrium of the complexation as discussed above. To further understand the effect of pH on the sensitivity, a static test was done to study the effect of buffer pH on the background signal in the presence of 0.005 M HIBA. Figure 3.23 (buffer pH 3.85) shows a higher background signal than figure 3.24, because the metal-HIBA complex can still release the free metal ions in ~ 2 s at pH 3.85. However, at pH 4.00, the mole fraction of the HIBA anion (pKa_{HIBA} = 3.65) increases so that it take longer than 2 - 3 s for the complex to release the free metal cations.

3.4.7 Reproducibility of Sample Injection

The reproducibility of 10 electrokinetic injections is listed in Tables 3.3 and 3.4. The reproducibility is not as good as achieved with on-column detection (2 - 10%), perhaps due to the extra variance associated with post-column CL detection.

Table 3.3 Reproducibility of 10 Electrokinetic Injections of Co^{2+}

Peak Height 1.0×10^{-9} M Co^{2+}	Mean	Standard Deviation	RSD
10 injections	5.64	0.67	11.89%

Sample: 1.0×10^{-9} M Co^{2+}; buffer: 2.0×10^{-4} M luminol, 0.01 M acetic acid, pH = 4.75. Capillary: 50 μm i.d. x 363 μm o.d. x 50 cm long fused silica capillary. Separation voltage: 10 kV. Amplifier: 10^8 V/A, 3 ms response time. PMT voltage: 800 V. Post-column reagents: 0.05 M H_2O_2, 0.1 M phosphate (pH = 12.50), flow rate: 3 μL/min per channel. Voltage of injection: 10 kV. Time of injection: 4s.

Table 3.4 Reproducibility of 10 Electrokinetic Injections of Co^{2+}

Peak Height 1.0×10^{-6} M Cr^{3+}	Mean	Standard Deviation	RSD
10 injections	3.45	0.62	17.98%

Sample: 1.0×10^{-9} M Co^{2+}, 1.0×10^{-6} M Cr^{3+} in deionized distilled water; separation buffer: 2×10^{-4} M luminol, 0.010 M NaAc/HAc, pH: 4.74; post-column CL reagents: 0.025 M H_2O_2, 0.050 M phosphate, pH = 12.49; flow rate: 6 μL /s; electrophoretic current: 2.0 μA; PMT voltage: 800 V; amplifier: 10^8 V/A; amplifier rise time: 3 ms; separation voltage: 10 kV; sample injection: 10 s at 10 kV; capillary: 50 μm i.d. x 363 μm x 40 cm long.

3.4.8 Number of Theoretical Plates with Post-Column Chemiluminscence Detection

The number of theoretical plates is influenced by many factors such as sample, and separation conditions. We estimated the number of theoretical plates for 1.0×10^{-11} M Co^{2+} based on figure 3.25. The peak showed a migration time of 188.9 s and a peak width of 1.3 s at the baseline. The number of plates was calculated from the equation 3.8:

$$N = 16\left(\frac{t_r}{w}\right)^2 \tag{3.8}$$

Here t_r is the migration time of the sample zone, and w is the peak width at the baseline.

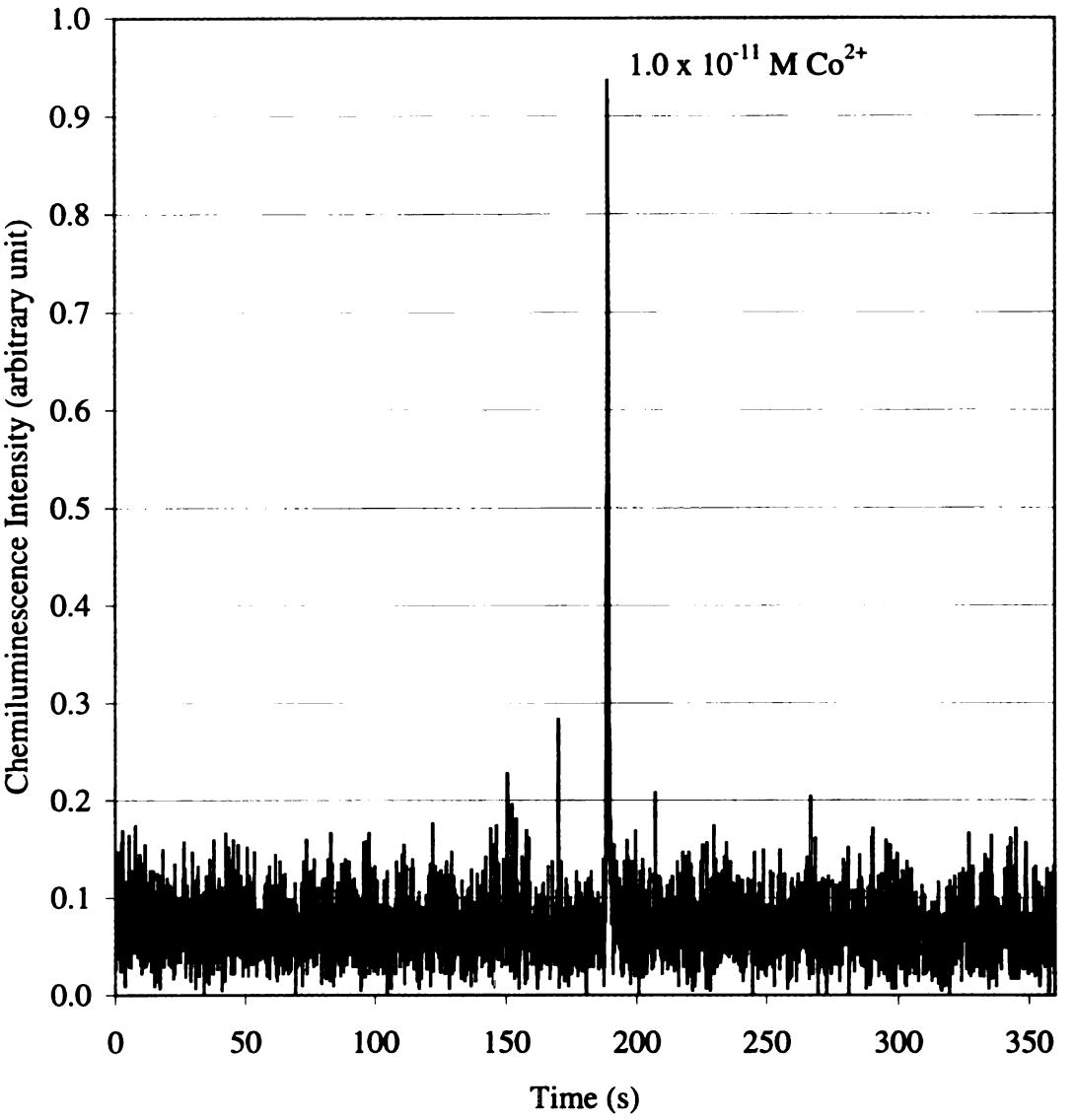

Figure 3.25 Theoretical plates for 1.0×10^{-11} M Co^{2+} (t_r: 188.9 s; peak width: 1.3 s) Sample: 1.0×10^{-11} M in deionized distilled water; separation buffer: 2×10^{-4} M luminol, 0.010 M NaAc/HAc, pH: 4.74; post-column CL reagents: 0.025 M H_2O_2, 0.1 M phosphate, pH = 12.49; flow rate: 6 µL /s; electrophoretic current: 2.0 µA; PMT voltage: 800 V; amplifier: 10^8 V/A; amplifier rise time: 3 ms; separation voltage: 10 kV; sample injection: 10 s at 10 kV; capillary: 50 µm i.d. x 363 µm o.d. x 40 cm long.

We were able to achieve 340,000 plates for 10^{-11} M Co^{2+}, which is superior to the 200,000 plates for isoluminol as reported by other workers (7) using CL detection in CE. This plate number matches those with on-column detection, meaning that there is little additional contribution to peak broadening from the post-column CL reaction. Figure 3.2a gives 189,225 plates for 1.0 x 10^{-6} M Cr^{3+} and 116,64 plates for 1.0 x 10^{-6} M Cu^{2+}.

3.4.9 Calibrations for Transition Metal Cations

A series of standard solutions containing various levels of Co^{2+}, Cr^{3+}, and Cu^{2+} was prepared using deionized distilled water. All these standard solutions were used under the same experimental conditions.

The peak areas for Co^{2+}, Cr^{3+}, and Cu^{2+} were plotted against concentrations as shown in figures 3.26, 3.27, and 3.28 respectively. The curves deviate from linearity at high concentrations because of the increased adsorption to the capillary wall. Based on a S/N ratio of 3, the detection limit is estimated in table 3.5. The detection limit for Co^{2+} with CL detection is 6 orders of magnitude lower than that with UV detection and electrochemical detection (ECD); the detection limit of Cr^{3+} with CL detection is 3 orders of magnitude lower than that with ECD. The detection limit of Cu^{2+} with CL detection is two orders of magnitude lower than that with UV detection and ECD.

Table 3.5 Detection limits for some transition metals using CL and other detectors

Cations	Detection Limit (UV) Ref. (21)	Detection Limit (ECD) ref (4)	Detection Limit (CL)
Co^{2+}	110 ppb or 1.8 x 10^{-6} M	5.1 x 10^{-6} M	1.5 x 10^{-12} M
Cr^{3+}		3.8 x 10^{-5} M	5.0 x 10^{-8} M
Cu^{2+}	206 ppb or 3.2 x 10^{-6} M	5.0 x 10^{-6} M	3.0 x 10^{-8} M

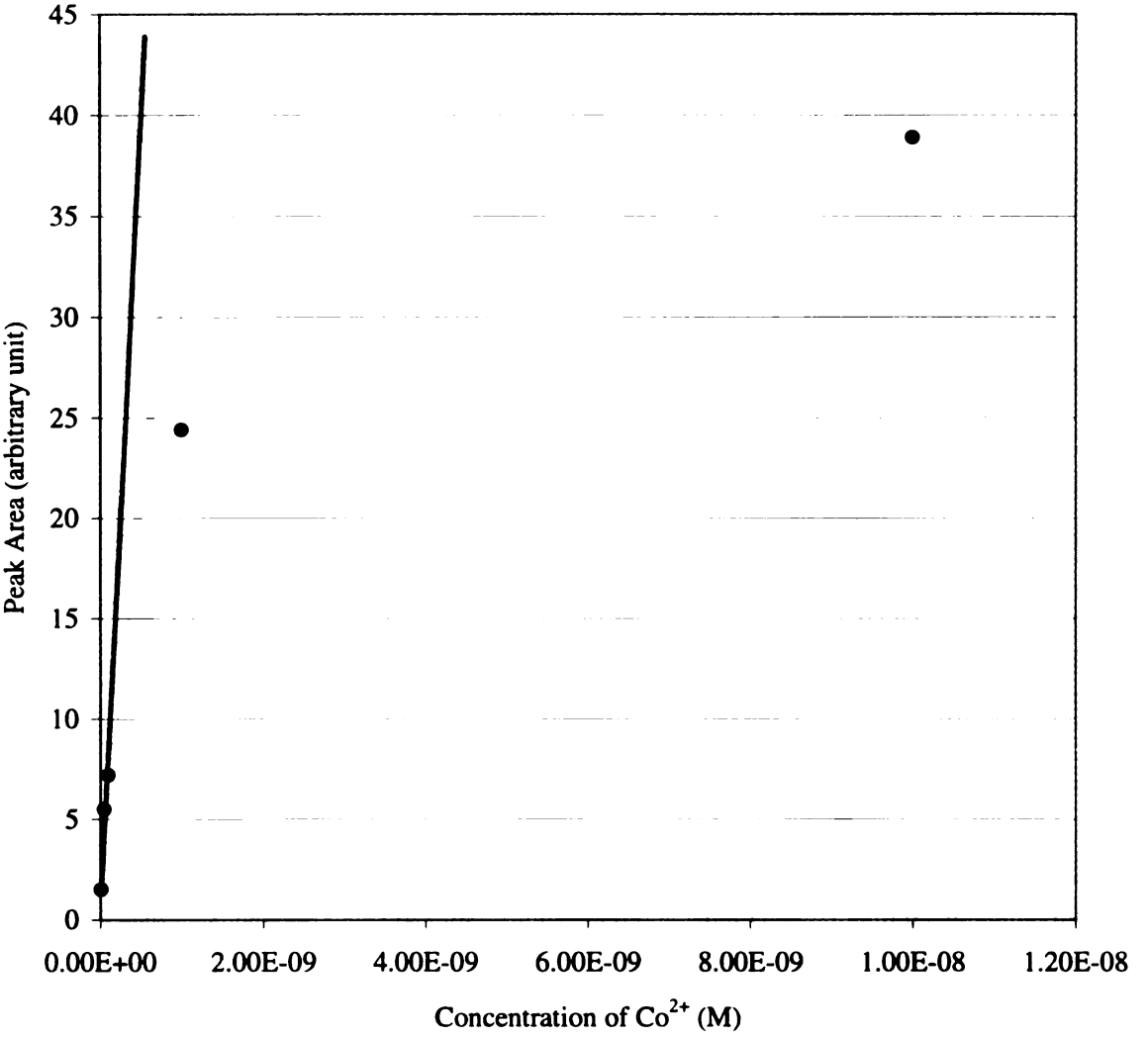

Figure 3.26 Calibration curve for Co^{2+}.
Sample: 1.0 x 10^{-11} M - 1.0 x 10^{-8} M Co^{2+} in deionized distilled water; separation buffer: 2 x 10^{-4} M luminol, 0.010 M NaAc/HAc, pH: 4.74; post-column CL reagents: 0.025 M H_2O_2, 0.1 M phosphate, pH = 12.49; flow rate: 6 μL /s; electrophoretic current: 2.0 μA; PMT voltage: 800 V; amplifier: 10^8 V/A; amplifier rise time: 3 ms; separation voltage: 10 kV; sample injection: 10 s at 10 kV.

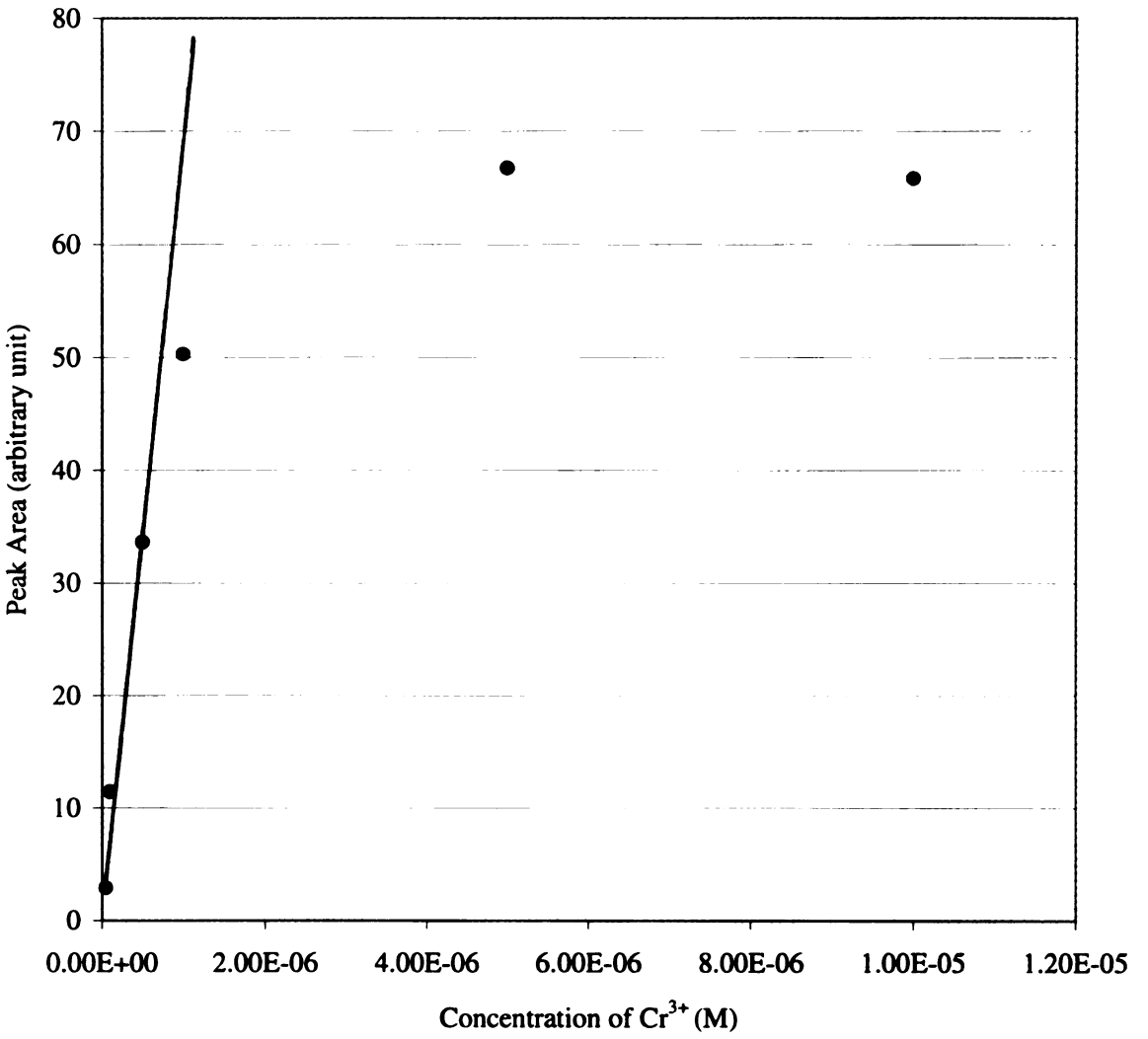

Figure 3.27 Calibration curve for Cr^{3+}.
Sample: 5.0 x 10^{-8} M - 1.0 x 10^{-5} M Cr^{3+} in deionized distilled water; separation buffer: 2 x 10^{-4} M luminol, 0.010 M NaAc/HAc, pH: 4.74; post-column CL reagents: 0.025 M H_2O_2, 0.1 M phosphate, pH = 12.06; flow rate: 6 μL /s; electrophoretic current: 2.0 μA; PMT voltage: 800 V; amplifier: 10^8 V/A; amplifier rise time: 3 ms; separation voltage: 10 kV; sample injection: 10 s at 10 kV.

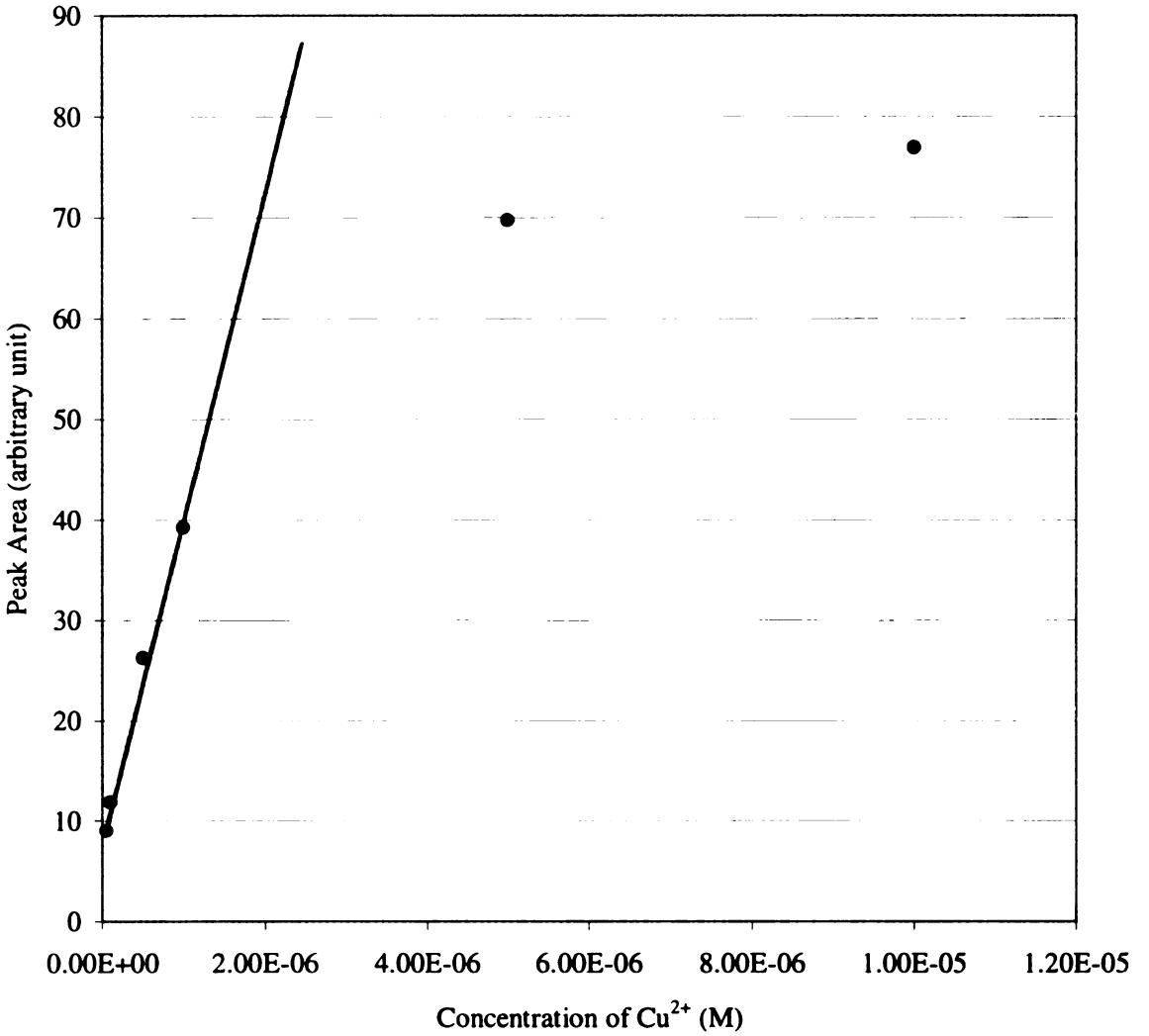

Figure 3.28 Calibration curve for Cu^{2+}.
Sample: 5.0 x 10^{-8} M - 1.0 x 10^{-5} M Cu^{2+} in deionized distilled water; separation buffer: 2 x 10^{-4} M luminol, 0.010 M NaAc/HAc, pH: 4.74; post-column CL reagents: 0.025 M H_2O_2, 0.1 M phosphate, pH = 12.06; flow rate: 6 μL /s; electrophoretic current: 2.0 μA; PMT voltage: 800 V; amplifier: 10^8 V/A; amplifier rise time: 3 ms; separation voltage: 10 kV; sample injection: 10 s at 10 kV.

3.10 Conclusions

This work demonstrates the sensitivity of chemiluminescence detection compared to other techniques such as electrochemical and UV detection. The post-column CL reactor demonstrates a high separation efficiency of 340,000 plates, which is even competitive with those with on-column detection in capillary zone electrophoresis. Many factors such as the pH of the post-column CL reagents and separation buffer were optimized. Reproducibility of post-column CL detection is not as good as that with on-column detection due to the extra variance introduced by the post-column mixing and reaction. The calibration curve showed deviations from linearity at high concentration due to the increased adsorption of metal ions to the active sites on the capillary surface. It is necessary to reduce the adsorption of transition metal cations, particularly at high concentrations.

List of References

1 Hara, T.; Okamura, S.; Kato, J.; Yokogi, J.; Nakajima, R. *Anal. Sci.* **1991**, *7*, 261-264.

2. Dadoo, R.; Colon, L.A.; Zare, R. N. *J. High Resolution Chromatography*, **1992**, *15*, 133.

3. Evans, C. E. *Anal. Chem.* **1997**, *69*, 2952-2954.

4. Lu, W. Z.; Cassidy, R. M. *Anal. Chem.* **1993**, *65*, 1649-1653.

5. Fuller, R. R.; Sweedler, J. V. *Anal. Chem.* **1999**, *71*, 4014-4022.

6. Ingle, J. D.; Crouch, S. R., *Spectrochemical Analysis*, Prentice Hall, Englewood Cliffs, New Jersey, **1988**, p 479-485.

7. J. Y. Zhao, J. Labba, and N. J. Dovichi, *J. of Microcolumn Separation*, **1993**, *5*, 331.

8. CRC Handbook of Chemistry and Physics, 72th edition, 195.

9. Peng, C. H., *"Application of Micro-Machining Technology for the Construction of End-Column Conductivity Detector in Capillary Zone Electrophoreis", M. Sc. Thesis,* p 57, University of Alberta, **1993**.

10. Riviello, J M.; Harrold, M. P. J of Chromatography A, **1993**, *652*, 385-392.

11. Kuban, P.; Karlberg, B. *Anal. Chem.* **1998**, *70*, 360-365.

12. Weston, A.; Brown, P. R.; Jandik, P.; Jones, W. R.; Heckenberg, A. L. *J. Chromatogr.* **1992**, *593*, 289-295.).

13. Foret, F.; Fanali, S.; Nardi, A.; Bocek, P. *Electrophoresis* **1990**, *11*, 780-783.

14. Chen, M.; Cassidy, R. M. *J. Chromatogr.* **1993**, 640, 425-431.

15. Lin, T. I.; Lee, Y. H.; Chen, Y. C. *J. Chromatogr.* **1993**, *654*, 167-176.

16. Shi, Y.; Frits, J. S. *J. Chromatogr.* **1993**, *640*, 473-479.

17. Swaile, D. F.; Sepaniak, M. J. *Anal. Chem.* **1991**, *63*, 179.

18. Mikkers, F. E. P.; Everaerts, F. M.; Verheggen, Th. P. E. M *J Chromatogr.*, **1979**, *169*, 1-10.

19. Foret, F.; Fanali, L.; Ossicini, L.; Bocek, P. *J Chromatogr.*, **1989**, *470*, 299.

20. Perrin, D. D. Stability Constants of Metal Ion Complexes, Part B; IUPAC Chemical Data Series 22; Pergamon Press: Oxford, 1982; p187.

21. Weston, A.; Brown, P. R.; Jandik, P.; Jones, W. R.; Heckenberg, A. L. *J. Chromatogr.* **1992**, *593*, 289-295.

Chapter 4

Automatic Sample Injection System with No Interruption of High Voltage in Capillary Zone Electrophoresis

Sample introduction is one of the very challenging aspects of capillary zone electrophoresis. Electrokinetic introduction and hydrodynamic introduction are the most commonly used sample introduction methods. In electrokinetic introduction, an electric field is applied across the capillary for a certain period of time to move the sample into the capillary. In hydrodynamic introduction, the sample is forced into the capillary using the siphoning effect. Electrokinetic introduction causes differential injection of species due to difference in their mobilities. Hydrodynamic injection causes a parabolic profile of sample zones due to frictional forces at the capillary walls.

The common drawback of these two injection methods is the relocation of the separation capillary during sample injection, which is not convenient for automation. Another drawback is the low sample throughput limited by the migration time. In this chapter, we describe an automatic sample injection system, which requires neither the relocation of separation capillary nor the disconnection of the electric field during sample injection. In this automatic sample injector, the sample is stored in a reservoir 76 cm higher than the high voltage reservoir. There are two identical capillaries, one for sample injection, one for separation. The two capillaries are accurately aligned. Upon injection, the sample capillary mounted on a sample platform rotates toward the separation capillary and meets the separation capillary for a time period controlled by computer. During this

process, the sample flows from sample capillary into the separation capillary driven by gravity. After injection, the sample capillary moves away from the separation capillary. The automatic sample injector allows sample injection without the interruption of high voltage, unlike traditional electrokinetic or hydrodynamic injection.

4.1 Instrumentation for the Automatic Sample Injector

The automatic injection system includes a mechanical system, an electronic control circuit and a computer. A 10" x 18" x ½ " aluminum plate with ¼"-20 holes spaced 1" apart was used as a breadboard for mounting various parts. The computer can give a ± 12 V voltage output with 2 μA of current. This current running through the electromagnet is too low to attract the steel plate glued to the Plexiglas rotary platform shown in figure 4.1. As we can see from figure 4.1, the pinch valve and the solenoid are synchronized. The pinch valve is normally closed, which prevents the leakage of sample solution. As the solenoid is actuated to pull the sample platform, the pinch valve opens in 30 ms and sample solution is ready to be delivered into the separation capillary. It takes 1.04 s for the sample platform to move into position to join the separation capillary. This period of time must be reproducible or else the time required for joining the sample and the separation capillary will not be consistent.

This automatic sample injection system uses two segments of fused silica capillaries as sample capillary and separation capillary respectively, and requires the accurate alignment of the two segments for reproducible sample injection. When the computer sends out a trigger signal (4V), the DC power supply gives 12 V to the solenoid and the

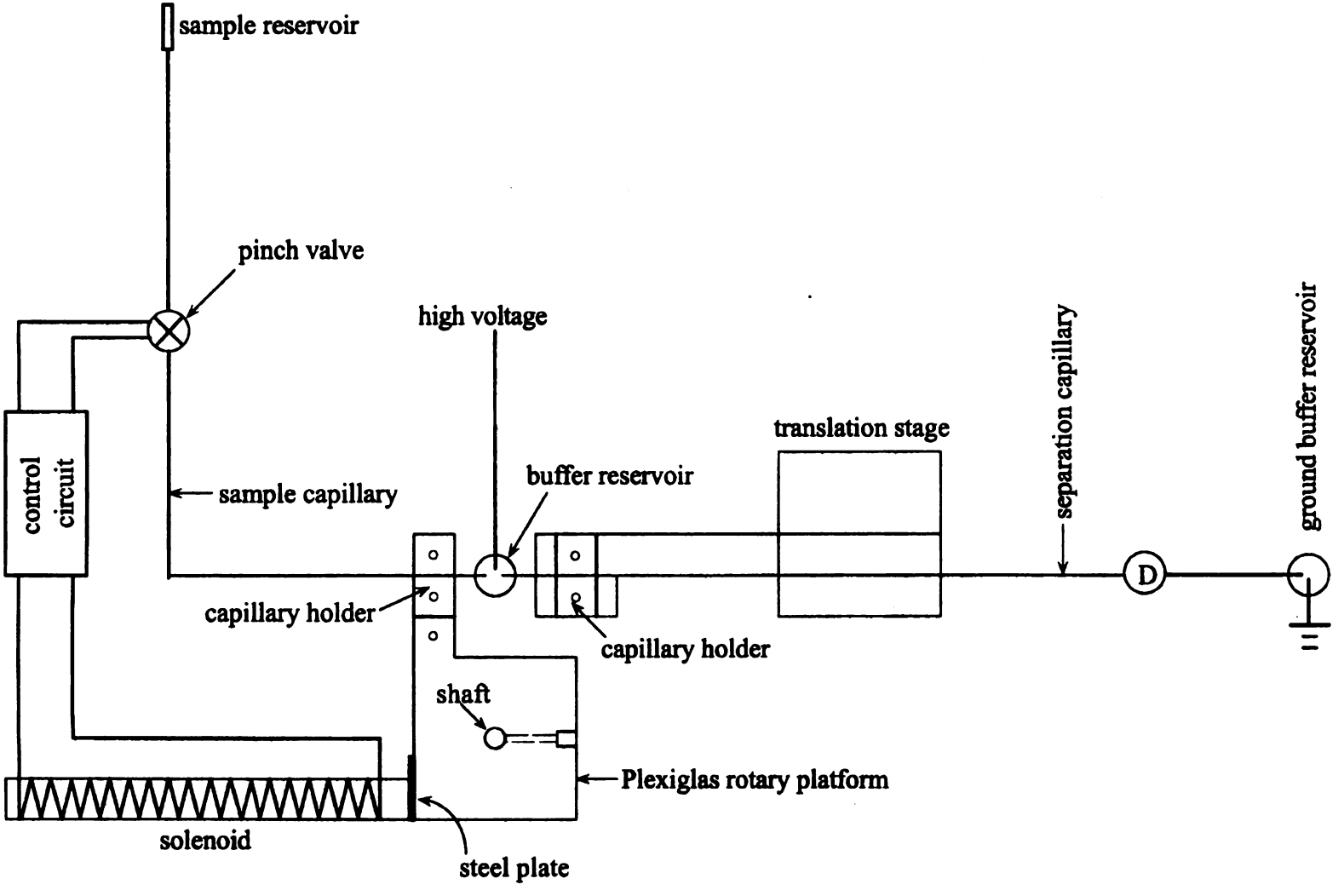

Figure 4.1 Automatic sample injection system in capillary electrophoresis

pinch valve in less than 1 μs, through the electronic circuit shown in figure 4.2. Here the field effect transistor (MTP3ONO6EL, Motorola) acts as a switch. A ¾" x 1" x 1/64" thick steel plate is glued to the left side of the sample platform for electromagnetic attraction. The sample capillary is held on a Plexiglas sample platform sitting on a ¼" shaft. The separation capillary is held on another Plexiglas platform mounted on a translation stage. Upon activation of the electronic circuit in figure 4.2, the sample platform with the steel plate is attracted by the electromagnet. The sample capillary on the sample platform slowly meets the separation capillary with the assistance of the damping device described in figure 4.3. It is very important to align the sample capillary to the separation capillary for a good reproducibility. The alignment of the sample capillary is assured by the two precision ball bearings described in figure 4.4.

The normally closed pinch valve opens upon its activation. The sample capillary delivers the sample and is detached from the separation capillary upon the repelling of the spring and the attraction from the permanent magnet mounted on the solenoid support as shown in figure 4.5. The pinch valve is closed and the injection is over. This is how the automatic sample injection system works.

4.2 Electronic Circuit

The power supply to the sample injection system should have a short turn on/off time (< 1 ms). Any delay will cause inaccurate sample injection time. The 12 V DC power-supply can not be turned on and off directly due to the delay. The electronic circuit was thus designed to solve the problem of delay as shown in figure 4.3. The field effect transistor has a very fast response time (< 1 μs). The electronic circuit is able to give 12 V

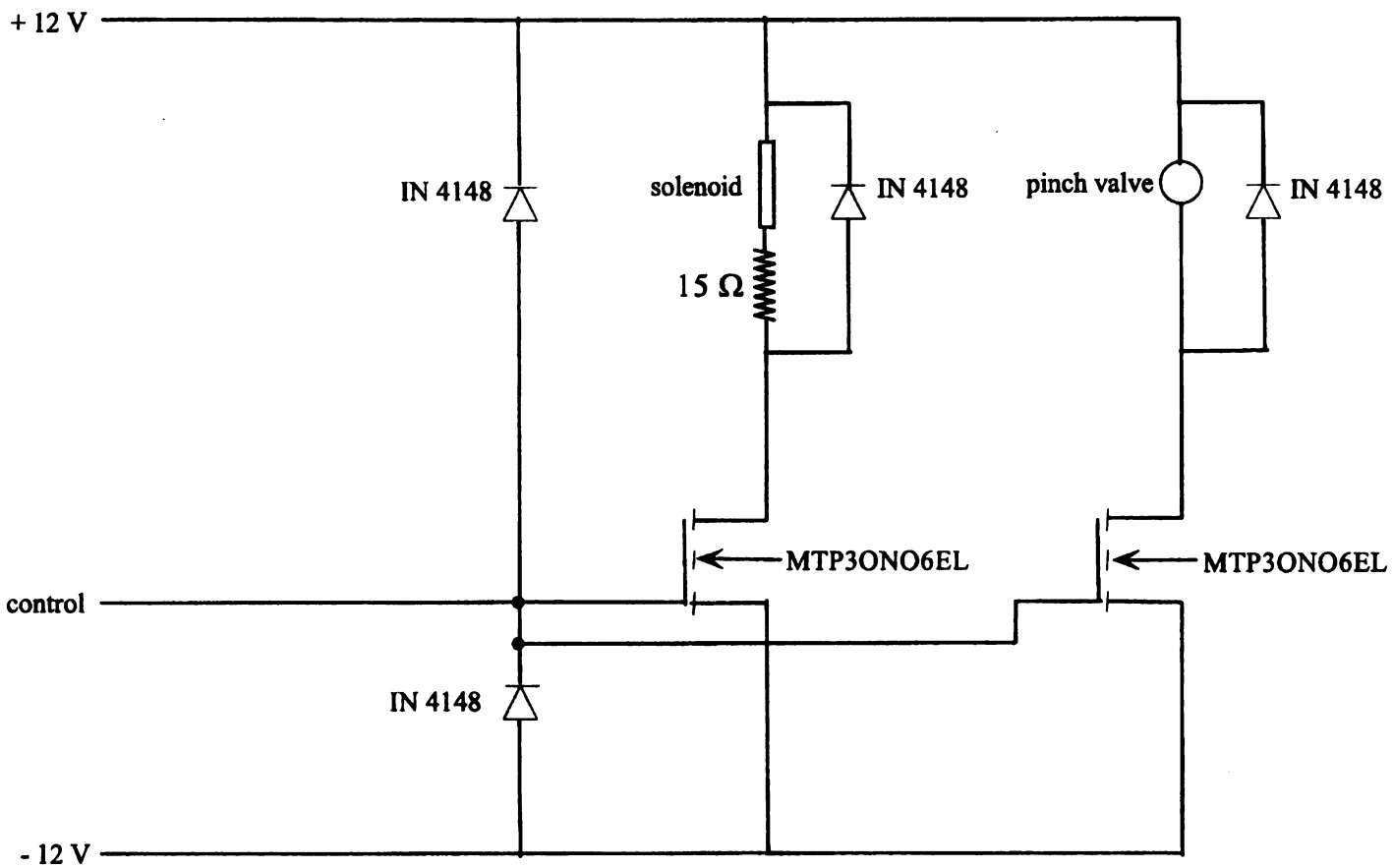

Figure 4.2 Electronic circuit for automatic injection system in capillary electrophoresis
MTP3ONO6EL: 0.05 Ω turn on resistance; maximum current: 15 A; response time: 0.7 μs.

DC output in less than 1 μs to the solenoid and the pinch valve. The solenoid is made of the coated copper wire (28 gauge or 0.013" diameter, 8054 copper wire, Belden Corp., Chicago, IL 60644). The copper wire was wound around a 1/2" x 10" diameter steel rod for about 7 inches. The total resistance of the copper wire is 4.4 Ω. A 15 Ω power resistor is connected in series with the copper coil to prevent the coil from excessive current. On the other hand, this resistor limits the strength of the electromagnetic field so that the attraction of the sample capillary toward the solenoid is not too strong otherwise impact damping can be difficult.

4.3 Damping Device

A dashpot (Airpot Corp., series 160s) for damping the shock which results when the sample and separation capillary meet is shown in figure 4.3 The dashpot was mounted on the solenoid support described in section 4.5. Maximum damping or time delay occurs when the adjustment screw is turned clockwise until it seats. More turns make the screw slip toward the open position which results in a slight decrease in damping. Another clockwise turn will restore maximum damping. To reduce damping, the screw is turned counter-clockwise.

The dashpot cannot be used directly in the sample injection system. The threaded ball joint was cut off and a stainless steel tube was glued on the tiny piston rod. The piston retainer was replaced with a homemade Plexiglas retainer which fit exactly into the glass cylinder. A 1/16" hole was drilled on the Plexiglas retainer to allow the stainless steel tubing to go through. The retainer is then screwed onto the ½"-13 threaded hole on the right side Plexiglas plate.

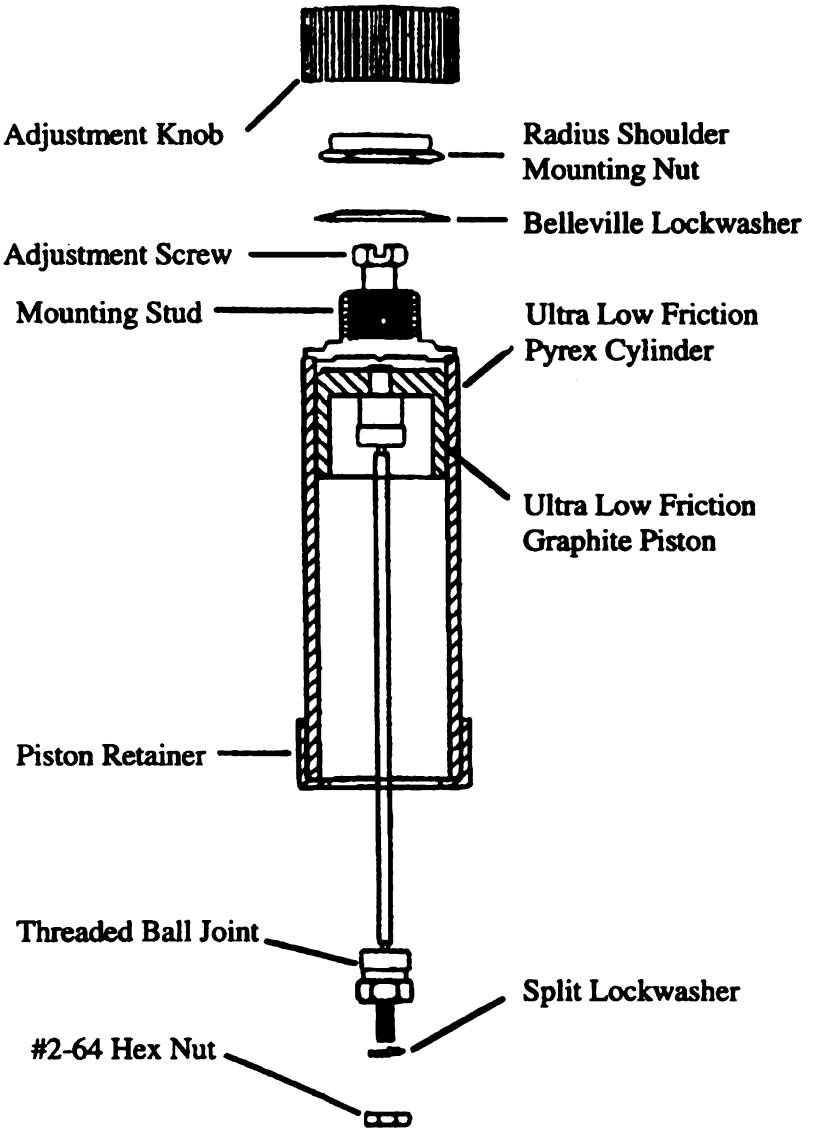

Figure 4.3 Dashpot for damping the shock between sample and separation capillary

4.4 Rotary Alignment System

Ideally, when the sample capillary and the separation capillary are joined, the alignment should be excellent and the contact slow and gentle. The most difficult work is the accurate alignment of the sample capillary and separation capillary due to their small dimensions. Some commercially available linear motion devices give repeatability up to 1 μm. However, the cost is too expensive (~ $9000) for sample injection in CE. Perhaps it

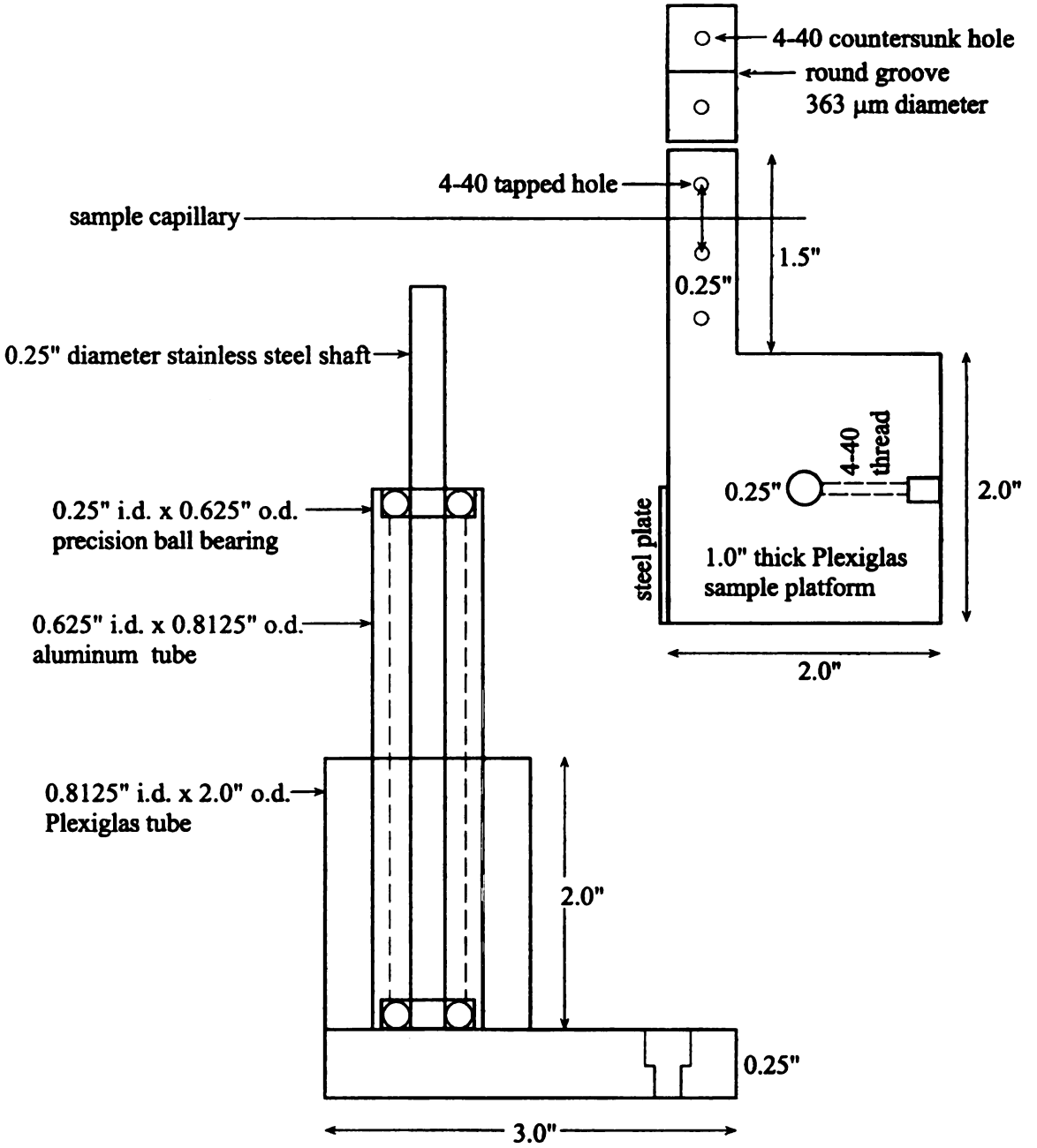

Figure 4.4 Rotary alignment system for automatic sample injection

is not necessary to use such expensive equipment if we can construct an alternative. Attempts to build a linear motion device were not successful. We then constructed the rotary system for alignment shown in figure 4.4, and the result was satisfactory. The precision of the two ball bearings (Barden Inc., product No. SR4SS) determines the quality of alignment. The aluminum tube holding the two precision ball bearings is glued to the Plexiglas with epoxy. The sample capillary is held on the sample platform with a special capillary holder described in section 4.4.

4.5 Holder for the Separation Capillary

Figure 4.5 shows the schematic diagram of the capillary holder made of ½" thick Plexiglas. The machining of the groove to hold the capillary is somewhat tricky. A short segment of the capillary (same dimension of those used for separation) was fixed on the centerline using scotch tape between the two holes of the capillary holder. Another piece of Plexiglas was used to sandwich the capillary. The Plexiglas block was then placed in the chuck of the milling machine; the chuck was then tightened, so that pressure carved a round groove on the centerline of the capillary holder. The round groove was carefully examined under the microscope, and it was found to be smooth and uniform. The capillary was then mounted onto the Plexiglas support block. The Plexiglas support block is then fixed onto a right-angle bracket (Newport Inc.) which is screwed onto the top of a two-dimensional translation stage, for precise position adjustment.

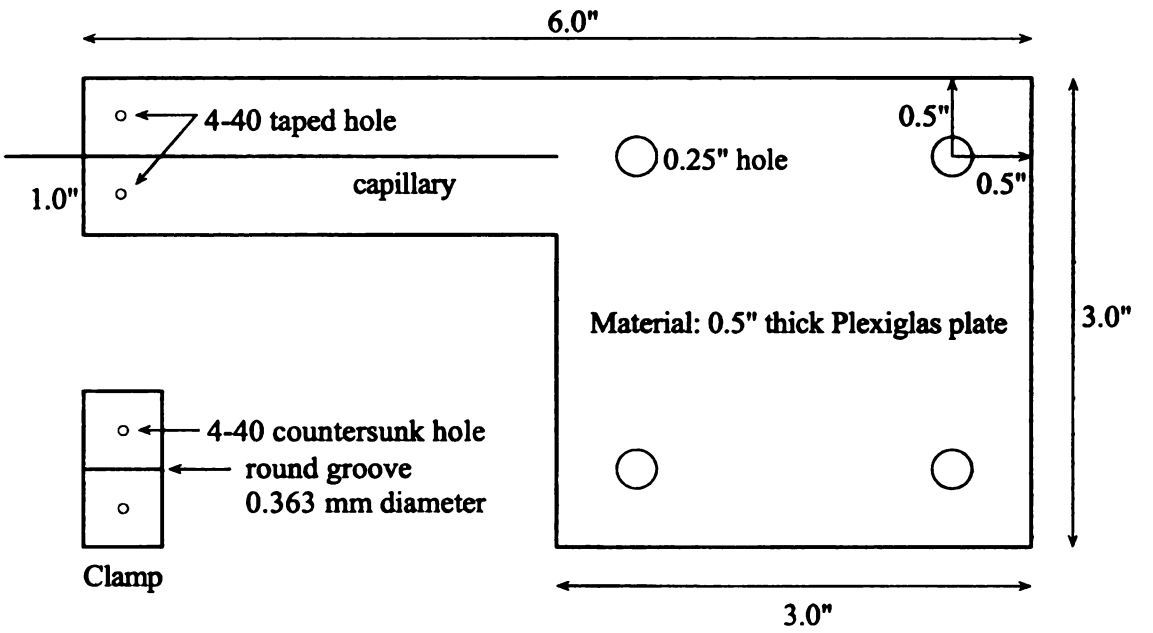

Figure 4.5 Separation capillary holder in automatic injection system

4.6 Solenoid Support

The solenoid support is shown in figure 4.6. It is made of three pieces of Plexiglas, a bottom piece and two side pieces. A ½ hole is drilled on each of the side Plexiglas plate in order to hold the solenoid in position with a set-screw. Two ¼" holes were drilled on the bottom to hold the solenoid support in position on the aluminum breadboard. The side pieces were connected to the bottom piece with six ¼-20" screws.

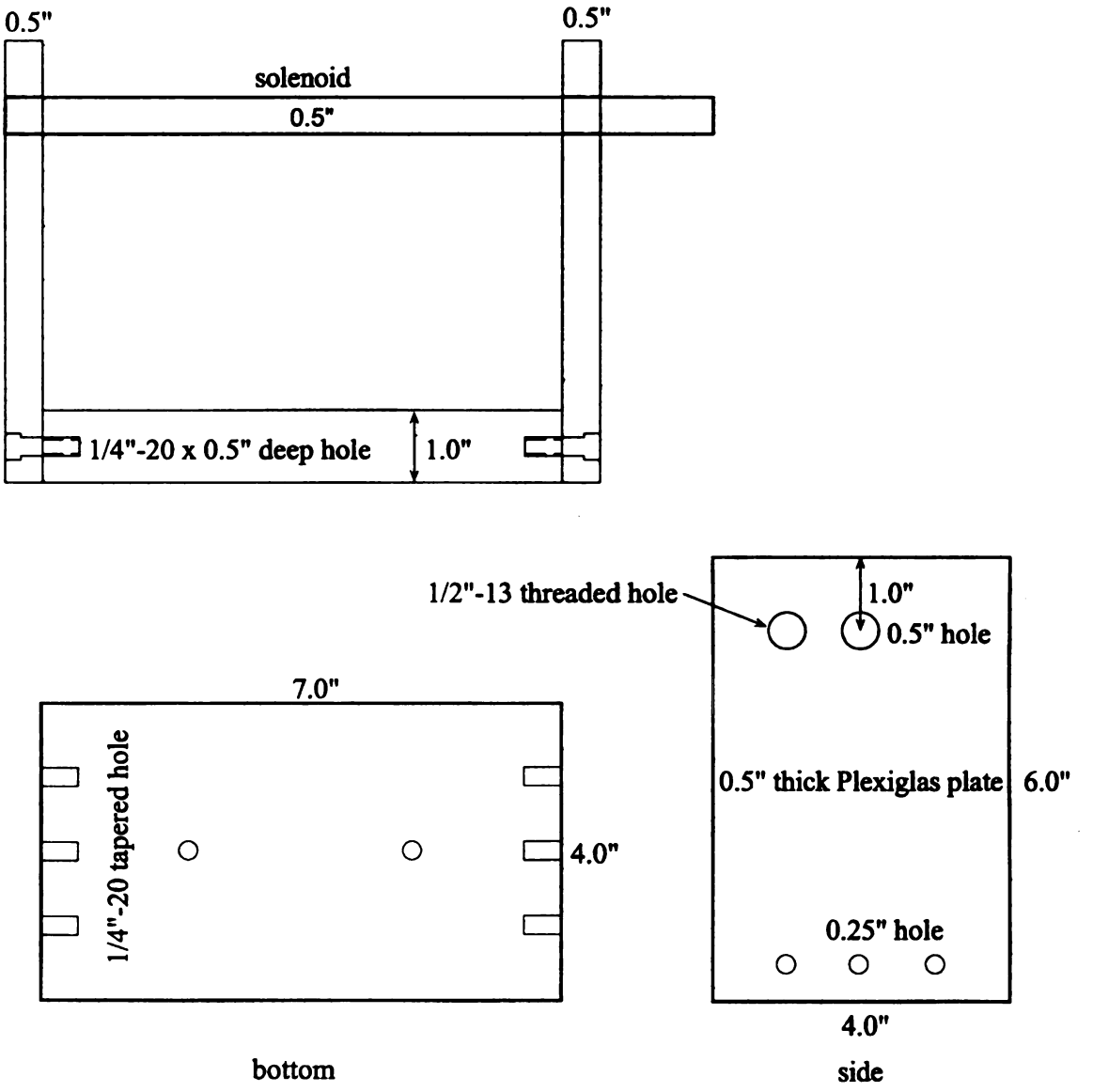

Figure 4.6 Support for the solenoid and the shock-damping dashpot

4.7 Capillary Polishing Tools

The end of the sample and separation capillary must be very flat in order to have the good contact required for sample introduction. A home-made polishing tool, shown in figure 4.7, is used to do the polishing work. About 20 capillaries (50 μm i.d. x 363 μm o.d.) are clamped in the ½" wide x 0.150 mm deep slot of the polishing tool. The end of the capillaries protrudes out of the bottom for about 0.5 mm. The tool is slowly moved in a circular motion on a piece of wet fine sand-paper for about 5 minutes. The end of the capillaries is then inspected under the microscope, and the polishing repeated until a smooth surface is obtained. A few capillaries were clogged by the particles from sandpaper. The clogged capillaries were then placed in the ultrasonic bath and a syringe filled with water was used to clear the clogged capillaries.

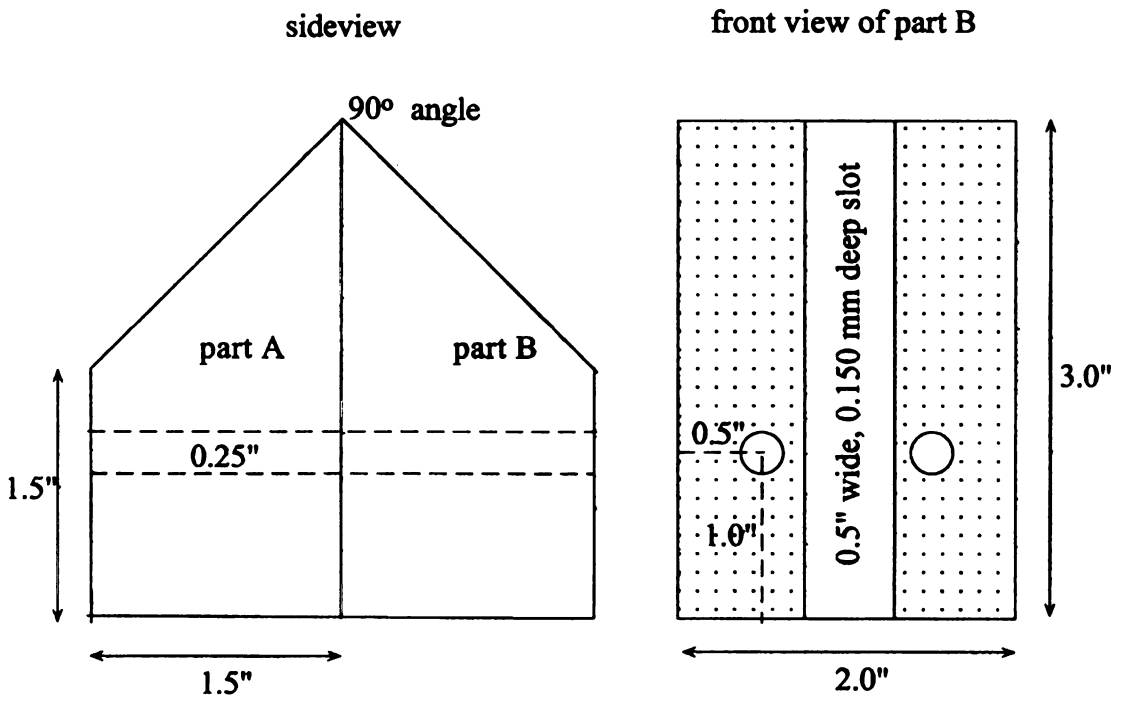

Figure 4.7 Polishing tools for the sample and the separation capillary

4.8 Tubing Connector and Pinch Valve

Sample solution is stored in a plastic syringe. The sample capillary enters the buffer reservoir under high voltage upon the activation of the solenoid. A short piece of silicon rubber tubing is used to connect the sample syringe with the sample capillary. The regular disposable needle (Becton Dickinson & Co.) should not be used directly since the stainless steel needle may cause interruption of the high voltage. The needle is pulled out and then a 1/16" hole is drilled on the plastic socket. A 500 μm i.d. x 1/16" o.d. PEEK sleeve (Upchurch Scientific Inc., product No. F230) is forced into the hole. One end of a silicone rubber tubing 0.015" i.d. x 1/32" o.d. (Manostat Corp., product # 75-300-015) is connected to the PEEK sleeve, and the other end is connected to the sample capillary (50 μm i.d. x 363 μm o.d. x 20 cm long). The silicon tubing is installed on the pinch valve, which is normally closed to prevent the leakage of sample solution. The end of the silicon tubing is fixed onto the high voltage box.

The pinch valve is screwed on the four small holes (1/2" spacing) of the Plexiglas pinch valve holder as shown in figure 4.8. The pinch valve holder is inserted into a ½" aluminum rod through the ½" center hole shown in top-view of figure 4.8 and held in position about 65 cm above the breadboard with a ¼"-20 set-screw. The sample syringe is mounted 76 cm above the breadboard.

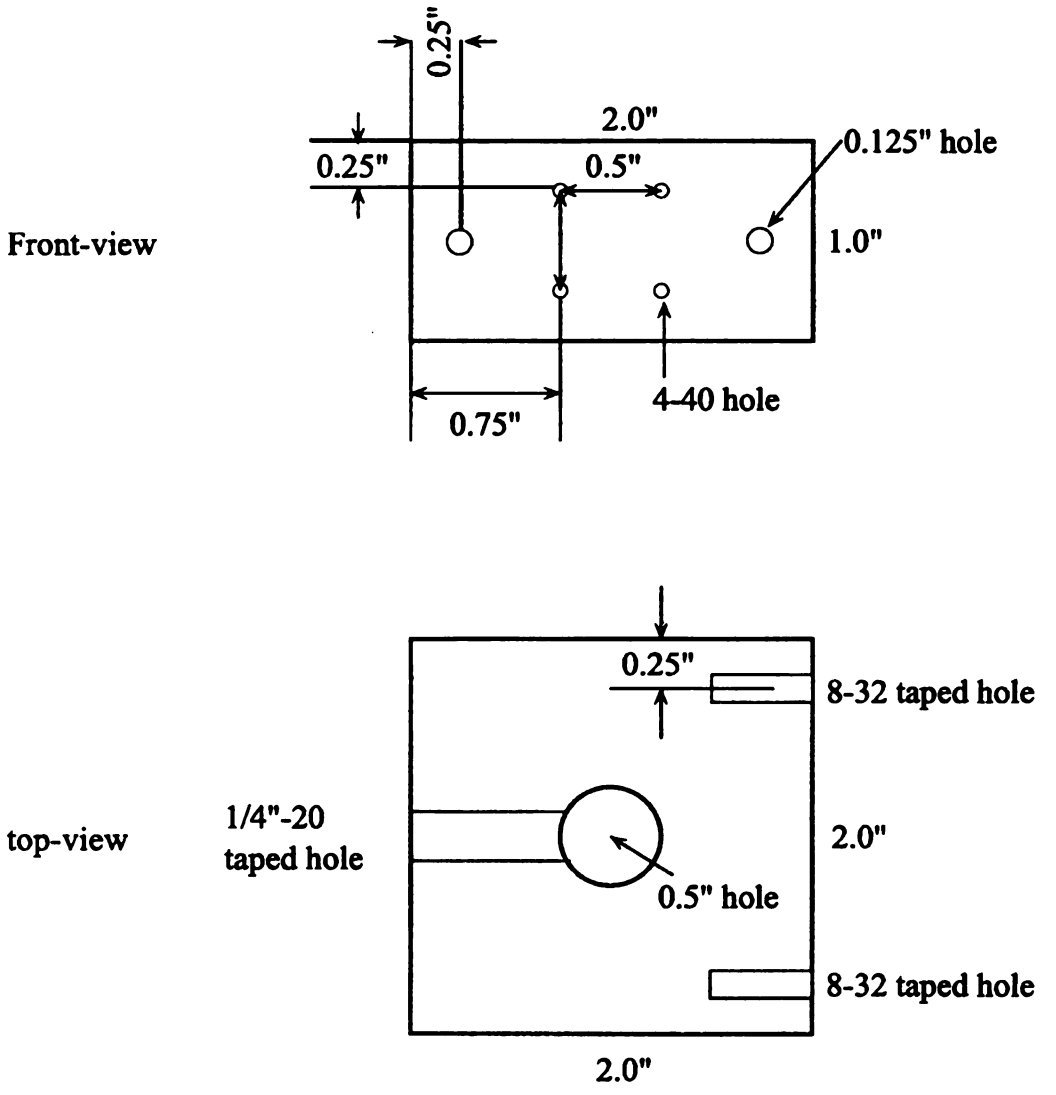

Figure 4.8 Pinch valve holder for automatic injection system

Chapter 5

Characterization of the Automatic Sample Injection System in Capillary Zone Electrophoresis

Sample injection in CE is different from that in LC, GC or FIA where a loop of fixed volume is used for injection. Since the capillary bore is very small, a loop injector is not technically practical at the moment. The amount of sample injected into the separation capillary in CE is time-controlled; therefore human error usually plays a big part in the overall error. The injection error in CE includes timing error and the transfer error. Timing error is one of the most important sources of error in capillary electrophoresis in manual injection. It is not uncommon to see 10% or higher relative standard deviation (RSD) in peak height due to irreproducible injections in CE.

Transfer error occurs when the capillary is moved from the sample to the buffer; this period of time can last about 2 - 4 seconds during which there is no electric field across the separation capillary. During this time, the sample zone can diffuse back and forth in the capillary, making the zone wider. Any motion of the separation capillary during this transfer process can further broaden the sample zone. Unfortunately, no CE system, including those commercially available, is able to eliminate diffusion occurring during this transfer. If we can reduce the timing error to some extent, we can certainly enhance the reproducibility of sample injection in capillary electrophoresis.

Sample throughput is defined in flow injection analysis as the number of sample injections performed per unit time. In CE with conventional injection, the manual

injections usually limit the sample throughput to ~10 injections/hour. In our automatic injection system, 10 consecutive sample injections were accomplished in 7 minutes, which converts to about 85 injections/hour. The higher throughput is attributed to the continuous injections during the electrophoretic run.

Many other factors such as sample composition, and detection scheme, may affect the reproducibility of injections in CE. In general, the RSD of injections can vary from 3% to 10% for on-column detection (2, 3). The RSD for post-column detection is higher due to the additional source of error. In this chapter, an automatic sample injection system is characterized. The linear flow rate ν, of sample in the sample capillary (open tubular) can be estimated by the Hagen-Poiseuille equation:

$$\nu = \frac{8 L \eta \Delta P}{r^2} \tag{5.1}$$

Here ΔP is the pressure drop along an open tubular capillary of length L with radius r containing a flowing solution of viscosity η.

5.1 Reproducibility of Timing

We repeated 10 tests to calculate the reproducibility of this time period using a stopwatch and obtained a mean value of 1.04 s with a travel time standard deviation of 0.04 s. The measured RSD of the automatic injection system is 3.7%. This is perhaps an upper limit because of the irreproducibility of the manual time measurement. Knowing the 0.04 s travel time standard deviation, we measured the precision of the injection time under various preset values of injection time. The measured time includes the travel time and the injection time ($t_{meas} = t_{inj} + t_{travel}$); hence the injection time is that measured time

minus the 1.04 s travel time. The means are reported for 10 injections. The RSD decreases with longer injection time.

Table 5.1 Reproducibility of the Injection System without Sample Injection

	Nominal injection time		
	2 s	5 s	10 s
Measured time (t_{meas})	2.95 ± 0.04	6.01 ± 0.05	11.00 ± 0.03
Injection time (t_{inj})	1.91 ± 0.06	4.97 ± 0.06	9.96 ± 0.05
RSD	3.1%	1.2 %	0.5%

5.2 Reproducibility of Peak Height

Figure 5.1 shows the reproducibility of 10 consecutive injections using the automatic injection system and a 0.96 s injection (nominal injection: 2 s). The relative standard deviation (RSD) of the peak height is 10.7%. The automatic injection system can efficiently reduce the timing uncertainty. The advantage of automatic injection is seen clearly here. For a 1 s manual injection in CE, accurate timing is difficult. The fourth peak is relatively low probably due to the vibration between the sample capillary and the separation capillary when they were joined. As we discussed earlier, good pressure damping is essential for reproducible results. Figure 5.2 shows the reproducibility of 10 consecutive injections using the automatic injection system for 3.96 s injections. The RSD of the peak height is 10.9%. In manual sample injection, the RSD is larger for shorter injection due to timing error. In automatic injection, the timing error is reduced; consequently the RSD for the two sets of sample injections under different injection time (0.96 s and 3.96 s) shows no significant variation (F-test at 95% confidence level).

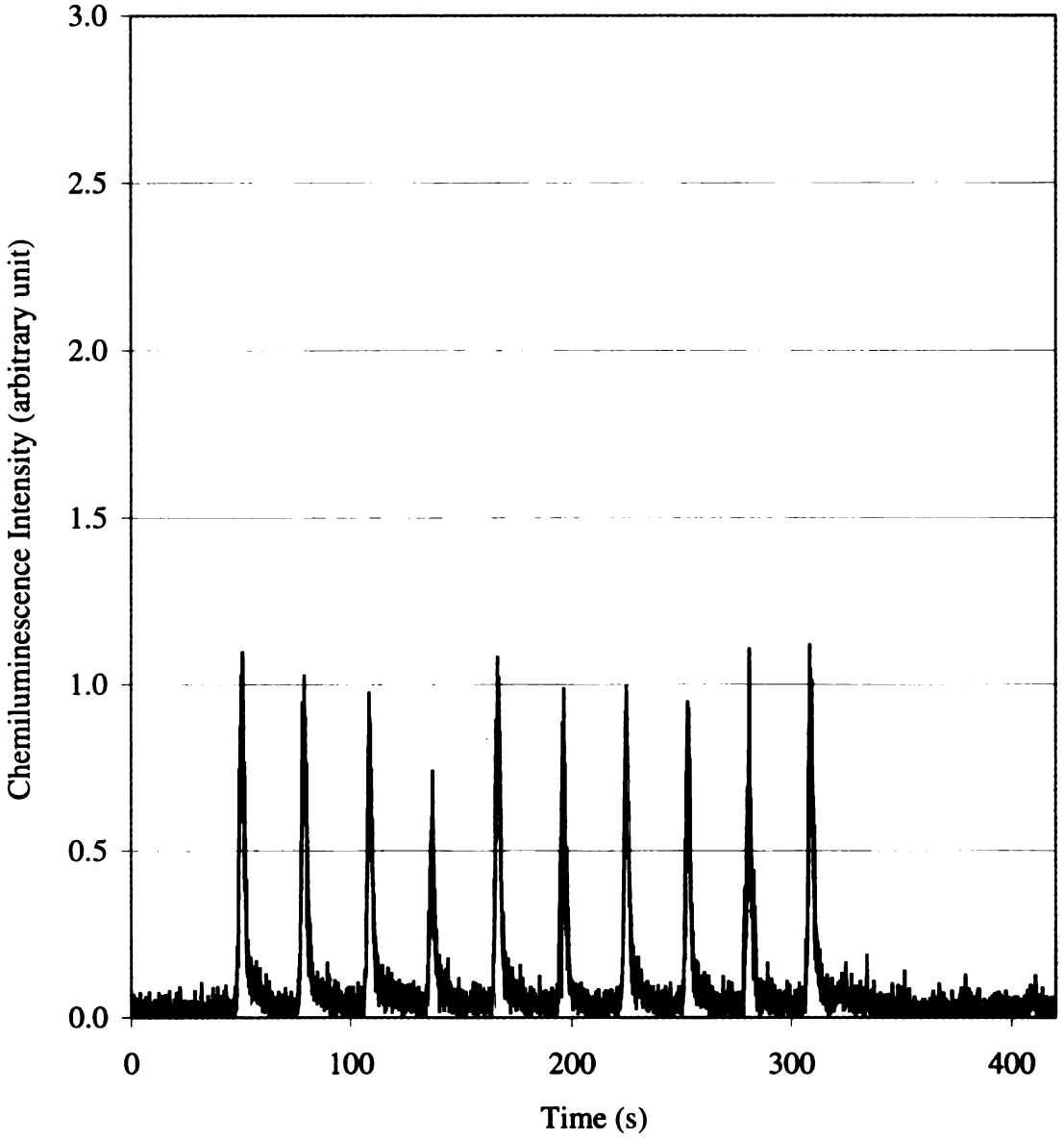

Figure 5.1 Reproducibility of 10 consecutive injections using the automatic injection system for 0.96 s. Sample: 1.0 x 10^{-8} M Co^{2+}; buffer: 2.0 x 10^{-4} M luminol, 0.01 M acetic acid, pH = 4.75. Capillary: 50 μm i.d. x 363 μm o.d. x 50 cm long fused silica capillary. Separation voltage: 10 kV. Amplifier: 10^{8} V/A, 3 ms response time. PMT voltage: 800 V. Post-column reagents: 0.05 M H_2O_2, 0.1 M phosphate (pH = 12.50), flow rate: 3 μL/min per channel. Height of sample injection: 76 cm. Injection interval: 30 s. Mean of the peak height: 1.00. RSD of the peak height: 10.7%.

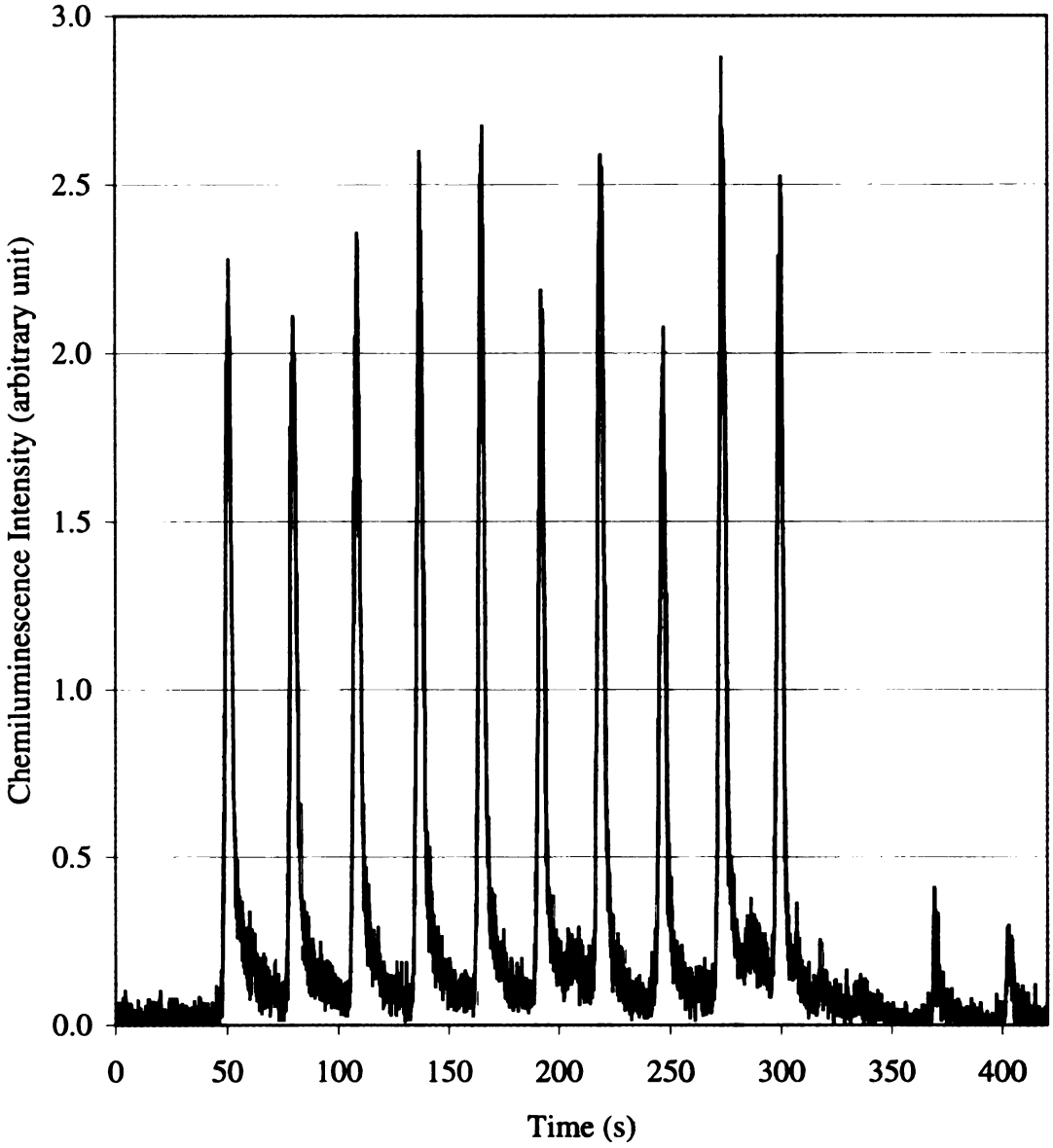

Figure 5.2 Reproducibility of 10 consecutive injections using automatic injection system for 3.96 s. Sample: 1.0 x 10^{-8} M Co^{2+}; buffer: 2.0 x 10^{-4} M luminol, 0.01 M acetic acid, pH = 4.75. Capillary: 50 μm i.d. x 363 μm o.d. x 50 cm long fused silica capillary. Separation voltage: 10 kV. Amplifier: 10^{8} V/A, 3 ms response time. PMT voltage: 800 V. Post-column reagents: 0.05 M H_2O_2, 0.1 M phosphate (pH = 12.50), flow rate: 3 μL/min per channel. Height of sample injection: 76 cm. Injection interval: 30 s. Mean of the peak height: 2.42. RSD of the peak height: 10.9%.

5.3 Function of Pinch Valve

The sample could continuously leak out in our automatic injection system. To solve

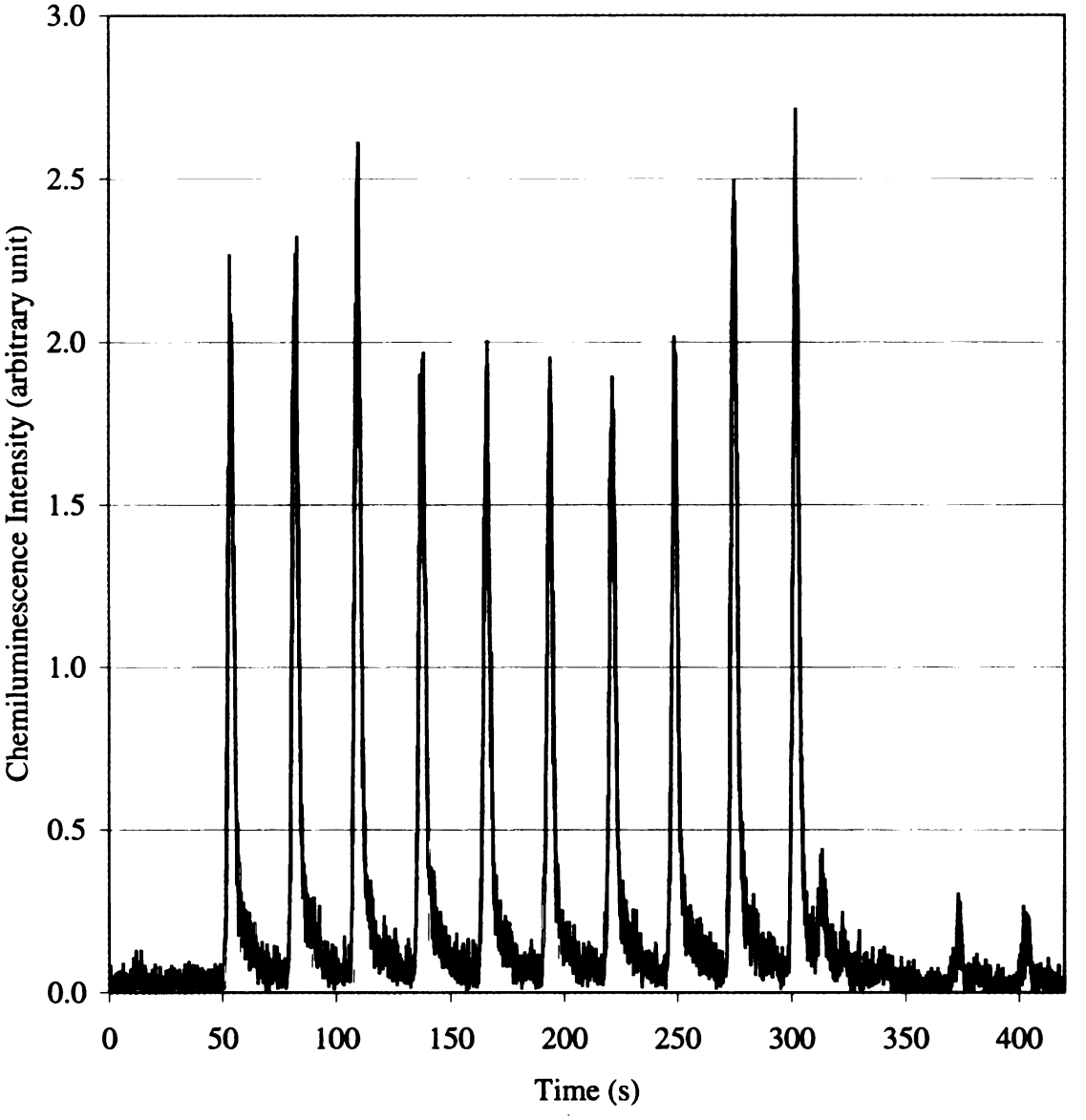

Figure 5.3 Reproducibility of 10 consecutive injections using automatic injection system with pinch valve for 3.96 s. Sample: 1.0 x 10^{-8} M Co^{2+}; buffer: 2.0 x 10^{-4} M luminol, 0.01 M acetic acid, pH = 4.75. Capillary: 50 μm i.d. x 363 μm o.d. x 50 cm long fused silica capillary. Separation voltage: 10 kV. Amplifier: 10^{8} V/A, 3 ms response time. PMT voltage: 800 V. Post-column reagents: 0.05 M H_2O_2, 0.1 M phosphate (pH = 12.50), flow rate: 3 μL/min per channel. Height of sample injection: 76 cm. Injection interval: 30 s. Mean of the peak height: 2.22. RSD of the peak height: 13.4%.

this problem, a pinch valve was installed as described previously. Figure 5.3 shows the reproducibility of automatic injection when a pinch valve is engaged. RSD for figure 5.3. (13.4%) differs only slightly from that for figure 5.2 (10.9%). The mean of the peak height in figure 5.2 (2.42) is close to that in figure 5.3 (2.22). Without the pinch valve, the sample is driven out continuously by the siphoning effect and a tiny growing droplet of sample remains at the tip of the sample capillary between sample injection. When the sample injection is actuated, the sample capillary joins the separation capillary and brings the tiny droplet of sample into the buffer reservoir. This small contamination of the buffer seems to affect neither the peak height nor the baseline as shown in figure 5.2 and 5.3. However, if the injection height is increased and the droplet is growing at higher rate, this could be a problem. Therefore, it is still desirable to install the pinch valve.

5.4 Comparison between the Automatic Injection System and other Injection Systems

The RSD in CE injections vary between 2 ~ 10% (2, 3, 4, 5) for on-column detection. In manual injection, the RSD may be higher when the injection time is short. The RDS under a 4 s injection is reported in table 5.2. The mean of the peak height is 1.74, and the

Table 5.2 Reproducibility of 10 Manual Injections for 4 s Injection

Peak Height	Mean	Standard Deviation	RSD
4 s Manual injection	1.74	0.47	27.0%

Sample: 1.0×10^{-9} M Co^{2+}; buffer: 2.0×10^{-4} M luminol, 0.01 M acetic acid, pH = 4.75. Capillary: 50 μm i.d. x 363 μm o.d. x 50 cm long fused silica capillary. Separation voltage: 10 kV. Amplifier: 10^8 V/A, 3 ms response time. PMT voltage: 800 V. Post-column reagents: 0.05 M H_2O_2, 0.1 M phosphate (pH = 12.50), flow rate: 3 μL/min per channel. Voltage of injection: 10 kV. Time of injection: 4s.

standard deviation is 0.47. The RSD of the 10 manual injections with a 4 s injection is 27.0%, substantially larger than the RSD (10.9%) of the10 automatic injection shown in figure 5.2.

5.5 Conclusions

This work demonstrates several advantages of the automatic sample injection system over manual injection in capillary zone electrophoresis. Several sources of injection error are reduced significantly in the new injection system. As a result, the new injection system presents a unique approach to sample introduction in CE. With some instrumental improvements in alignment and in the damping device, the RSD should be improved. The new injection system also gives higher sample throughput. This unique advantage can be particularly useful in some CE separations where long separation times are required so that a series of injection can be performed before the previous run is finished. It saves time and operation cost.

List of References

1. Evans, C. E. *Anal. Chem.* **1997**, *69*, 2952-2954
2. Fuller, R. R.; Sweedler, J. V. *Anal. Chem.* **1999**, *71*, 4014-4022.
3. Bachmann, K.; Boden, J.; Haumann, I. *J Chromatogr.* **1992**, *626*, 259-265.
4. Weston, A.; Brown, P. R.; Heckenberg, A. L.; Jandik, P.; Jone, W. R. *J. Chromatogr.* 1992, 602, 249-256.

Chapter 6

Summary and Conclusions

In this work, we have constructed a miniaturized chemiluminescence (CL) detector for capillary electrophoresis (CE) which provides high collection efficiency (≈ 58%). This CL detector is well grounded and significantly cuts down the electrical noise associated with AC power supply. The miniaturized CL detector is characterized using a few transitional metal cations (Co^{2+}, Cr^{3+}, and Cu^{2+}) as the sample species. We found these metal cations are all strongly adsorbed to the wall of fused-silica capillary at high concentrations. We obtained the best theoretical plate number, 500,000, for a post-column reaction detector in capillary electrophoresis. We were able to achieve a detection limit of 1.5×10^{-12} M for Co^{2+}, 5.0×10^{-8} M Cr^{3+}, and 3.0×10^{-8} M Cu^{2+}. These limits of detection are significantly lower than those obtained by other methods of detection such as electrochemical and UV detection.

We also constructed an automatic sample injection system for CE. This new injection system greatly enhances the sample throughput in CE, compared to manual injections. The automatic sample injection system shows a better reproducibility of injection (10.9%) than the manual injection system (27.0%) in our CL-CE system for a 4s injection, based on 10 consecutive injections.

Chapter 7

Future Work

7.1 The Chemiluminescence Detection System

The fused silica capillary is so far the most widely used capillary in capillary electrophoresis; the majority of CE separations have been performed in untreated fused-silica capillaries. The walls of untreated fused-silica capillaries are chemically reactive. They can adsorb solutes by electrostatic and/or chemical interactions, especially in the case of transition metal cations and large molecules like proteins. The adsorption results in band broadening, and in some cases the peak is lost completely (1).

Inert capillaries such as Teflon, and PEEK (Polyether Ether Ketone) are ideal for the separation of transition metal cations if their mechanical property matches that of the fused-silica capillary. PEEK tubing of 63 μm i.d. x 1/16" o.d. is commercially available (Upchurch Scientific Inc.), but the outside diameter (1/16") is so large that it cannot be inserted into the reaction capillary. A portion of the PEEK capillary must be machined to a smaller outside diameter in order to fit the reaction capillary; so far we have not found a practical way of doing that.

A number of approaches for suppressing the electroosmosis and/or minimizing wall adsorption for fused-silica capillaries have been explored. These methods include adjustment of the buffer pH (2-5), addition of high concentrations of ionic salts (6-8) or zwitterions (9, 10), addition of buffer modifiers (11, 12), application of an external electric field (13-15), and permanent wall coatings (16-37).

Several groups have tried to eliminate adsorption by covalently bonding organic phases to the wall, or physically coating the wall. Chemical modification of the inner capillary wall is the most practical method, and it includes coating the capillary inner wall with methylcellulose (16), chitosan (17), acrylamide (18, 19), trialkoxysilane (11, 20-23), epoxydiols (24), maltose (25), polyethylene glycol (26, 27), poly(vinylpyrrolidine) (1), arylpentafluoro (28), polyethyleneimine (29), polyelectrolyte multilayers (30), OV-1 (31), Carbo-wax 20M (31, 32), and Plexiglas (33).

Generally speaking, capillaries coated with cross-linked polymers which are bonded to the inner wall are stable, and provide high efficiency separations (34, 35). Chemical bonding with trialkoxysilane involves blocking the silanol groups with an uniform addition of an organic monolayer, which subsequently serves as a link for attachment of a polymer layer. The primary purpose of the latter is to provide a "comfortable" medium for the separated solutes, with minimum interaction.

Physical coating provides a new alternative for achieving long and narrow-bore capillaries. Shao and coworkers from Lee 's group (36) used Plexiglas to physically modify fused silica capillary. The procedure was carried out using a dynamic coating method at room temperature. Greatly suppressed electroosmosis was observed at pH 3-10. Plexiglas coating shields the surface Si-OH group so that the adsorption of metal ions can be greatly depressed. The electroosmotic flow shows little dependence on the pH of the separation buffer. The adsorption of transition metal cations has been a serious problem at high pH (pH > 4.50). Plexiglas is resistant to alkali, dilute acids, and aqueous solutions of inorganic salts (37). With Plexiglas-coated capillaries, strict control of buffer pH is not necessary. Separation of transition metal cations can be performed at higher

buffer pH, which allows a faster post-column pH switching. No capillary preconditioning is necessary. These approaches should be explored in the future for use with the metal ions, CL CL system. We anticipate that adsorption to the walls of the capillary can be eliminated or minimized.

7.2 Automatic Injection System in Capillary Electrophoresis

Linear injection devices can be a good alternative for automatic sample injection in CE. A linear motion device sweeps lesser area than a rotary alignment device. The linear motion device for sample injection in CE should present high repeatability, appropriate travel distance (~ 10 mm) and travel speed (~5 mm/s). Newport Corp. provides a variety of motorized precision translation stages and drive modules that meet these requirements. The mid-range travel translation stage (UTM25CC1DD) gives the following features: travel distance 25 mm, repeatability to 0.5 μm, maximum speed > 20 mm/sec, load capacity to 20 kg. Its weakness is the high cost. The translation stage costs about $3000, and the drive module costs $2000-3000. For easy position manipulation, we need free adjustment in three dimensions, which can be done by mounting a motorized translation stage via a right-angle bracket on top of a two-dimensional translation stage ($450). Therefore, the motorized translation stage and drive module are the major cost.

7.2.1 Linear Motion Device for Alignment

In order to make the linear motion device cost-efficient for use in CE as a sample injector, it is necessary to modify the drive system by replacing the precision screw with other methods such as an air cylinder or electromagnetic coils. In such cases, a damping

device (i.e., airpot from Airpot Corp.) is needed to reduce the shock upon contact of the sample and separation capillaries. The cost of the linear injection system can be significantly reduced if the number of translation stages for alignment can be reduced from three dimensions (XYZ directions) to one dimension. The translation stage for the Z direction can be removed if the sample and the separation capillary can be set at the same height on two different plates. A right angle V-groove can be machined so that the two plates are in precise alignment. The sample capillary and the separation capillary can be placed in the right angle V-groove to achieve good alignment, and a capillary holder can be used to hold the capillary in position. In this way, only one translation is needed to bring the sample and separation capillary into contact with good alignment for sample injection.

7.2.2 Timing Device

The timing device described in chapter 4 counts from the moment of rotation of the rotary alignment system, rather than the moment of contact between the sample and the separation capillary. Therefore, we have to offset the traveling delay. It is better to time from the moment of contact in order to reduce the timing error caused by the variation of traveling time of the rotary alignment system. This can be accomplished by installing a timer which can be actuated when the sample and separation capillaries are met.

List of References

1. Chen, M.; Cassidy, R. M. *J. Chromatogr.* **1992**, *602*, 227.
2. McCormick, R. M. *Anal. Chem.* **1988**, *60*, 2322.
3. Lauer, H. H.; McManigill, D. *Anal. Chem.* **1986**, *58*, 166.
4. Walbroehl, Y.; Jorgenson, J. W. *J. Microcolumn Sep.* **1989**, *1*, 41.
5. Vinther, A.; Bjorn, S. E. Sorenson, H. H.; Soeberg, H. *J. Chromatogr.* **1990**, *516*, 175.
6. Green, J. S.; Jorgenson, J. W.; *J. Chromtgr.* **1989**, *478*, 63.
7. Lauer, H. H.; McManigill, D. *Trent. Anal. Chem.* **1986**, *5*, 11.
8. Bushey, M. M.; Jorgenson, J. W. J. Chromatgr. **1989**, *480*, 301.
9. Stover, F. S.; Haymore, B. L.; McBeath, R. J. *J. Chromatogr.* **1989**, *470*, 241.
10. Yeung, K. K.-C.; Lucy, C. A. *Anal. Chem.* **1997**, *69*, 3435.
11. Hjerten, S. *J. Chromatgr.* **1985**, *347*, 191.
12. Corradini, D.; *J. Chromatogr. B* **1997**, *699*, 221.
13. Lee, C. S.; Blanchard, W. C.; Wu, C. T. *Anal. Chem.* **1990**, *62*, 1550.
14. Lee, C. S.; McManigill, D.; Wu, C. T.; Patel, B. *J. Chromatogr.* **1991**, 63, 1519.
15. Lee, C. S.; Wu, C. T.; Lopes, T.; Patel, B.; J. Chromatogr. **1991**, *559*, 133.
16. Hjerten, S. *J. Chromatgr. Rev.*, **1967**, *9*, 122.
17. Sun, P.; Landman, A.; Hartwick, R. A. *J. Microcol. Sep.* **1994**, *6*, 403-407.
18. Cobb, K. A.; Donik, V.; Novotny, M. *Anal. Chem.* **1990**, *62*, 2478.
19. Huang, X. Y.; Doneski, L. J.; Wirth, M. J. *Anal. Chem.* **1998**, *70*, 4023-4029.
20. Hjerten, S.; Kiessling-Johansson, M. *J. Chromatogr.*, **1991**, *550*, 811.

21. Huang, M. X.; Dubrovcakova-Schneiderman, E.; Novotny, M. V.; Fatunmbi, H.; Wirth, M. J. *J. Microcol. Sep.*, **1994**, *6*, 571-576.

22. Jorgenson, J. W.; Lukacs, *Science (Washington, D.C.)*, **1983**, *222*, 266.

23. Shao, X. W.; Shen, Y. F.; O'Neil, K.; Lee, M. *J. Chromatogr. A*, **1999**, *830*, 415.

24. Bruin, G. J. M.; Huiden, R.; Kraak J. C.; Poppe, H. *J. Chromatogr.* **1989**, *480*, 339.

25. Bruin, G. J. M.; Huiden, R.; Kraak J. C.; Poppe, H. *J. Chromatogr.* **1989**, *480*, 339.

26. Bruin, G. J. M.; Chang, R. H.; Kuhlman, R. H.; Zegers, K.; Kraak, J. C.; Poppe, H. *J. Chromatgr.* **1988**, *471*, 429.)

27. Herren, B. J.; Shafer, S. G.; Alstine, J. V.; Hams, J. M.; Snyder, R. S. J. *Colloid Interface Sci.* **1987**, *115*, 46.

28. Maa, Y.; Hyner, K. J.; Swedberg, S. A. *J. High Resolut. Chromatogr.* **1991**, *14*, 65.

29. Towns, J. K.; Regnier, F. E.; *J. Chromatogr.* **1990**, *516*, 69.

30. Graul, T. W.; Schlenoff, J. B. *Anal. Chem.* **1999**, *71*, 4007-4013.

31. Lux, J. A.; Yin, H.; Schomberg, G. *J. High Resolut. Chromatogr.* **1990**, *13*, 145.

32. Chen, M.; Cassidy, R. M. *J. Chromatogr.* **1992**, *602*, 227.

33. Shao, X. W.; Shen, Y. F.; O'Neil,K.; Lee, M. *J. Microcolumn Separations*, **1999**, *11 (5),* 325.

34. Gilges, M.; Kleemiss, M. H.; Schomburg, G. *Anal. Chem.* **1994**, *66*, 2038.

35. Ren, X.; Shen, Y; Lee, M. *J. Chromatogr. A 741*, **1996**, 115.

36. Shao, X. W.; Shen, Y. F.; O'Neil,K.; Lee, M. *J. Microcolumn Separations*, **1999**, *11 (5),* 325.

37. Harrison, D. J.; Flury, K.; Seiler, K.; Fan, Z.; Effenhauser, C. S.; Mans, A. *Science* **1993**, *261*, 895.